Effizienz einer Kombinationstherapie aus G-CSF und mononukleären Knochenmarkzellen in einem präklinischen Schlaganfallmodell

Kumulative Dissertation
zur Erlangung des akademischen Grades
Dr. rer. med.

an der Medizinischen Fakultät
der Universität Leipzig

eingereicht von:
Dipl. Ing. (FH) Claudia Pösel
Geburtsdatum: 09. April 1982
Geburtsort: Gera

angefertigt am:
Fraunhofer-Institut für Zelltherapie und Immunologie, Abteilung Zelltherapie,
Arbeitsgruppe Ischämieforschung

Betreuer:
Prof. Dr. Frank Emmrich (Universität Leipzig)
Prof. Dr. Hans-Jürgen Mägert (Hochschule Anhalt, Köthen)

Beschluss über die Verleihung des Doktorgrades vom 14. Juli 2015

Inhaltsverzeichnis

Bibliografische Zusammenfassung

Claudia Pösel

Effizienz einer Kombinationstherapie aus G-CSF und mononukleären Knochenmarkzellen in einem präklinischen Schlaganfallmodell

Universität Leipzig, Kumulative Dissertation zur Erlangung des akademischen Grades Doctor rerum medicinae (Dr. rer. med.)

68 Seiten, 98 Literaturangaben, 1 Tabelle

Eine Vielzahl präklinischer Schlaganfallstudien zeigte die neuroprotektive und neuroregenerative Wirkung des hämatopoetischen Wachstumsfaktors G-CSF (Granulozyten-Kolonie stimulierender Faktor). Ein Wirkungsmechanismus des G-CSF ist die Mobilisation von protektiven Knochenmarkzellen in die ischämische Läsion, wobei diese zeitverzögert nach G-CSF-Gabe stattfindet. Eine zusätzliche frühzeitige Transplantation mononukleärer Knochenmarkzellen (BM MNC) könnte diese therapeutische Lücke füllen. Ziel der vorliegenden Studie war es, die Wirksamkeit dieser Kombinationstherapie in einem Schlaganfallmodell der spontan hypertensiven Ratte (SHR) zu testen. Syngene BM MNC wurden aus dem Knochenmark von SHRs durch immunmagnetische Depletion der Granulozyten isoliert. Nach Verschluss der Arteria cerebri media wurde den Tieren über insgesamt 5 Tage G-CSF verabreicht und zusätzlich zu einem frühen (6h nach Schlaganfall) oder späteren (48h nach Schlaganfall) Zeitpunkt BM MNC intravenös appliziert. Unbehandelte Schlaganfalltiere sowie Tiere mit alleiniger G-CSF-Therapie dienten als Kontrolle.

Das Infarktvolumen wurde weder durch die alleinige G-CSF-Gabe noch durch die zusätzliche Zelltherapie verändert. Dennoch wiesen Tiere mit G-CSF-Einzeltherapie eine anhaltende funktionelle Verbesserung des sensomotorischen Defizites auf. Während die zusätzliche frühzeitige Zelltransplantation (6h) keinen weiteren Therapieeffekt zeigte, führte die Zelltransplantation nach 48h zu einer Aufhebung des protektiven G-CSF-Effektes. Die G-CSF-Therapie bewirkte erwartungsgemäß einen deutlichen Anstieg der zirkulierenden Leukozyten. Interessanterweise wurde der Granulozytengehalt im Blut und in der Milz durch die einmalige Zelltherapie nach 48h signifikant erhöht. Ein Großteil der transplantierten BM MNC (48h) konnte in der Milz nachgewiesen werden und führte dort vermutlich zu einer kompetitiven Hemmung des Granulozytenabbaus. Dies hatte sowohl den Anstieg der zirkulierenden Granulozyten als auch deren vermehrte Infiltration in das ischämische Hirngewebe zur Folge und könnte schließlich den negativen Einfluss auf die funktionelle Verbesserung erklären. Die beobachteten Interaktionsmechanismen werfen ein interessantes Licht auf die mögliche Wirkungsweise von Zelltherapien und unterstreichen die entscheidende Rolle des Immunsystems in der Pathophysiologie des Schlaganfalls.

Abkürzungsverzeichnis

ARRIVE	engl. *Animals in Research: Reporting In Vivo Experiments*
ART	engl. *Adhesive Removal Test*
AUC	engl. *area under the curve*, Fläche unter der Kurve
Bcl-2	engl. *B-cell lymphoma 2,* B-Zellen-Lymphom 2
BM MNC	engl. *bone marrow mononuclear cells,* mononukleäre Zellen des Knochenmarks
CD	engl. *cluster of differentiation,* Unterscheidungsgruppen immunphänotypischer Oberflächenmoleküle
cIAP2	engl. *cellular inhibitor of apoptosis,* zelluläre Apoptose-inhibitorische Proteine
CXCR4	CXC-Motiv-Chemokinrezeptor 4
DAMPs	engl. *damage associated molecular patterns,* Schaden-assoziierte molekulare Strukturen
DGZ	Dichtegradientenzentrifugation
G-CSF	engl. *granulocyte-colony stimulating factor,* Granulozyten-Kolonie stimulierender Faktor
G-CSFR	Rezeptor des Granulozyten-Kolonie stimulierender Faktor, CD114
GFAP	engl. *glial fibrillary acidic protein*, saures Gliafaserprotein
h	Stunde
HLA	engl. *human leukocyte antigen*, humanes Leukozytenantigen
%HLVe	engl. *hemispheric lesion volume,* Ödem-korrigiertes Infarktvolumen
HSC	engl. *hematopoietic stem cell*, hämatopoetische Stammzelle
ia	intraarteriell
ICAM	engl. *intercellular adhesion molecule,* Intrazelluläres Adhäsionsmlekül
IL	Interleukin
iv	intravenös
kDa	Molekulargewicht in Kilodalton
MACS	engl. *magnetic activated cell sorting*, magnetische Zellselektion
MCAO	engl. *middle cerebral artery occlusion,* Verschluss der mittleren zerebralen Hirnarterie
mmHg	Millimeter Quecksilbersäule
MZM	engl. *marginal zone macrophages,* Makrophagen der Marginalzone
pMCAO	engl. *permanent middle cerebral artery occlusion,* permanenter Verschluss der mittleren zerebralen Hirnarterie

PMN	engl. *polymorphonuclear leukocytes*, Granulozyten
rt-PA	engl. *tissue plasminogen activator,* gewebsspezifischer Plasminogenaktivator
SCID	engl. *severe combined immunodeficiency,* schwerer kombinierter Immundefekt
SDF-1	engl. *stromal cell-derived factor 1,* CXCL12
SHR	spontan hypertensive Ratte
STAIR	engl. *The Stroke Treatment and Academic Roundtable*
STEPS	engl. *Stem Cell Therapy as an Emerging Paradigm for Stroke*
SVZ	Subventrikuläre Zone
tCCA	engl. *transient common carotid artery occlusion*, transienter Verschluss der Halsschlagader
Th1	T-Helferzelle des Typ 1
tMCAO	engl. *transient middle cerebral artery occlusion,* transienter Verschluss der mittleren zerebralen Hirnarterie
TNF-α	Tumornekrosefaktor-α
TVV	Tierversuchsvorhaben
α	Wahrscheinlichkeit des Fehlers 1. Art
ß	Wahrscheinlichkeit des Fehlers 2. Art
σ	Varianz

1 Einführung

1.1 Der ischämische Schlaganfall

1.1.1 Epidemiologie

Der Schlaganfall (Synonym: Hirninfarkt, Apoplex, engl. stroke) stellt eine sozioökonomisch bedeutsame, zerebrovaskuläre Erkrankung dar und ist weltweit die dritthäufigste Todesursache. Er ist zugleich der häufigste Grund für erworbene Behinderungen im Erwachsenenalter und erfordert des Öfteren eine langfristige rehabilitative Behandlung. Die mit dem Auftreten eines Schlaganfalls verbundenen Risikofaktoren wie Bluthochdruck und Diabetes mellitus nehmen mit steigendem Alter zu. Somit ist im Hinblick auf die demografische Entwicklung in den nächsten Jahrzehnten ein deutlicher Anstieg der Schlaganfall-Inzidenz zu erwarten. Dank verbesserter medizinischer Versorgung überleben immer mehr Patienten einen Schlaganfall; dem stehen steigende Gesundheitskosten für rehabilitative Nachbehandlung, Pflege und Berufsunfähigkeit gegenüber, die sich in Deutschland auf bis zu 7,1 Milliarden Euro pro Jahr belaufen (1).

1.1.2 Pathogenese und Klinische Symptomatik

Die den Schlaganfall verursachenden Durchblutungsstörungen lassen sich auf ischämische Verschlüsse (87%; ischämischer Infarkt), intrazerebrale Blutungen (10%; hämorrhagischer Infarkt) und Subarachnoidalblutungen (3%) zurückführen (2). Diese Arbeit befasst sich ausschließlich mit dem ischämischen Schlaganfall, bei dem es aufgrund einer Verengung oder eines Verschlusses von zerebralen Blutgefäßen zur Ischämie des Versorgungsgebietes kommt. Der lokale, transiente oder permanente Verschluss kann durch ein Blutgerinnsel aus dem Herzen (kardiale Embolien), Erkrankungen kleiner zerebraler Blutgefäße (Mikroangiopathien) oder auch Stenosen großer, zuführender Blutgefäße verursacht werden (3). Die daraus resultierende Minderdurchblutung des Gehirns und Unterversorgung mit Glukose und Sauerstoff führt zu einem Zusammenbruch des Funktions- und Erhaltungsstoffwechsels in dem betroffenen Hirnareal. Als Konsequenz können Symptome wie leichte sensible Missempfindungen, Sprachstörungen, Gesichtsfeldausfälle und Halbseitenlähmung auftreten und bei schwerem Ausmaß bis hin zu Koma und Tod führen. Sowohl die Lokalisation und Dauer der Ischämie als auch die Ersatzversorgung durch umliegende Kollateralgefäße bestimmen die Ausprägung der klinischen Symptome.

1.1.3 Pathophysiologie

1.1.3.1 Exzitotoxizität

Nach einem ischämischen Hirninfarkt wird das Ausmaß der Gewebeschädigung durch das Zusammenspiel komplexer pathophysiologischer Mechanismen beeinflusst. In der akuten ischämischen Phase führt die Minderdurchblutung der betroffenen Hirnareale bereits nach wenigen Minuten zu einer Unterversorgung der Zellen mit Glukose und Sauerstoff und damit zu einem Mangel an energiereichem Adenosintriphosphat in den Zellen. Infolgedessen fallen die Funktionen der energieabhängigen neuronalen Ionenpumpen in den Zellmembranen reversibel aus. Es kommt zum unkontrollierten Ionenaustausch. Durch die Verschiebung der Ionengradienten dringt zunehmend Wasser in die Zelle ein, und es bildet sich ein hyperosmotisches, zytotoxisches Ödem aus. Darüber hinaus bewirkt der zytosolische Kalziumanstieg eine mitochondriale Freisetzung membranschädigender Sauerstoffradikale sowie eine massive Ausschüttung des exzitatorischen Neurotransmitters Glutamat. Extrazelluläres Glutamat aktiviert glutamatabhängige Kalziumkanäle der postsynaptischen Membran und führt zu einem weiteren exzessiven Kalziumeinstrom in die Zelle (Exzitotoxizität) (4). Dieser resultiert in einer Aktivierung verschiedener intrazellulärer Enzyme wie Calpain, Stickstoffmonoxidsynthethasen, Phospholipasen, Endonukleasen sowie Caspasen, welche im Wesentlichen in ihrer Funktion den programmierten Zelluntergang (Apoptose) induzieren (5). Der anhaltende Energiemangel der Zelle leitet zudem kurzzeitig die anaerobe Metabolisierung ein und führt mit der Bildung von saurem Laktat zur metabolischen Azidose.

Die beschriebenen molekularen und zellulären Mechanismen treten zunächst lokal und irreversibel am Ursprungsort der Minderdurchblutung auf und bilden dort den Infarktkern aus. Im subakuten Verlauf der Ischämie können diese Kaskaden jedoch auf das umgebende Randgebiet (Penumbra) übergreifen und folglich den ischämischen Gewebeschaden ausweiten. Obwohl die Funktionen in diesem Bereich durch die Versorgung der Kollateralgefäße zum Teil aufrecht erhalten werden, können die extrazellulären, toxischen Ansammlungen von Kalium und exzitatorischen Aminosäuren spontane Depolarisationen im Infarktrand initiieren. Im Gegensatz zu denen im Infarktkern sind diese jedoch reversibel und stellen somit im Rahmen der Neuroprotektion einen therapeutischen Angriffspunkt dar (6).

1.1.3.2 Bedeutung der Immunantwort nach Schlaganfall

Nach einer lokalen Zellschädigung kommt es wie auch in anderen Organen zu einer Entzündungsreaktion. Initial setzen ischämische Neurone Schaden-assoziierte molekulare

Strukturen (engl. damage associated molecular patterns, DAMPs) frei. Diese DAMPs induzieren die umliegende residente Mikroglia oder Astrozyten zur Synthese und Freisetzung pro-inflammatorischer Signalmoleküle wie Interleukin (IL) 1β oder Tumornekrosefaktor-α (TNF-α). Diese Mediatoren erhöhen die Expression von Adhäsionsmolekülen (engl. *Intercellular Adhesion Molecule* 1, ICAM-1; P-Selektine; E-Selektine) an der Zelloberfläche des umliegenden Endothels und erleichtern somit das Einwandern von peripheren Leukozyten aus dem Blut in das Hirnparenchym. Nach dem Zusammenbruch der Blut-Hirn-Schranke kommt es zu einer Infiltration von neutrophilen Granulozyten, Makrophagen und schließlich T- sowie B-Lymphozyten. Die durch die Leukozyteninfiltration bedingte sekundäre Entzündungswelle kann ein Infarktwachstum zur Folge haben (4;7).

Neben der lokalen, sterilen Entzündungsreaktion im Hirnparenchym tritt bei den betroffenen Schlaganfallpatienten oft eine lang anhaltende systemische Immundepression auf, die zu schweren bis hin zu tödlichen Infektionen führen kann (8). Die Herabsetzung der systemischen Immunantwort nach Schlaganfall wird vor allem durch die Aktivierung der Hypothalamus-Hypophysen-Achse und des sympathischen Nervensystems eingeleitet. Diese Aktivierung von nervalen als auch neurohumoralen Efferenzen bewirkt eine massive Apoptose von Immunzellen in der Peripherie, welche sich in einer Leukozytopenie im Blut als auch in einer Atrophie der sekundären lymphatischen Organe, wie Milz und Lymphknoten, äußert (8-10). Darüber hinaus wird über den parasympathischen, cholinergen Signalweg des Nervus vagus die Sekretion pro-inflammatorischer Zytokine in Gewebsmakrophagen unterdrückt und somit ein anti-inflammatorisches Milieu eingestellt (11;12). Das Ausmaß der systemischen Immundepression und der damit einhergehenden Infektionsanfälligkeit ist von der Infarktgröße, von dem klinischen Schweregrad des neurologischen Defizits und dem Alter der Patienten abhängig (11).

1.1.4 Experimenteller Schlaganfall

1.1.4.1 Eigenschaften des Modellsystems und Qualitätsrichtlinien

Der ischämische Schlaganfall wird durch einen transienten oder permanenten Verschluss einer hirnversorgenden Arterie operativ induziert. Dies kann durch intraluminalen Verschluss, transkranielle permanente oder transiente Okklusion einer versorgenden Hirnarterie (bspw. engl. middle cerebral artery occlusion, MCAO), Induktion einer Thromboembolie oder eines photo-induzierten Verschlusses (bspw. Photothrombose) im Bereich der Arteria cerebri media erfolgen (13). In der Schlaganfallforschung werden vorrangig Ratten oder Mäuse eingesetzt, da es in diesen Kleintiermodellen bereits umfassende Kenntnisse über den Ablauf von pathophysiologischen Mechanismen gibt.

Die Anforderungen an das gewählte Modell sind eine einfache Durchführbarkeit, eine Reproduzierbarkeit der Läsion und die entsprechende Vergleichbarkeit zum klinischen Bild des Schlaganfalls.
Um eine effiziente Translation der präklinischen Ergebnisse in die Klinik gewährleisten zu können, wurden durch Expertenkomitees Qualitätskriterien zur Durchführung von präklinischen Studien erstellt (STAIR – engl. ‚The Stroke Treatment and Academic Roundtable' (14); STEPS – engl. ‚Stem Cell Therapy as an Emerging Paradigm for Stroke' (15); ARRIVE Richtlinien – engl. 'Animals in Research: Reporting In Vivo Experiments' (16)). Im Allgemeinen werden dabei die folgenden Empfehlungen zur Generierung sowie Interpretation von präklinischen Daten gegeben:

- die Verwendung verschiedener Spezies sowie Tiere unterschiedlichen Geschlechts;
- die Verwendung von prämorbiden Tieren unter Berücksichtigung der relevanten Begleiterkrankungen bei Risikopatienten;
- die a priori Bestimmung der notwendigen Tierzahlen (primärer Studienendpunkt) sowie a priori Festlegung von Ein- und Ausschlusskriterien;
- die vollständige Randomisierung und Verblindung der Operationen, Testdurchführungen und Auswertungen;
- das Definieren von multiplen Endpunkten (Verhaltenstests, Infarktentwicklung und histologische Auswertung);
- die Bestimmung einer optimalen Dosis und eines optimalen Transplantationszeitraums;
- die Durchführung von Langzeitexperimenten (Dauer von mindestens einem Monat) sowie die Validierung der Ergebnisse durch mehrere Forschungsgruppen.

1.1.4.2 Präklinisches Schlaganfallmodell dieser Studie

In Hinblick auf den klinisch multimorbiden Schlaganfallpatienten spielt die Wahl des Tiermodells eine entscheidende Rolle. So zeigt die Metaanalyse präklinischer Schlaganfallstudien eine Überschätzung der Therapieeffekte, wenn innerhalb der Studie gesunde anstelle von prämorbiden Tieren verwendet wurden (17). Aus diesem Grund wurde in dieser Studie mit spontan hypertensiven Ratten (SHR) gearbeitet. Diese von Wistar-Kyoto-Tieren abstammenden Ratten entwickeln spontan im Alter von 5-6 Wochen eine Hypertension mit einem systolischem Blutdruck zwischen 180 und 200 mmHg, welcher fortschreitend zur systemischen Schädigung des vaskulären und kardialen Mikrogefäßsystems führt. Weiterhin kennzeichnen SHR das Auftreten einer ausgeprägten Hyperinsulinämie, Hyperlipidämie sowie Hypercholestinämie (18). Neben den hämodynamischen Veränderungen wurden bei diesen Tieren auch immunologische

Einschränkungen der Leukozyten-Endothel-Interaktionen und der T-Lymphozytenfunktionen beschrieben (19).
In dieser Studie wurde an SHRs nach Kraniotomie durch gezielte Thermokoagulation eine permanente Okklusion der mittleren Zerebralarterie erzeugt (20) (genehmigtes Tierversuchsvorhaben, TVV 12/11), dessen Resultat eine kortikale Infarktläsion mit geringer Varianz in Größe waren. Die Effektstärke der Therapie auf das Infarktvolumen wurde mit einem Mittelwertunterschied von 30% festgesetzt und demnach die Versuchsgruppengröße mittels a priori Poweranalyse (α=0.05 and β=0.8) auf 18 Tiere je Gruppe berechnet. Basierend auf Vorexperimenten wurde die zu erwartende Varianz der Infarktvolumina von σ=3.2 %HLVe, (21) für die Berechnung angenommen. Die Datenerhebung und Datenanalyse wurde randomisiert sowie verblindet durchgeführt. Als Ausschlusskriterien wurden ein Gewichtsverlust von 20% oder mehr, das Fehlen einer kortikalen, ischämischen Läsion (Bildgebung) sowie eine unvollständige Therapie festgelegt.

1.2 Therapieverfahren zur Behandlung des Schlaganfalls

Trotz intensiver Untersuchungen der experimentellen und klinischen Schlaganfallforschung in den letzten Jahrzehnten existiert bis heute nur eine Therapiemöglichkeit, die auf der intravenösen Auflösung des Schlaganfall verursachenden Blutgerinnsels mit gewebsspezifischem Plasminogenaktivator (rt-PA) basiert (22). Das Zeitfenster für diese Behandlung nach einem akuten ischämischen Schlaganfall beträgt nur maximal viereinhalb Stunden, und weitere Ausschlusskriterien führen dazu, dass nur ca. 15% aller Schlaganfallpatienten kausal therapiert werden können (23). Neben der Lysetherapie wurden in der klinischen Routine mit der Einführung sogenannter „Stroke Units“ zusätzlich neurologische Stationen errichtet, welche sich auf die schnellstmögliche intensivmedizinische und interdisziplinäre Akutbehandlung von Schlaganfallpatienten sowie deren Rehabilitation spezialisiert haben.
In verschiedenen tierexperimentellen Studien konnten die nach Schlaganfall auftretenden pathophysiologischen Prozesse durch die Anwendung neuroprotektiver Medikamente gezielt moduliert werden. Dennoch ist es bis heute nicht gelungen, eine der in der Präklinik getesteten neuroprotektiven Substanzen in die klinische Routine zu überführen (24-26). So zum Beispiel konnten die protektiven Eigenschaften des Radikalfängers NXY-059 in fünf verschiedenen Tiermodellen des experimentellen Schlaganfalls evaluiert, jedoch letztendlich im Rahmen der klinischen Phase-III-Studie nicht bestätigt werden (27). Die Diskrepanz in der Translation der präklinisch erfolgreich getesteten Substanzen in die Klinik ist vordergründig in der komplexen sowie heterogenen klinischen Pathologie des Schlaganfalls zu suchen (28). Darüber hinaus wurde durch die bevorzugte Publikation von

Positivergebnissen eine statistisch verzerrte Datenlage der Präklinik dargelegt (25;29). Dennoch besteht ein großes Interesse, neue Therapiekonzepte zu entwickeln, die eine kausale Behandlung jenseits der bisher bestehenden Einschränkungen erlauben. Sowohl die Zelltherapie als auch der stammzellmobilisierende hämatopoetische Wachstumsfaktor G-CSF (engl. *granulocyte-colony stimulating factor*, Granulozyten-Kolonie stimulierende Faktor) zeigten in zahlreichen experimentellen Schlaganfallstudien ein vielfältiges neuroprotektives und –regeneratives sowie immunmodulatorisches Wirkungsspektrum auf (30-32).

1.2.1 Granulozyten-Kolonie stimulierender Faktor

Der Granulozyten-Kolonie stimulierende Faktor (G-CSF) ist ein aus 207 Aminosäuren bestehendes 19,6kDa großes hydrophobes Glykoprotein (33). Das humane G-CSF Molekül wurde bereits vor 25 Jahren charakterisiert und zeigt eine hohe Kreuzreaktivität zur murinen Spezies (34). G-CSF gehört zur Gruppe der hämatopoetischen Wachstumsfaktoren, welche im Organismus das Wachstum und die Reifung von Blutzellen regulieren. Das Zytokin wird bei Entzündungsreaktionen (35) vor allem von Immunzellen (36), mesenchymalen (37) oder endothelialen Zellen (38) sekretiert. Als hämatopoetischer Wachstumsfaktor reguliert G-CSF die Reifung, die Proliferation sowie das Überleben myeloider Zellen (39) und verbessert deren phagozytierenden sowie bakteriziden Eigenschaften (40;41). Aufgrund der stammzellmobilisierenden Eigenschaften (42) wird G-CSF bereits seit vielen Jahren klinisch für die Behandlung der Neutropenie nach Chemotherapie als auch im Rahmen von Knochenmarktransplantationen präventiv und therapeutisch eingesetzt (43). Darüber hinaus besitzt G-CSF immunmodulierende Eigenschaften (44). So konnte nach G-CSF-Behandlung eine verminderte Ausschüttung pro-inflammatorischer und eine erhöhte Freisetzung anti-inflammatorischer Zytokine beobachtet werden (45-47).

Die Wirkungsweise von G-CSF basiert auf der Interaktion mit seinem hoch-affinen G-CSF-Rezeptor (G-CSFR; CD114) (48) welcher vor allem auf myeloiden Vorläuferzellen sowie reifen Granulozyten und Monozyten vorkommt (49). Darüber hinaus konnte dieser Transmembranrezeptor sowohl Thrombozyten (50), Lymphozyten (51), Endothelialzellen (52) als auch Neuronen (53) nachgewiesen werden, wobei seine Expression durch seinen Liganden G-CSF selbst reguliert wird (54). Die Expressionsdichte des Rezeptors auf Neutrophilen ist sehr gering und lässt daher vermuten, dass eine Aktivierung von nur wenigen Rezeptormolekülen durch G-CSF schon eine massive biologische Antwort induziert. Kommt es zur Bindung von G-CSF an seinen Rezeptor, so wird intrazellulär über die Aktivierung diverser Kinasen und Transkriptionsfaktoren eine komplexe Signalkaskade ausgelöst, welche in der Expression verschiedenster Gene für Proliferation

oder Reifung resultiert (49). Unter anderem zeigen die Ergebnisse einer Mikroarraystudie, dass Gene für die Neutrophilenaktivierung vermehrt transkribiert werden, wohingegen Gene, welche mit der Immunantwort in Verbindung stehen, wie beispielweise für den T-Zell Rezeptor oder HLA-Komplex kodierende Gene, herunterreguliert sind (55).

1.2.1.1 Neuroprotektive und -regenerative Wirkungsweise des G-CSF

Die therapeutische Wirkung von G-CSF zur Behandlung der zerebralen Ischämie wurden erstmals vor über 10 Jahren experimentell im murinen Schlaganfallmodell beschrieben (56). Die Therapie mit G-CSF führte zu einem signifikant verringerten Infarktvolumen. Nachfolgende präklinische Studien im transienten Schlaganfallmodell bestätigten diese Effekte mit einer durchschnittlichen Reduktion des Infarktvolumens von bis zu 40% sowie einer Verbesserung der neurologischen Defizite um 24-40% (31;32). Arbeiten mit G-CSF-defizienten Knockout-Mäusen zeigten außerdem einen Anstieg des Infarktvolumens, welchem mit substituiertem G-CSF entgegen gewirkt werden konnte (57). Als Wirkungsmechanismus wird zum einen eine Geweberegeneration durch G-CSF-mobilisierte Knochenmarkzellen angenommen, zum anderen kann G-CSF die Blut-Hirn-Schranke passieren (53) und somit direkte zelluläre Schutzmechanismen induzieren. Interessanterweise wurde der G-CSF-Rezeptor hauptsächlich auf Neuronen im Cortex, Hippocampus, der Subventrikulären Zone (SVZ) als auch im Cerebellum bestimmt und in Folge des Schlaganfalls konnte ein Anstieg der endogenen, neuronalen G-CSF-Synthese als eine Art intrinsische Stressantwort beobachtet werden (53;58).

Die anti-apoptotischen Eigenschaften des G-CSF wurden zum ersten Mal in *in vitro* Kulturen von zerebellären Körnerzellen nach glutamatinduzierter Exzitotoxizität nachgewiesen (59). Weitere Studien belegten diese Effekte und verzeichneten die Aktivierung anti-apoptotischer Signalkaskaden sowie eine erhöhte Transkription der Bcl-2 Proteinfamilie (engl. *B-cell lymphoma 2*) welche mit der Regulation des programmierten Zelltodes in Verbindung stehen (53;60). Beispielsweise führte die G-CSF-Behandlung in einem transienten Schlaganfallmodell der Ratte zu einem Anstieg des Apoptose inhibierenden Proteins cIAP2 (engl. *cellular inhibitor of apoptosis*) und folglich zu einer Abnahme der Caspase-3-Enzymaktivität (61).

In weiteren *in vitro* Studien wurde der funktionelle Einfluss von G-CSF auf die neuronale Differenzierung von adulten neuralen Vorläuferzellen demonstriert. Dabei erhöhte G-CSF die Expression neuronaler Marker wie β-III Tubulin und neuronenspezifische Enolase, wohingegen die Expression glialer Marker wie dem sauren Gliafaserprotein GFAP (engl. *Glial fibrillary acidic protein*) und dem Proteolipid-Protein nicht reguliert war (53). Des Weiteren konnte für G-CSF eine Neurogenese fördernde Wirkung beobachtet werden. Nach einer Ischämie kommt es im Gyrus dentatus des Hippokampus sowie in der SVZ

der ischämischen und nicht-ischämischen Hemisphäre zu einer Neubildung von neuralen Vorläuferzellen. Nach G-CSF-Therapie wurden sowohl im Gyrus dentatus als auch im Randgebiet der ischämischen Läsion eine erhöhte Anzahl proliferierender Vorläuferzellen nachgewiesen (53). G-CSF scheint außerdem die Gefäßneubildung zu stimulieren. So konnte nach Schlaganfall durch die G-CSF-Therapie sowohl eine erhöhte Proliferation von endothelialen Zellen im Infarktrand als auch ein Anstieg der Gefäßverzweigung und -länge registriert werden. Die erhöhte Expression der Angiogenesemarker Angiopoetin 2 und endothelialen Stickstoffmonooxidsynthetase bestätigte diese Resultate (62;63).
Aufgrund der vielversprechenden präklinischen Ergebnisse wurde die Effektivität von G-CSF in einer multizentrischen klinischen Phase-II-Studie (Axis-2) an 328 Schlaganfallpatienten eingehend untersucht (64). Diese zeigte jedoch keine statistisch relevanten funktionellen Verbesserungen zwischen der G-CSF- und placebobehandelten Patientengruppe. Die Diskrepanz in der Translation der vielversprechenden präklinischen Vordaten wurde mit der variablen Pathologie des Schlaganfalls innerhalb der Patientengruppe, sowie mit der im Vergleich zur Präklinik höheren Dosis an G-CSF (135µg G-CSF/kg Körpergewicht gegenüber 50µg G-CSF/kg Körpergewicht) als auch der geringen Behandlungsdauer von 3 Tagen begründet.

1.2.1.2 Immunmodulierende Wirkungsweise von G-CSF nach Schlaganfall

In der Anwendung beim Schlaganfall verändert G-CSF als hämatopoetisches Wachstumshormon auch immunologische Parameter. Zum einen bewirkt die G-CSF-Therapie eine massive Leukozytose, welche hauptsächlich in einer Akkumulation von Granulozyten (PMN, engl. *polymorphonuclear leukocytes*) resultiert. Es ist jedoch umstritten, ob diese G-CSF-vermittelte Neutrophilie eine erhöhte Leukozyteninfiltration ins Hirngewebe und somit eine verstärkte postischämische Entzündungsreaktion zur Folge hat. Taguchi et al. konnte nach G-CSF-Behandlung eine vermehrte Infiltration myeloider Zellen ins Infarktgewebe detektieren (63), andere Arbeiten widerlegten jedoch diese Ergebnisse (62). Des Weiteren wurde gezeigt, dass G-CSF die Expression der Matrix-Metalloproteinase 9 supprimiert (57), welche nachweislich zu Blut-Hirn-Schranken-Störungen, Ödembildung und Zelluntergang führt (65;66). Während der Ischämie senden ischämische Neurone, aktivierte Mikroglia oder Astrozyten pro-inflammatorische Signalmoleküle wie IL1-β oder TNF-α aus, welche eine Entzündungsreaktion induzieren. G-CSF kann die Expression dieser pro-inflammatorischen Zytokine reduzieren und hierdurch neuroprotektive Effekte vermitteln (61;67). In einer aktuellen Studie werden die immunmodulatorischen Effekte einer präklinischen Niedrig- und einer klinischen Hochdosis an G-CSF im Vergleich zu unbehandelten Schlaganfalltieren dargestellt (68).

Diese Studie zeigte, dass beide Dosen die Sekretion des pro-inflammatorischen IL-6 im Serum reduzierten. Im Gegensatz dazu erhöhte die 24-stündige Gabe einer G-CSF-Hochdosis die Frequenz an Interferon-γ produzierenden Th1 Lymphozyten in der Milz und bewirkt darüber hinaus eine vermehrte Infiltration von T-Lymphozyten, Makrophagen als inflammatorischen Monozyten ins ischämische Hirngewebe.

G-CSF besitzt somit vielseitige Wirkungsansätze. Es steuert nicht nur das Wachstum, die Reifung und die Mobilisation von potenziell regenerativen Knochenmarkzellen, sondern weist sowohl lokale neuroprotektive als auch neuroregenerative Wirkungsmechanismen nach einer Ischämie auf.

1.2.2 Mononukleäre Zelltherapie beim Schlaganfall

In Hinblick auf das enge Zeitfenster der Neuroprotektion und der häufig verspäteten Diagnose und Behandlungsmöglichkeit der Schlaganfallpatienten gewinnen zelltherapeutische Ansätze zunehmend an Bedeutung. Die Wirkungsweise der Zelltherapie erstreckt sich über die Inhibierung des apoptotischen oder nekrotischen Zellsterbens (69;70), den Wiederaufbau eines nährstoffversorgenden Gefäßsystems (71-73), die Förderung der neuronalen Plastizität (74;75), die Unterstützung der endogenen Neubildung von neuralen Zellen (76) bis hin zum lokalen Gewebeersatz durch Einwanderung der Zellen ins ischämische Gewebe. Des Weiteren wurden für Zelltransplantate immunmodulierende Effekte nachgewiesen, indem sie beispielsweise die inflammatorische Reaktion der Milz unterbinden und somit lokale Entzündungsreaktionen im geschädigten Hirngewebe vermindern.
Insbesondere mononukleäre Zellen des Knochenmarks (BM MNC, engl. *bone marrow mononuclear cells*) stellen als heterogenes Zellgemisch aus reifenden Immunzellen (v.a. B-Lymphozyten, T-Lymphozyten, Monozyten) sowie hämatopoetischen, endothelialen und mesenchymalen Stammzellen ein vielversprechendes Zelltransplantat dar. Im Vergleich zu mesenchymalen oder hämatopoetischen Stammzelltransplantaten ist die Konzentration an Vorläuferzellen in der Zellfraktion der BM MNC sehr gering. Dennoch weisen BM MNC mit variablen Anteilen verschiedener Immun- und Vorläuferzellen möglicherweise ein umfassenderes Wirkungsspektrum auf als homogene Stammzelltransplantate. So bewirkte die mononukleäre Zelltherapie in der akuten oder subakuten Phase nach Schlaganfall eine Reduktion des Infarktvolumens, eine verminderte Aktivierung der residenten Mikrogliazellen sowie eine Verbesserung motorischer Funktionen (siehe Tabelle 1, (77-81)). Als zugrunde liegender neuroprotektiver Mechanismus wird die Ausschüttung trophischer Faktoren angenommen welche sich mildernd auf die postischämische Entzündungsreaktion auswirken und so den

neuralen Gewebeschaden eingrenzen (80;82;83). Diese Effekte wurden vorrangig in Tieren ohne Vorerkrankungen mit einem therapeutischen Zeitfenster zwischen 3h und 24h ermittelt (77;79;80). Dagegen konnte eine aktuelle Studie in einem prämorbiden Schlaganfallmodell der Ratte trotz frühzeitiger BM MNC-Transplantation mit vergleichbaren Zelldosen weder eine Reduktion des Infarktvolumens noch eine verminderte Entzündungsreaktion im Hirnparenchym nachweisen (84).

Als neuroregenerative Effekte nach BM MNC-Transplantationen sind die Förderung der Neurogenese und der neuronalen Plastizität, der Wiederaufbau eines nährstoffversorgenden Gefäßsystems sowie immunmodulierende Funktionen beschrieben (81;85). In der Literatur gibt es nur wenige Anhaltspunkte für einen lokalen Gewebeersatz durch mononukleäre Zelltransplantate, so wird deren neurale Differenzierung und Integration ins geschädigte Hirngewebe kontrovers diskutiert (86;87). Stattdessen wurde nach intraarterieller oder intravenöser BM MNC-Injektion eine Migration und Akkumulation der BM MNC in Leber-, Nieren-, Lungen- und Milzgewebe beobachtet (88-90), welche auf eine immunmodulierende Wirkungsweise der Zellen schließen lassen.

Die Zelltherapie mit mononukleären Knochenmarkzellen bietet die Möglichkeit einer autologen Therapie ohne den Einsatz von Immunsuppressiva. Ein weiterer Vorteil des BM MNC-Transplantates ist die unkomplizierte Entnahme und Aufarbeitung innerhalb weniger Stunden. Die Isolation ohne aufwendige Kultivierungsschritte bewahrt das physiologische Zellvolumen und ermöglicht so die uneingeschränkte Zirkulation des Transplantates zum Wirkungsort (88). BM MNC werden aseptisch mittels standardisierter Dichtegradienten-zentrifugation (DGZ) schnell und sicher angereichert und können sowohl kryokonserviert gelagert als auch umgehend therapeutisch eingesetzt werden. Bereits in den 80er Jahren wurde diese Isolationsmethode für die klinische Anwendung zur Behandlung von Leukämien zugelassen und ist im Rahmen einer offenen klinischen Studie für die Schlaganfalltherapie als sicher und zulässig befunden worden (91). Dennoch gehen mit dieser Aufreinigungsmethode ein hoher Verlust an Vorläuferzellen und eine geringere Zellausbeute einher (92;93). Darüber hinaus können die verwendeten Separationsmedien zytotoxisch wirken.

Tab.1: Übersicht über präklinische Schlaganfallstudien mit BM MNC Therapie

Literatur	Modell	BM MNC-Transplantat		BM MNC-Transplantation			Primäre Endpunkte	Spezies/Stamm
		Gewinnung	Charakterisierung	Zeitpunkt	Dosis	Route		
Iihoshi et al., 2004 (77)	tMCAO, 45min	autolog, Ficoll DGZ	nein	3h, 6h, 12h, 24h, 72h	$1x10^7$	iv	Infarktvolumen, funktionelle Verhaltensanalyse, Biodistribution	Ratten/Spraque Dawley
Kamiya et al., 2008 (78)	tMCAO, 90min	autolog, Ficoll DGZ	nein	nach Reperfusion	$1x10^7$	ia, iv	Infarktvolumen, funktionelle Verhaltensanalyse, Biodistribution	Ratten/Spraque Dawley
Giraldi-Guimardes et al., 2009 (79)	pMCAO	syngen, Ficoll DGZ	nein	24h	$3x10^7$	iv	funktionelle Verhaltensanalyse	Ratten/Wistar Kyoto
Minnerup et al., 2010 (94)	Photo-thrombose	xenogen, Ficoll DGZ	nein	3d	$5x10^6$	ia	funktionelle Verhaltensanalyse	Ratten/Wistar Kyoto
Nakano-Doi et al., 2010 (81)	pMCAO	allogen, Ficoll DGZ	ja	2d	$1x10^6$	iv	Verbesserung der Angio- und Neurogenese	Mäuse/SCID
Brenneman et al., 2010 (80)	tCCA+tMCAO 180min	autolog, Ficoll DGZ	ja	1h, 3h, 6h, 12h, 24h, 72h, 7d	$4x10^7$	ia	Infarktvolumen, funktionelle Verhaltensanalyse, Biodistribution	Ratten/Long Evans
Yang et al., 2011 (95)	tCCA+tMCAO 180min	autolog, Ficoll DGZ	nein	24h	$1x10^6$/kg, $1x10^7$/kg, $3x10^7$/kg	iv	Infarktvolumen, funktionelle Verhaltensanalyse, Biodistribution	Ratten/Long Evans
Wagner et al., 2012 (83)	pMCAO	xenogen, Ficoll DGZ	ja	24h	$8x10^6$/kg	iv	funktionelle Verhaltensanalyse, Infarktvolumen	Ratten/SHR
Yang et al., 2012 (96)	tMCAO, 90min	autolog, Ficoll DGZ	ja	24h	$1x10^7$	ia	Infarktvolumen, funktionelle Verhaltensanalyse, Biodistribution	Ratten/Long Evans
Yang et al., 2013 (90)	tMCAO, 90min	autolog, Ficoll DGZ	nein	24h	$1x10^6$/kg, $3x10^7$/kg	ia, iv	Infarktvolumen, funktionelle Verhaltensanalyse, Biodistribution	Ratten/Long Evans
Minnerup et al., 2014 (84)	tMCAO, 60min	syngen, MACS	nein	3h	$1x10^6$, $5x10^6$, $2x10^7$	iv	Infarktvolumen, funktionelle Verhaltensanalyse, Biodistribution	Ratten/SHR

1.2.3 Kombinatorische Therapieansätze beim Schlaganfall

In Hinblick auf die komplexen pathophysiologischen Vorgänge nach einem Schlaganfall stellt die Kombination aus mehreren therapeutisch wirksamen Kandidaten einen interessanten Ansatzpunkt dar. Eine aktuelle Metaanalyse zeigt, dass Kombinationstherapien sowohl die Effizienz der Einzeltherapie verstärken als auch das therapeutische Zeitfenster erweitern können (24;97). So konnte beispielsweise das Zeitfenster der Thrombolyse durch eine zusätzliche Behandlung von 4,5h auf 8h ausgedehnt werden und die Reduktion der Infarktvolumen in kombinatorischen Therapieansätzen von 20% auf 38% erhöht werden. Angesichts der Multimorbidität der Schlaganfallpatienten kommt es in der Klinik schon jetzt zur Anwendung verschiedener medikamentöser Therapien. Da die Kombination mehrerer Therapien auch schädigende Wechselwirkungen aufweisen oder sogar eine Aufhebung der Therapieeffekte zur Folge haben kann, besteht die dringende Notwendigkeit, kombinatorische Therapieansätze präklinisch zu testen.

Die Kombinationstherapie aus G-CSF und mononukleären Knochenmarkzellen könnte eine innovative Therapieoption darstellen. Sowohl G-CSF als auch die mononukleäre Zelltherapie zeigten in experimentellen Schlaganfallstudien vielfältige und insbesondere identische Wirkungsmechanismen. Sie können sowohl das apoptotische Zellsterben nach Ischämie vermindern, die Neurogenese als auch die Gefäßneubildung erhöhen sowie die Immunantwort nach Schlaganfall beeinflussen. Als hämatopoetischer Wachstumsfaktor ist G-CSF darüber hinaus für die Mobilisation von Knochenmarkzellen verantwortlich. Die G-CSF-abhängige Freisetzung der Knochenmarkzellen wird unter anderem durch die Unterbrechung der SDF-1/CXCR-4-Achse vermittelt, welche jedoch nach Schlaganfall zeitverzögert stattfindet (98). Eine zusätzliche frühzeitige Transplantation von mononukleären Knochenmarkzellen stellt somit eine synergistische Therapieoption zur Behandlung des Schlaganfalls dar.

1.3 Zielstellung dieser Arbeit

Das primäre Ziel dieser Arbeit ist die Prüfung der therapeutischen Wirksamkeit einer Kombinationstherapie aus G-CSF und mononukleären Knochenmarkzellen in einem präklinischen Schlaganfallmodell. Diese multimodale Therapie setzt sich aus der wiederholten Applikation von G-CSF sowie einer einmaligen mononukleären Zelltherapie nach 6h oder 48h nach Schlaganfall zusammen. Die Effizienz der Kombinationstherapie wird im Vergleich zu unbehandelten Schlaganfalltieren oder Schlaganfalltieren mit alleiniger G-CSF-Therapie bewertet.

Die Studie wurde unter Anwendung empfohlener Qualitätskriterien für präklinische Schlaganfallstudien durchgeführt. Diese Vorgaben schlossen die detaillierte Charakterisierung des verwendeten Zellproduktes, die Verwendung von prämorbiden Versuchstieren, eine Langzeituntersuchung mit funktionell aussagekräftigen Tests, die a priori Definition von Ausschlusskriterien, eine verblindete und randomisierte Durchführung sowie die Verwendung von multiplen Studienendpunkten ein.
Der Zustand des Zelltransplantates stellt ein wichtiges Qualitätskriterium der Studie dar. Es wird zu Beginn die Etablierung einer reproduzierbaren Methode zur Isolation von mononukleären Knochenmarkzellen aus der Ratte beschrieben und deren Vergleich mit standardisierten Aufreinigungsmethoden über Dichtegradientenzentrifugation dargestellt (Kapitel 2.1: Density Gradient Centrifugation Compromises Bone Marrow Mononuclear Cell Yield; Pösel et al., PLoS One 2012). Die detaillierte Charakterisierung des Zelltransplantates während des Isolationsprozesses sowie vor der Applikation ist von hoher Relevanz für diese Studie.

Im Anschluss wird unter Verwendung eines prämorbiden Rattenstamms (SHR) der Einfluss der Kombinationstherapie auf die Studienendpunkte Infarktwachstum sowie sensomotorische Defizite untersucht. Zusätzliche Analysen geben Aussage über den Wirkungsmechanismus der Therapie und zeigen potenzielle Wechselwirkungen auf (Kapitel 2.2: Bone marrow cell transplantation time-dependently abolishes efficacy of G-CSF after stroke in hypertensive rats; Pösel et al., Stroke 2014).

Aus der Zielstellung ergaben sich folgende Fragen:

1. Welchen Einfluss hat die Aufreinigungsmethode auf das Zelltransplantat? In welcher Zusammensetzung und Vitalität steht das mononukleäre Zelltransplantat für die multimodale Therapie zur Verfügung?

2. Können die vielversprechenden neuroprotektiven und neuroregenerativen Effekte von G-CSF auch in einer prämorbiden Ratte nach experimentellem Schlaganfall nachgewiesen werden? Welche zusätzliche Wirkung ist durch die wiederholte G-CSF-Behandlung zu beobachten?

3. Wie wirkt sich die zusätzliche Zelltherapie 6h oder 48h nach Schlaganfall auf die Studienendpunkte aus? Welche Wechselwirkungen können innerhalb der Kombinationstherapie beobachtet werden?

2 Publikationen

2.1 Density Gradient Centrifugation Compromises Bone Marrow Mononuclear Cell Yield

Titel: Density Gradient Centrifugation Compromises Bone Marrow Mononuclear Cell Yield

Autoren: Claudia Pösel*, Karoline Möller*, Wenke Fröhlich, Isabell Schulz, Johannes Boltze*, Daniel-Christoph Wagner*
* geteilte Autorenschaft

eingereicht am: 26.04.2012

akzeptiert am: 22.10.2012

Veröffentlichung: PLoS One 2012;7(12)
online seit 06.12.2012
doi: 10.1371/journal.pone.0050293

OPEN ACCESS Freely available online

PLOS ONE

Density Gradient Centrifugation Compromises Bone Marrow Mononuclear Cell Yield

Claudia Pösel[1*☯], Karoline Möller[1☯], Wenke Fröhlich[1,2], Isabell Schulz[1], Johannes Boltze[1,2☯], Daniel-Christoph Wagner[1,2☯]

1 Fraunhofer Institute for Cell Therapy and Immunology, Leipzig, Germany, **2** Translational Centre for Regenerative Medicine, Leipzig, Germany

Abstract

Bone marrow mononuclear cells (BMNCs) are widely used in regenerative medicine, but recent data suggests that the isolation of BMNCs by commonly used Ficoll-Paque density gradient centrifugation (DGC) causes significant cell loss and influences graft function. The objective of this study was to determine in an animal study whether and how Ficoll-Paque DGC affects the yield and composition of BMNCs compared to alternative isolation methods such as adjusted Percoll DGC or immunomagnetic separation of polymorphonuclear cells (PMNs). Each isolation procedure was confounded by a significant loss of BMNCs that was maximal after Ficoll-Paque DGC, moderate after adjusted Percoll DGC and least after immunomagnetic PMN depletion (25.6±5.8%, 51.5±2.3 and 72.3±6.7% recovery of total BMNCs in lysed bone marrow). Interestingly, proportions of BMNC subpopulations resembled those of lysed bone marrow indicating symmetric BMNC loss independent from the isolation protocol. Hematopoietic stem cell (HSC) content, determined by colony-forming units for granulocytes-macrophages (CFU-GM), was significantly reduced after Ficoll-Paque DGC compared to Percoll DGC and immunomagnetic PMN depletion. Finally, in a proof-of-concept study, we successfully applied the protocol for BMNC isolation by immunodepletion to fresh human bone marrow aspirates. Our findings indicate that the common method to isolate BMNCs in both preclinical and clinical research can be considerably improved by replacing Ficoll-Paque DGC with adapted Percoll DGC, or particularly by immunodepletion of PMNs.

Citation: Pösel C, Möller K, Fröhlich W, Schulz I, Boltze J, et al. (2012) Density Gradient Centrifugation Compromises Bone Marrow Mononuclear Cell Yield. PLoS ONE 7(12): e50293. doi:10.1371/journal.pone.0050293

Editor: Beatriz Pelacho, Foundation for Applied Medical research, Spain

Received April 26, 2012; **Accepted** October 22, 2012; **Published** December 6, 2012

Funding: This work was supported by the German Federal Ministry of Education and Research (BMBF), http://www.bmbf.de/en/index.php, grant number 01GN0981. The funders had no role in study design, data collection and analysis, decision to publish, or preparation of the manuscript.

Competing Interests: The authors have declared that no competing interests exist.

* E-mail: claudia.poesel@izi.fraunhofer.de

☯ These authors contributed equally to this work.

Introduction

Bone marrow transplantation was originally established to treat hematological malignancies [1] and is nowadays widely used in different branches of regenerative medicine. The bone marrow is a capable source of autologous cells with distinct regenerative properties, which can be quickly harvested and are thus applicable for both chronic and acute diseases. Preclinical and clinical safety, feasibility and efficacy have been reported, inter alia, for ischemic limb injury [2,3], cerebral ischemia [4,5] and in particular for myocardial infarction [6,7] for which by now more than 30 placebo controlled randomized trials have been accomplished [8].

In the majority of studies, aspirated bone marrow was further processed in order to isolate the mononuclear cell fraction (BMNC), a heterogeneous population containing differentially matured B-cells, T-cells and monocytes, as well as rare progenitor cells such as hematopoietic stem cells (HSC), mesenchymal stromal cells (MSC), endothelial progenitor cells (EPC) and very small embryonic-like cells (VSEL). It has been constantly described that this cell mixture promotes distinct angiogenic properties [2], mediates vascular repair, expresses several cytoprotective growth factors and cytokines [9] and restores pathologically altered genes after ischemic heart injury [10]. However, which component or combination of components exactly determines the efficacy of BMNCs is not entirely understood, hence impeding full realization and further advancement of the therapeutic concept [11]. Some groups suggested that conflicting results in large-scale clinical trials [12,13] are, at least to some extent, due to different cell isolation protocols and a subsequently altered BMNC composition [14]. In fact, it has been proven that efficacy and functionality of BMNCs are significantly influenced by red blood cell contamination [15], the content of apoptotic cells [16], different washing steps [14] and even by the centrifugation speed [17].

Another decisive point seems to be the choice of the density gradient medium. Most preclinical and clinical studies used Ficoll-Paque (hereafter indicated as Ficoll) as density medium in order to enrich the mononuclear cell population as well as the rare progenitor cells therein [18]. However, it is a well-known problem that Ficoll-based density gradient centrifugation (DGC) causes a significant reduction of BMNCs to only 15–30% of the initial content [17,19]. This is critical since the efficacy of autologous BMNC transplantation is likely dose-dependent [20], and little data is available on a possible asymmetry of the cell loss [21,22]. Recently, it was described that Ficoll DGC even depleted cells with a high regenerative potential, such as MSC [23] and VSEL [24], and irreversibly impaired cell function by decreasing expression of chemokines receptors [25,26]. Accordingly, the objective of this study was to determine whether and

how Ficoll DGC affects the yield and composition of the cell graft compared to alternative methods such as adjusted Percoll DGC [27] and immunomagnetic bead separation of granulocytes [28]. Our findings indicate that the common method to isolate BMNC in both preclinical and clinical research can be considerably improved by replacing Ficoll with adapted Percoll or preferably by immunodepletion of unwanted constituents of bone marrow.

Methods

Rat Bone Marrow Harvest and Lysis of Erythroid Cells

Animal experiments were conducted according to the Guide for the Care and Use of Laboratory Animals published by the US National Institutes of Health (NIH Publication No. 85-23, revised 1996). Rat bone marrow was obtained from 12-week-old male Sprague-Dawley rats. Femurs and tibiae were aseptically opened and bone marrow was harvested by repeated flushing with phosphate buffered saline (PBS). In order to dissolve remaining cell aggregates, the solution was resuspended using a 20 G cannula and sieved through a 100 μm cell strainer. Erythroid bone marrow cells were lysed by short-term incubation (30 seconds) with hypotonic ammonium chloride buffer (0.155 M NH4Cl, 10 mM KHCO3 and 0.01 mM Na2EDTA) followed by repeated washing steps with PBS containing 3% fetal calf serum (PBS/3% FCS). Viability and cell count were determined by the trypan blue exclusion method using a hemocytometer.

Rat Mononuclear Cell Isolation by Density Gradient Centrifugation

Bone marrow cells from 5 donor rats were separated using Ficoll-Paque 1.084 (which is used to isolate rat mononuclear cells (MNC; GE Healthcare, Munich, Germany) with 3 technical replicates per sample. A total of 10E7 bone marrow cells were resuspended in 10 mL HBSS/3% FCS and carefully layered upon 7.5 mL of Ficoll separation medium. Ficoll gradients were centrifuged for 40 min at 400 g without brake. The bone marrow mononuclear cell (BMNC) layer was then collected, washed in PBS/3% FCS, counted and prepared for flow cytometric analysis.

Next, we aimed to establish an appropriate density gradient for isolating BMNC using Percoll medium (GE Healthcare, Munich, Germany). Concentrated Percoll was diluted in 1.5 M NaCl to an isotonic Percoll stock solution (SIP) with a density of 1.1228 g/mL. We then prepared a series of different separation media (1.071, 1.073, 1.075, 1.077, 1.080 and 1.084 g/mL) by mixing SIP with varying volumes of Hank's balanced salt solution (HBSS) containing 3% FCS. Likewise, an invariant bottom layer was adjusted to 1.095 g/mL. For each of the separation gradients, 10E7 bone marrow cells from two donor rats were resuspended in 5 ml Percoll medium with the highest density (1.095 g/mL). This layer was then carefully covered with 5 ml of the respective lower concentrated Percoll dilutions and finally capped with 5 mL of HBSS/3% FCS. Discontinuous gradients were centrifuged for 40 min at 480 g without brake. After centrifugation, the cell layers located between HBSS/separation medium or in between the two Percoll layers were separately collected and washed twice in PBS/3% FCS. Cells were counted and prepared for flow cytometric analysis. The Percoll medium density leading to the highest BMNC yield along with the lowest polymorphonuclear cells (PMN) contamination (1.080 g/mL) was then chosen for according BMNC isolation from 5 donor rats with 3 technical replicates per sample.

Rat BMNC Isolation by Immunomagnetic Depletion of PMNs

A total of 10E8 bone marrow cells obtained from 6 donor rats (with 3 technical replicates per sample) were incubated with 5 ng/ml phycoerythrin conjugated anti-rat granulocytes antibody (clone RP1; BD Pharmingen, Heidelberg, Germany) for 15 min at 4°C. After washing in cold PBS/0.5% FCS, bone marrow cells were further incubated with 50 μL magnetic anti-phycoerythrin microbeads (Miltenyi Biotech, Bergisch Gladbach, Germany) for 12 min at 4°C. Non-adsorbed microbeads were eliminated by an additional washing step. Finally, bone marrow cells were resuspended in 500 μL PBS/0.5% FCS. Magnetic separation was performed on LD columns using a magnetic QuadroMACS separator according to manufacturer's instructions (Miltenyi Biotech). Both discharge and the fraction that was magnetically trapped were separately collected, counted and prepared for flow cytometry.

Flow Cytometric Characterization of rat BMNCs

Cellular composition of lysed rat bone marrow and separated BMNCs following different isolation protocols were analyzed by flow cytometry. For labelling, 2.5×10E5 cells were incubated with a mixture of monoclonal antibodies (Table 1) for 20 min at 4°C. Erythroid cells were labeled by biotinylated anti-erythroid-antibody which was secondly conjugated with streptavidin PerCP (BD Pharmingen, Heidelberg, Germany). After incubation, cells were washed and resuspended in 300 μL PBS/3% FCS. Flow cytometric acquisition and analysis was performed using a FACS Canto II equipped with FACS Diva software (BD Biosciences, Heidelberg, Germany). Cellular subpopulations were identified by specific antigen expression (Table 1) and categorized according to the gating strategy displayed in Figure 1.

Determination of Progenitor Frequency in Rat Samples

The frequency of hematopoietic or non-hematopoietic progenitors was assessed by granulocyte-macrophage (CFU-GM) and fibroblast (CFU-F) colony forming unit assays. For CFU-GM, 1.5×10E4 vital cells were seeded in duplicates with 1.1 ml Methocult medium (GF R3774, Stem Cell technologies, Grenoble, France) into 35 mm suspension dishes and further cultivated at 37°C, 5% CO_2 and 95% humidity for 14 days. Proliferating CFU-GM colonies were counted and the frequency was calculated and normalized to leukocytes counts. CFU-GM frequency was analyzed from 8 (lysed bone marrow) or 4 (Percoll, Ficoll and MACS) donor rats with 2 technical replicates per sample.

Accordingly, to determine CFU-F frequency, 10E7 vital cells from 8 (lysed bone marrow) or 4 (Percoll, Ficoll and MACS) donor rats (with 2 technical replicates per sample) were plated into 35 mm culture dishes in Dulbecco's modified Eagle's medium containing 4.5 g/L glucose (PAA Laboratories, Cölbe, Germany), 10% FCS plus 1% Penicillin/Streptomycin and maintained at 37°C, 5% CO_2 and 95% humidity for 21 days. Medium was initially changed after 5 days and twice a week thereafter. After 3 weeks, cells were fixed in ice-cold methanol and stained with Giemsa. Fibroblast colonies were counted and frequencies were calculated.

Pretreatment of Human Bone Marrow Aspirates

Next, we aimed to validate the protocol of BMNC isolation by immunodepletion in human samples. Human bone marrow aspirates from 3 donors were purchased from Lonza Walkersville (Lonza, Walkersville, MD; FDA-registered company for the processing of human cells, tissue and cellular and tissue based

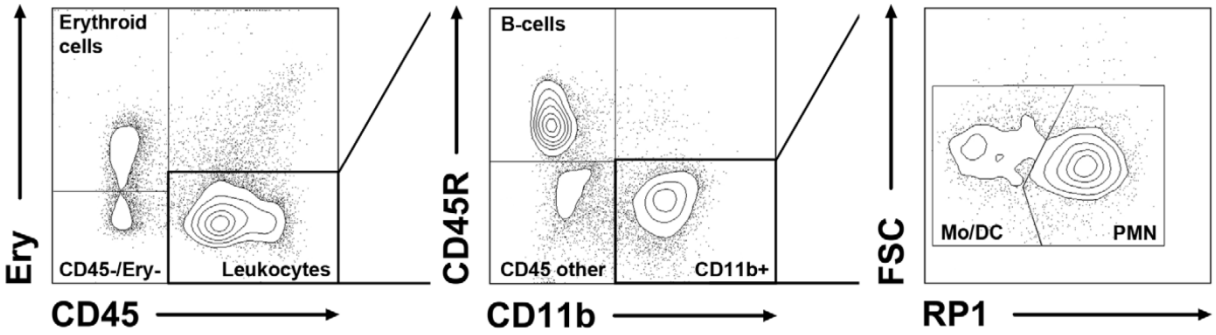

Figure 1. Representative illustration of the gating strategy in rat samples. The cells of interest were first categorized into cells belonging to the erythroid lineage (CD45−/Ery+), CD45−/Ery- cells and leukocytes (CD45+/Ery-). The latter were then differentiated into B-cells (CD45R+/CD11b−), CD11b+ cells (CD45+/CD45R−/CD11b+) and other CD45+ cells (CD45+/CD45R−/CD11b−). Next, CD11b+ cells were separated into RP1+ polymorphonuclear cells (PMN) and RP1- monocytes/dendritic cells (Mo/DC).
doi:10.1371/journal.pone.0050293.g001

products in accordance with the US Code of Federal Regulations (21 CFR Par 1271)). Human bone marrow was diluted 10-fold with PBS/3% FCS and 5 mM EDTA and sieved through a 30 µm cell strainer (pluriSelect, Leipzig, Germany) to exclude fat and bone fragments. After centrifugation for 5 min at 440 g, human bone marrow was resuspended in PBS/3% FCS and 5 mM EDTA to the original volume.

Each of the three bone marrow samples was then split into two experimental groups: (i) whole human bone marrow and (ii) lysed human bone marrow. For lysis, human bone marrow cells were incubated with a 4 fold volume of hypotonic ammonium chloride buffer (0.155 M NH4Cl, 10 mM KHCO3 and 0.1 mM Na2EDTA) for 10 min at room temperature followed by repeated washing steps with PBS/3% FCS. Viability and total cell count were determined by the trypan blue exclusion method in a hemocytometer. Leukocytes were separately stained and counted with Turk's solution.

Immunodepletion of PMNs from Human Bone Marrow

First, PMNs were depleted from lysed human bone marrow by means of magnetic-activated cell sorting (MACS). One mL of lysed bone marrow was incubated with 50 µL CD15 whole blood MicroBeads (for human PMNs; Miltenyi Biotech) for 20 min at 4°C. Non-adsorbed MicroBeads were eliminated by washing with PBS/0.5% FCS. The labeled cell suspension was then resuspended in 2 mL of PBS/0.5% FCS. Subsequently, magnetic separation was performed on LS columns using a QuadroMACS separator according to the manufacturer's instructions (Miltenyi Biotech). LS columns were successively loaded with 0.5 mL of CD15-labeled lysed bone marrow cells and 1 mL of PBS/0.5% FCS. Both discharge and the magnetically trapped CD15+ fraction were separately collected, counted and prepared for flow cytometry.

Alternatively, PMNs were depleted from lysed human bone marrow using the PluriBead technology (PluriB) that bases on differentially sized beads (rosetted with according antibodies) that can be separated by cell strainers (pluriStrainer, pluriSelect). One mL of lysed bone marrow was incubated with anti-human CD15 whole blood S-pluriBeads (pluriSelect; with a ratio of 2 pluriBeads per 3 target cells) on a pluriPlix shaker (pluriSelect) for 30 min at room temperature. Next, the labeled cell suspension was passed through an S-pluriStrainer (pluriSelect) accompanied by continuous rinsing with 15 mL of washing buffer (pluriSelect). Cells that were trapped in the S-pluriStrainer were detached from the pluriBeads using 1 mL detachment buffer (pluriSelect) for 10 minutes at room temperature and flushed through the strainer with 6 mL of washing buffer. Both fractions were separately collected, counted and prepared for flow cytometry.

In the next step, we considered to replace lysis by immunodepletion of erythrocytes. For immunomagnetic depletion of erythrocytes, whole human bone marrow was incubated with 300 µL of CD235a MicroBeads (Glycophorin A; for human erythroid cells; Miltenyi Biotech) for 20 min at 4°C. Further steps correspond to those described for the immunomagnetic CD15 depletion (above), except for the loading of the LS columns. Due to the significantly higher number of magnetically labeled cells (ratio of leucocytes to erythrocytes in whole bone marrow was 1:200),

Table 1. Anti-rat monoclonal antibodies used for flow cytometry.

FC panel				Cell population					
Antigen	**Fluorochrome**	**Clone**	**Manufacturer**	**B-cells**	**Mo/DC**	**PMNs**	**CD45 other**	**Erythroid cells**	**CD45 −/Ery-**
CD45R	FITC	HIS24	BD	+	−	−	−	−	−
Granulocytes	PE	RP-1	BD	−	−	+	−	−	−
Erythroid	Biotin	HIS49	BD	−	−	−	−	+	−
CD45	APC-Cy7	OX-1	BD	+	+	+	+	−	−
CD11b	Pacific Blue	MRC-OX42	Abd Serotec	−	+	+	−	−	−

doi:10.1371/journal.pone.0050293.t001

1 mL of CD235a-labeled whole bone marrow was loaded onto 3 LS columns. Both discharge and the mobilized CD235a+ cells were separately collected, counted and prepared for flow cytometry. In a second step, discharge was further immunomagnetically depleted of CD15+ PMNs as described above.

Finally, we used the pluriBead technology to combine multiple protocol steps by using differentially sized beads to simultaneously deplete erythrocytes and PMNs. Whole human bone marrow was incubated with anti-human CD235a M-pluriBeads (with a ratio of 1 M-pluriBead per 140 target cells) and CD15 whole blood S-pluriBeads (with a ratio of 2 pluriBeads per 3 target cells) for 30 min at room temperature on a pluriPlix shaker. Further steps correspond to those described for the CD15 pluriBead depletion (above).

Flow Cytometric Characterization of Human BMNC

Cellular composition of human bone marrow cells and subsequently separated cell fractions were analyzed by means of flow cytometry according to the protocols described for the analysis of rat BMNCs (above). Human cellular subpopulations were identified by expression of specific antigens (Table 2).

Statistical Analysis

Statistical differences were analyzed using t-tests (in case of 2 groups) or by one way analysis of variance (ANOVA; in case of more than 2 groups) and Holm-Sidak post hoc test. A p-value of 0.05 or less was considered statistically significant. All data was shown as mean ± standard deviation (SD).

Results

Rat Bone Marrow Cell Yield and Effect of Lysis

Rat bone marrow obtained from femurs and tibiae was pooled and yielded 1.2×10E9±2.4×10E8 cells per animal that were composed of CD45+ leukocytes (62.3±3.7%) and CD45- cells (37.8±3.7%; Figure 2A). The latter population primarily belonged to the erythroid lineage (CD45−/Ery+ cells), but also contained a small number of CD45−/Ery- cells (Figure 2D). As intended, short-term incubation of bone marrow cells with lysis buffer caused a 90% decrease of erythroid cells that was accompanied by a significant loss of about 35% of the CD45+ leukocytes (Figure 2A, B). However, we found the leukocyte loss being equally distributed to the major bone marrow subpopulations (Figure 2B, C). Both unprocessed and lysed bone marrow consisted of two-third BMNCs and one-third PMNs. The BMNC fraction was further classified into B-cells (52.1±5.5%), monocytes/dendritic cells (Mo/DC) (5.1±1.4%) and other CD45+ cells (9.4±1.7%; Figure 2C). The small CD45−/Ery- cell population was hardly affected by lysis and increased to approximately 40% of the CD45- cells within lysed bone marrow (Figure 2D). Interestingly, we found that the isolation of BMNCs (irrespectively of the method used; data not shown) resulted in a further enrichment of CD45/Ery double-negative cells alongside with an additional decrease of erythroid cells (Figure 2D).

Establishing an Adapted Density Separation Gradient using Percoll

We used a series of different Percoll separation gradients to identify the density gradient most suitable to separate MNC and PMN from rat bone marrow. The main endpoints were BMNC loss and yield as well as PMN contamination. We found a positive relation between escalating Percoll densities and BMNC yield (Figure 3) with highest BMNC yield at densities 1.080 g/mL and 1.084 g/mL. However, at a density of 1.084 g/mL, we observed a distinct increase of PMN contamination (Figure 3).

Rat BMNC Recovery following Different Isolation Protocols

We next compared BMNC yield and composition after applying either the Percoll gradient selected above (1.080 g/mL), a standard Ficoll gradient or an immunomagnetic depletion (MACS) of PMNs. Pre-isolation, 10E7 lysed bone marrow cell contained about 5.7×10E6 BMNCs, 2.6×10E6 PMNs and 1.7×10E6 CD45- cells (Figure 4A). As expected, all isolation protocols caused a nearly complete depletion of PMNs (Ficoll: 2.5±1.3%, Percoll 11.5±6.1% and MACS 9.5±8.5% recovery of total PMNs in lysed bone marrow) and, to a lesser extent, of the CD45- population, particularly of the erythroid cells (Figure 4A,C). Depletion of the CD45- cell population was significantly more severe after Ficoll DGC compared to Percoll DGC and MACS (14.6±8.3% versus 41.2±5.1% and 51.0±6.0% recovery of total CD45- cells in lysed bone marrow). One major result of this study is the significant decrease of the BMNC population after each of the isolation procedures. This cell diminution, however, was especially pronounced after Ficoll DGC, during which almost 75% of the BMNC were lost. The adjusted Percoll gradient yielded two-fold more BMNC than the Ficoll DGC, but still showed

Table 2. Anti-human monoclonal antibodies used for flow cytometry.

FC panel				Cell population						
Antigen	**Fluorochrome**	**Clone**	**Manufacturer**	**B-cells**	**T-cells**	**Monocytes**	**PMNs**	**Erythroid cells**	**MSC**	**HSC**
CD15	FITC	VIMC6	Miltenyi	−	−	−	+	−	N/A	N/A
CD3	PE	UCHT1	BD	−	+	−	−	−	N/A	N/A
CD235a	PE-Cy5	GA-R2 (HIR2)	BD	−	−	−	−	+	N/A	N/A
CD14	PE-Cy7	M5E2	BD	−	−	+	−	−	N/A	N/A
CD19	APC	HIB19	BD	+	−	−	−	−	N/A	N/A
CD45	APC-Cy7	2D1	BD	+	+	+	+	−	−	+
CD133	PE	AC133	Miltenyi	−	−	−	−	−	−	(+)
CD105	PerCPCy5.5	266	BD	−	−	−	−	−	+	−
CD34	APC	AC136	Miltenyi	−	−	−	−	−	−	+

doi:10.1371/journal.pone.0050293.t002

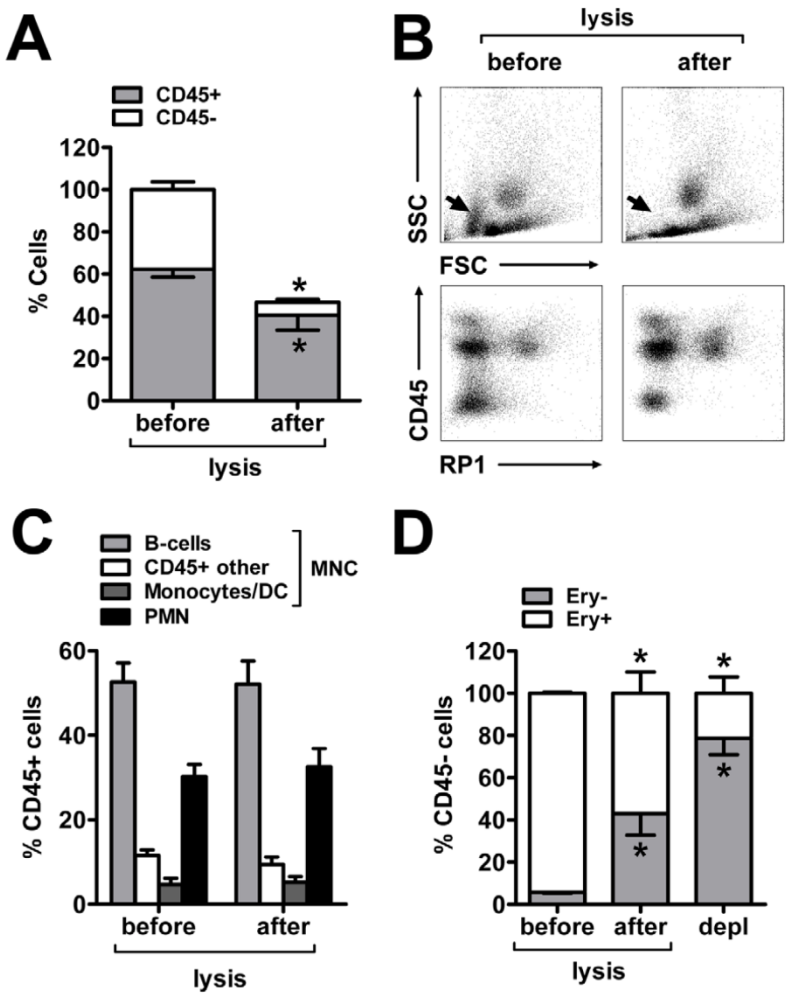

Figure 2. Influence of ammonium chloride lysis on rat bone marrow composition. (A) Freshly isolated rat bone marrow consists of 60% CD45+ and 40% CD45- cells. Lysis caused a significant decrease of CD45- (−85%) and CD45+ (−36%) cells. (B) The forward/sideward scatter diagram revealed an almost complete depletion of erythroid cells (arrow) whereas other main bone marrow populations remained largely unchanged. (C) Quantification of the cell fractions revealed that the loss of CD45+ cells due to lysis occurred symmetrically among the main leukocyte subpopulations. (D) Staining against an erythroid marker supported the finding that most cells of the erythroid line (CD45−/Ery+) disappeared following lysis whereas other CD45−/Ery- cells were significantly enriched. This was further potentiated after the application of Ficoll, Percoll or MACS depletion leading to an extended loss of erythroid cells in favor of CD45−/Ery-. Values are means ± SD for 5 samples. *$p<0.05$ by t-test.
doi:10.1371/journal.pone.0050293.g002

a BMNC loss of about 50%. By contrast, immunomagnetic depletion of PMN showed a BMNC deficit of less than 30% (Figure 4A). Proportions of leukocyte subpopulations within the respective BMNC fractions resembled those of lysed bone marrow (Figure 4B) indicating symmetric BMNC loss independent of the isolation protocol.

To investigate the amount and composition of cell loss after isolation, we analyzed the cells within layer 2 after Percoll DGC and the eluate after MACS. As expected, we detected large amounts of PMNs both after Percoll and MACS separation (61.3±18.0% versus 75.8±16.5% recovery of total PMNs in lysed bone marrow). By contrast, the incidence of BMNCs was significantly increased within the waste after Percoll DGC compared to MACS (10.6±1.2% versus 4.4±2.7% recovery of total BMNCs in lysed bone marrow; Figure 4D).

Determination of Rat Progenitor Frequencies

Additional experiments were performed to clarify whether or not the different isolation protocols influence the progenitor frequencies within rat BMNCs. To answer this question we used both CFU-GM and CFU-F to assess the proportion of bipotent hematopoietic stem cells (HSC) and of non-hematopoietic progenitors such as mesenchymal stromal cells (MSC). In lysed bone marrow, the CFU-GM frequency was 0.37±0.08% which corresponds to 3.5×10E4 HSCs in 1×10E7 bone marrow cells (Figure 5A, B). Separation of BMNCs by means of Ficoll DGC caused an enrichment of HSCs resulting in a CFU-GM frequency of 0.63±0.12%. This effect was less pronounced after Percoll DGC and disappeared after immunomagnetic separation (0.5±0.13% and 0.37±0.05%; Figure 5A). However, considering the significant different BMNC yields (Figure 4A), only one-third of all HSCs were harvested after Ficoll DGC. By contrast, after

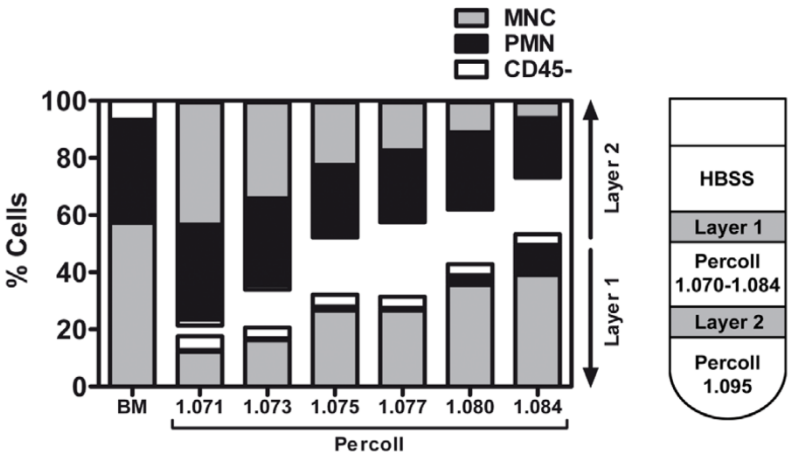

Figure 3. Adjusted density gradient centrifugation by using Percoll. Percoll of different densities (1.071 to 1.084 g/mL) differentially separated the major subclasses of lysed rat bone marrow. The higher the density, the higher was the BMNC yield (within layer 1) and the lower the BMNC loss (within layer 2), respectively. The CD45- population remained stable in layer 1 at densities from 1.073 g/mL upwards. At a density of 1.084 g/mL the BMNCs were increasingly contaminated with PMNs. Values are means from 2 pooled samples per density.
doi:10.1371/journal.pone.0050293.g003

adjusted Percoll DGC and immunomagnetic separation, the HSC yield was two-fold higher as compared to Ficoll DGC and increased to two-third of the total amount in lysed bone marrow (Figure 5B). As described previously [29], CFU-F frequency was extremely low in lysed bone marrow (0.00007±0.00002%) representing only 7 of non-hematopoietic progenitors per 1×10E7 bone marrow cells. We did not detect any CFU-F within the BMNCs after Ficoll, Percoll or immunomagnetic separation nor within the discharge of the latter two.

Isolation of Human BMNCs

To further validate whether the concept of immunodepletion is a feasible method to isolate BMNCs also from human samples, we used four different approaches to deplete both erythrocytes and PMNs of fresh human bone marrow aspirates. After harvest and pretreatment, whole human bone marrow contained 22.6±3.6×10E6 CD45+ leukocytes per mL compared to 4.68×10E9±3×10E8 CD45- cells per mL, compromising predominately CD235+ erythrocytes. Thus, a ratio of leukocytes and erythroid cells of 1:200 was determined (Figure 6A). Depletion of erythrocytes was hence indispensable for the further flow cytometric characterization and antibody-based processing of human bone marrow. Standard lysis led to a significant decrease of CD45- cells yielding a ratio of leukocytes and erythroid cells of 1:5. Immunodepletion of erythrocytes by either MACS or pluriBeads (PluriB) was even more effective and resulted in a ratio of 20:1 and 1:1, respectively (Figure 6A).

Next, we isolated BMNCs from lysed bone marrow by immunodepletion of CD15+ PMNs using either MACS or PluriB. Both methods were effective to significantly decrease PMN numbers to less than 1% of the content in whole bone marrow and recovered almost 60% of the lysed bone marrow MNCs (Figure 6B). The combined depletion of erythrocytes and PMNs by either MACS (two-step approach) or PluriB (one-step approach) showed a comparable BMNC yield and purity except for a slightly, statistically not significant higher BMNC yield after PluriB depletion (Figure 6B).

Flow Cytometric Determination of Human Progenitor Cell Populations

In addition to the BMNC yield and the remaining PMN content, we used flow cytometry to quantify progenitor populations within the obtained BMNC populations. Hematopoietic stem cells (HSCs) were identified as CD34+, CD105- and CD45dim cells which appeared along the lymphoid population in the forward/sideward scatter plot (Figure 6C; 1). In contrast, CD105+ and CD45- mesenchymal stromal cells (MSCs) were characterized by increased size and granularity (Figure 6C; 2). The HSC population was further differentiated into CD133- and CD133+ cells (Figure 6C; 3). Overall, the CD133+ HSCs accounted for approximately 40% of the CD34+ cells in all experimental groups (data not shown).

Flow cytometric quantification of HSCs and MSCs was not feasible in human whole bone marrow, owing to the extremely low rate of progenitor cells (approximately 0.005% (HSCs) and 0.0005% (MSCs) of all events in whole bone marrow). However, after lysis of human bone marrow, we ascertained 10.2±0.2×10E4 HSCs and 1.6±0.2×10E4 MSCs per mL (Figure 6D). The subsequent isolation of BMNCs was responsible for a significant loss of both HSCs and MSCs (on average of 30% for HSCs and of 55% for MSCs). The decrease of HSCs was thereby mostly pronounced after one-step depletion of erythrocytes and PMNs using PluriB (Figure 6D). However, the proportion of progenitors to the amount of total nucleated cells (i.e. frequency) increased after BMNC isolation, simply as a consequence of selective PMN depletion. Thus, the HSC frequencies increased from 0.76±0.04% in lysed bone marrow to 3.51±0.16% (lysis+MACS), 2.97±0.05% (lysis+PluriB), 3.8±0.06% (MACS+MACS) and 1.58±0.3% (PluriB combination). The MSC frequencies increased from 0.12±0.007% in lysed bone marrow to 0.34±0.01% (lysis+MACS), 0.37±0.11% (lysis+PluriB), 0.44±0.04% (MACS+MACS) and 0.26±0.04% (PluriB combination).

Discussion

In this study, we provide evidence that the application of density gradient centrifugation (DGC) for isolation of the

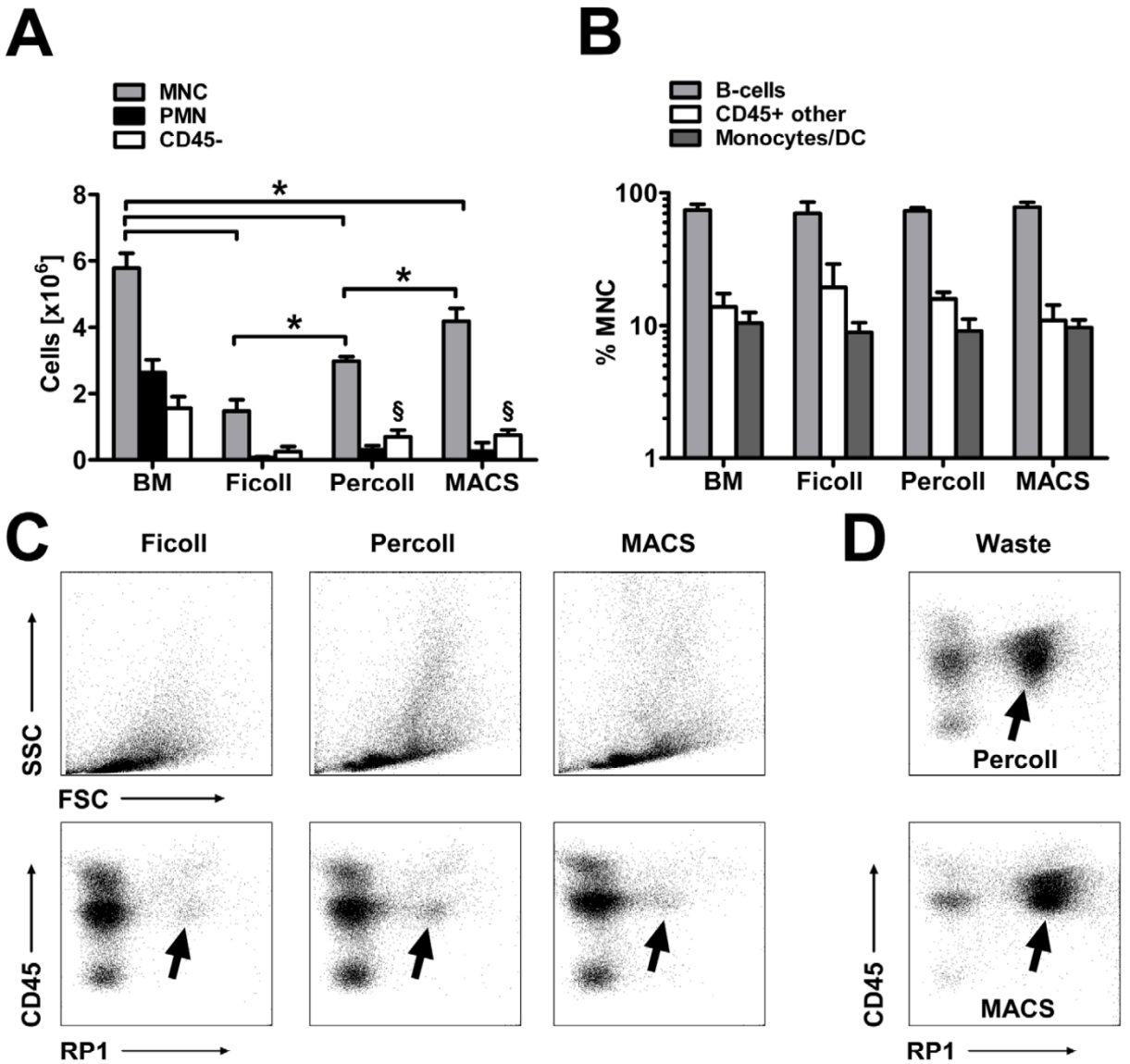

Figure 4. Rat BMNC yield following different isolation procedures. (A) Compared to lysed bone marrow, each of the isolation procedures caused an almost complete depletion of PMNs (C; arrows indicate the remaining RP1+ PMNs). As an unwanted side effect, this was accompanied by a significant loss of BMNCs and CD45- cells (A). BMNC loss was maximal after Ficoll DGC followed by Percoll DGC and MACS separation (*$p<0.05$). Both Percoll and MACS preserved the CD45- population compared to Ficoll (A; $^{\S}p<0.05$). Further analysis revealed a symmetric cell loss among the BMNC subpopulations (B; C, representative forward/sideward scatter diagrams). (D) For both Percoll and MACS, primarily RP1+ PMNs but also particular BMNC populations were detected within the waste (Percoll: layer 2; MACS: content of the columns). Values are means ± SD for 5 samples. $^{*,\S}p<0.05$ by one-way ANOVA.
doi:10.1371/journal.pone.0050293.g004

mononuclear cell fraction from rat bone marrow (BMNC) is confounded by a significant loss of the cells of interest. When using Ficoll as density medium, only 25% of the BMNCs being detectable in lysed bone marrow were recovered. These findings are consistent with other studies investigating human bone marrow that show BMNC recovery rates between 15 to 30% after Ficoll DGC [17,19]. Interestingly, we found that DGC using Percoll with an equal density to that of Ficoll (1.084 g/mL) yielded significantly more BMNCs (Figure 3), suggesting that excessive cell loss during Ficoll DGC is a consequence of density medium-related cytotoxicity [30]. Moreover, Ficoll based DGC has been primarily established for separation of blood into its components. In contrast to peripheral blood mononuclear cells (PBMNCs), BMNCs exhibit an increased variability of cell maturity and consequently of buoyant density [31]. Hence, BMNCs with densities deviating from those of PBMNCs might less likely accumulate within the correct Ficoll density layer. To address this problem, we used a series of different layer densities by diluting Percoll and found that the optimal density range for isolating rat BMNCs is in between 1.080 to 1.084 g/mL,

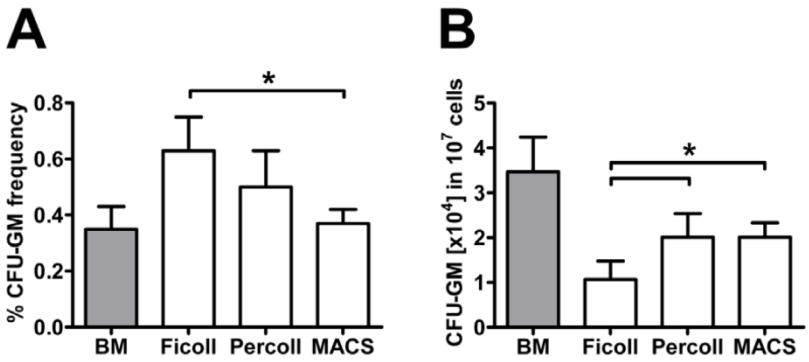

Figure 5. Recovery of rat hematopoietic progenitors. (A) Analysis of the CFU-GM frequency revealed a significant enrichment of hematopoietic stem cells (HSC) by Ficoll compared to MACS. However, when relating the CFU-GM number to the absolute BMNC yield, Ficoll DGC resulted in a significant loss of HSCs compared to both Percoll and MACS separation. Values are means ± SD for 4 samples. *$p<0.05$ by one-way ANOVA.
doi:10.1371/journal.pone.0050293.g005

bounded above by unwanted polymorphonuclear cell (PMN) contamination and below by decreasing BMNC yields (Figure 3). However, even after adjustment of the density layers, density gradient separation of BMNCs was generally confounded by a cell loss of at least 50%. This is highly relevant for clinical practice, since meta-analyses revealed a clear dose-dependency of autologous BMNC transplantation [20]. A profound cell loss during DGC may hence directly attenuate therapeutic efficacy.

Consequently, we looked for an alternative method to separate BMNCs with a higher yield, and decided to immunomagnetically deplete PMNs as it has been described for human blood samples from patients with sepsis or burn [28]. Immunomagnetic separations by either positive or negative selection of special cell populations can be conducted under conditions of good manufacturing practice [32] and have already been applied in several clinical studies [33–35]. In our experiment with rat samples, we show that this approach achieved a significantly higher BMNC yield compared to both DGC-based methods (Figure 4A), while the leukocyte composition was identical. We therefore conclude that immunomagnetic separation could be an appropriate method to isolate bone marrow mononuclear cells for transplantation purposes offering the advantage of higher BMNC doses for patients. To further validate this hypothesis, we performed a proof-of-concept study with fresh human bone marrow samples from three healthy donors. We found that immunomagnetic separation (MACS) of CD15+ PMNs from lysed human bone marrow was feasible and yielded a BMNC recovery of 55%. An alternative method for immunoselection based upon differently sized beads (PluriB) recovered slightly more cells (58%) with comparable effort and almost equal final composition of BMNCs. Generally, human BMNC yields were lower compared to what we observed in our rat study (72%), but we assume that a further optimization of the human proof-of-concept protocol, as it has been extensively done for the rat protocol, would approximate the BMNC yields.

One further important advantage of using immunoselection compared to density gradient centrifugation is the flexibility to adapt the protocol to a supposed mechanism of action by either depletion of adverse or enrichment of beneficial cell populations. We verified this concept in human bone marrow samples by immunoselection of both PMNs and erythrocytes, since it was shown that the content of erythroid cells directly impaired the function of BMNCs [15]. Interestingly, immunomagnetic depletion of erythrocytes resulted in a highly purified CD45+ cell population (ca. 5% erythroid cells; Figure 6A) compared to lysis (ca. 80% erythroid cells) or Ficoll DGC (ca. 70% erythroid cells [15]).

Hematopoietic CD34+ stem cells (HSC) account for approximately 1.5% of the BMNCs and have been discussed to have a crucial impact on the observed therapeutic effects [33]. DGC-based separation of BMNCs was hence often justified to augment these progenitors within the cell graft [27]. In fact, we and others [12] found a significant enrichment of HSCs after Ficoll DGC. An increased resistance against the toxicity of the density medium or a suitable buoyant density (i.e. close to lymphocytes) might explain HSC enrichment after Ficoll DGC. Nevertheless, due to the significant loss of BMNCs, the overall HSC yield was significantly decreased after Ficoll DGC. Enrichment might thus be beneficial in preclinical studies with a fixed, non-autologous BMNC transplantation scheme. However, in a clinical and autologous setting, DGC might rather result in a loss of effector cells. In fact, the amount of CD34+ cells in human whole bone marrow was described to be 1.5×10E5 per mL [36] whereas several clinical trials yielded between 1.4 to 7.2×10E4 CD34+ cells per mL [12,13]. After immunoselection of PMNs from lysed human bone marrow, we found 7.5×10E4 CD34+ cells per mL which is considerably higher compared to that what was reported recently in large scale clinical studies.

It is still controversially discussed which cell population within BMNCs is actually required for beneficial effects and which is not. Thus, for example, one recent study described the B-cells as being the effective cell population within the BMNCs [37]. In the present study we observed a distinct CD45- cell population within the rat bone marrow cells which clearly did not belong to the erythroid line (Figure 2D). In total the CD45- population was almost completely depleted after Ficoll DGC (15% recovery of total CD45- cells in lysed bone marrow), a finding that is supported by Medina et al. [38] who found many non-erythroid CD45- cells within the usually discarded pellet after DGC. By contrast, in our rat study, both Percoll and MACS separation conserved a large proportion of this population (41% and 57% of lysed bone marrow; Figure 4A). Interestingly, these CD45- cells seem to contain specific stem cell populations such as MSCs, VSEL, epithelial progenitors [38], multilineage inducible cells [39] and endothelial progenitor cells [40] and might thus be relevant for therapeutic effects of BMNCs. In line with these observations, it was recently described that most of the bone marrow MSCs were discarded during Ficoll DGC due to their aggregate nature

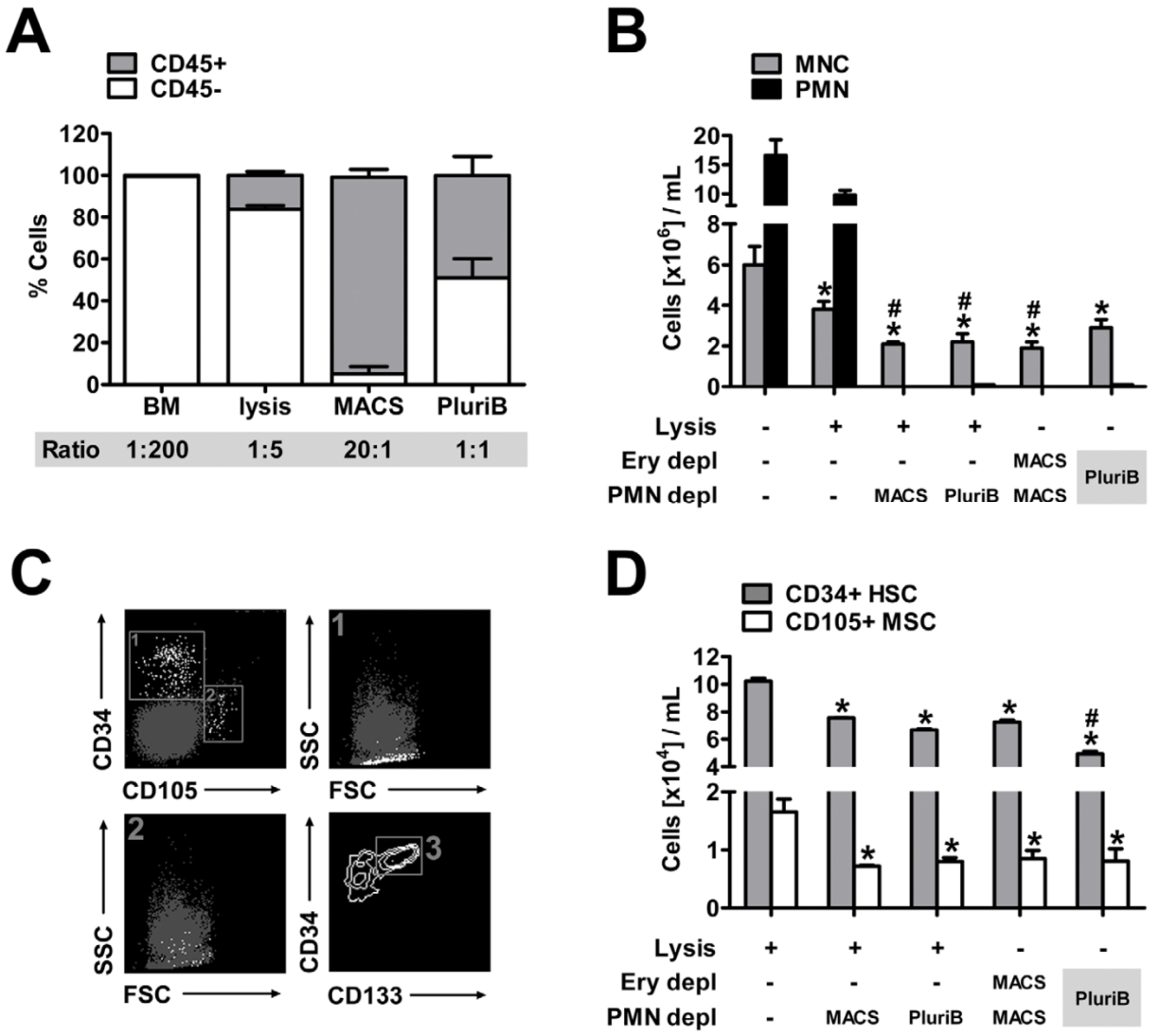

Figure 6. Isolation of BMNCs from fresh human bone marrow aspirates and determination of progenitor cells. (A) Fresh whole bone marrow (BM) contained a high proportion of CD45- erythroid cells. The amount of erythroid cells could be significantly decreased by lysis or by immunodepletion (MACS or PluriB) of erythrocytes whereas highest purity of CD45+ leukocytes was attained after immunomagnetic depletion (MACS). (B) Lysis of whole bone marrow caused a significant loss of BMNCs (*$p<0.05$ versus whole bone marrow) that was further extended by PMN depletion with either MACS or PluriB ($^{\#}p<0.05$ versus lysed bone marrow). The combined depletion of erythrocytes and PMNs by sequential MACS or by combined PluriB yielded comparable BMNC counts. The amount of remaining PMNs was constant at a low level after each of the isolation procedures. (C) Gating strategy for progenitor characterization. CD34+ hematopoietic stem cells (HSCs; C 1) featured a uniform, lymphoid-like phenotype and were partially CD133+ (C 3). In contrast, CD105+ mesenchymal stromal cells (MSC; C 2) exhibited increased variability of size and granularity. (D) Quantification of progenitors revealed that HSCs and MSCs were lost due to the different BMNC isolation procedures ($p<0.05$ versus lysed bone marrow). Cell loss was comparable in all experimental approaches except for the combined one-step depletion (PluriB), where the HSC yield was significantly lower compared to the other isolation protocols ($^{\#}p<0.05$ versus lysis+MACS, lysis+PluriB and MACS+MACS). Values are means ± SD for 3 samples. $^{*,\#}p<0.05$ by one-way ANOVA.
doi:10.1371/journal.pone.0050293.g006

[23], and that whole bone marrow, but not BMNCs obtained by Ficoll DGC improved functional recovery after experimental myocardial infarction [41]. Collectively, these considerations question whether the concept of stem cell enrichment during Ficoll DGC-based BMNC separation is true and reasonable in the setting of clinical studies.

In conclusion, our findings show that the isolation of BMNCs by density gradient centrifugation causes a distinct and symmetric cell loss that includes a decrease of therapeutically relevant stem cell populations. A higher cell yield can be obtained by using a customized Percoll protocol or by immunodepletion of unwanted constituents such as erythrocytes and granulocytes.

Acknowledgments

We would like to thank Dr. Gesa Weise and Dr. Alexander Deten for critically reviewing the manuscript and for helpful discussions. We also thank Dr. Jan-Michael Heinrich for valuable technical advice.

Author Contributions

Conceived and designed the experiments: CP KM JB DCW. Performed the experiments: CP KM WF IS. Analyzed the data: CP KM DCW. Wrote the paper: CP DCW.

References

1. Thomas ED, Lochte HL Jr, Lu WC, Ferrebee JW (1957) Intravenous infusion of bone marrow in patients receiving radiation and chemotherapy. N Engl J Med 257: 491–496.
2. Matoba S, Tatsumi T, Murohara T, Imaizumi T, Katsuda Y et al. (2008) Long-term clinical outcome after intramuscular implantation of bone marrow mononuclear cells (Therapeutic Angiogenesis by Cell Transplantation [TACT] trial) in patients with chronic limb ischemia. Am Heart J 156: 1010–1018.
3. Tateishi-Yuyama E, Matsubara H, Murohara T, Ikeda U, Shintani S et al. (2002) Therapeutic angiogenesis for patients with limb ischaemia by autologous transplantation of bone-marrow cells: a pilot study and a randomised controlled trial. Lancet 360: 427–435.
4. Savitz SI, Misra V, Kasam M, Juneja H, Cox CS Jr et al. (2011) Intravenous autologous bone marrow mononuclear cells for ischemic stroke. Ann Neurol 70: 59–69.
5. Friedrich MA, Martins MP, Araujo MD, Klamt C, Vedolin L et al. (2011) Intra-Arterial Infusion of Autologous Bone-Marrow Mononuclear Cells in Patients with Moderate to Severe Middle-Cerebral-Artery Acute Ischemic Stroke. Cell Transplant 21 Suppl. 1: S13–21.
6. Abdel-Latif A, Bolli R, Tleyjeh IM, Montori VM, Perin EC et al. (2007) Adult bone marrow-derived cells for cardiac repair: a systematic review and meta-analysis. Arch Intern Med 167: 989–997.
7. Strauer BE, Brehm M, Zeus T, Kostering M, Hernandez A et al. (2002) Repair of infarcted myocardium by autologous intracoronary mononuclear bone marrow cell transplantation in humans. Circulation 106: 1913–1918.
8. Clifford DM, Fisher SA, Brunskill SJ, Doree C, Mathur A et al. (2012) Stem cell treatment for acute myocardial infarction. Cochrane Database Syst Rev 2: CD006536.
9. Korf-Klingebiel M, Kempf T, Sauer T, Brinkmann E, Fischer P et al. (2008) Bone marrow cells are a rich source of growth factors and cytokines: implications for cell therapy trials after myocardial infarction. Eur Heart J 29: 2851–2858.
10. Lachtermacher S, Esporcatte BL, da Silva de Azevedo Fortes, Rocha NN, Montalvao F et al. (2012) Functional and transcriptomic recovery of infarcted mouse myocardium treated with bone marrow mononuclear cells. Stem Cell Rev 8: 251–261.
11. Rosenzweig A (2006) Cardiac cell therapy–mixed results from mixed cells. N Engl J Med 355: 1274–1277.
12. Schachinger V, Erbs S, Elsasser A, Haberbosch W, Hambrecht R et al. (2006) Intracoronary bone marrow-derived progenitor cells in acute myocardial infarction. N Engl J Med 355: 1210–1221.
13. Lunde K, Solheim S, Aakhus S, Arnesen H, Abdelnoor M et al. (2006) Intracoronary injection of mononuclear bone marrow cells in acute myocardial infarction. N Engl J Med 355: 1199–1209.
14. Seeger FH, Tonn T, Krzossok N, Zeiher AM, Dimmeler S. (2007) Cell isolation procedures matter: a comparison of different isolation protocols of bone marrow mononuclear cells used for cell therapy in patients with acute myocardial infarction. Eur Heart J 28: 766–772.
15. Assmus B, Tonn T, Seeger FH, Yoon CH, Leistner D et al. (2010) Red blood cell contamination of the final cell product impairs the efficacy of autologous bone marrow mononuclear cell therapy. J Am Coll Cardiol 55: 1385–1394.
16. Mouquet F, Lemesle G, Delhaye C, Charbonnel C, Ung A et al. (2011) The presence of apoptotic bone marrow cells impairs the efficacy of cardiac cell therapy. Cell Transplant 20: 1087–1097.
17. van Beem RT, Hirsch A, Lommerse IM, Zwaginga JJ, Noort WA et al. (2008) Recovery and functional activity of mononuclear bone marrow and peripheral blood cells after different cell isolation protocols used in clinical trials for cell therapy after acute myocardial infarction. EuroIntervention 4: 133–138.
18. Jaatinen T, Laine J (2007) Isolation of mononuclear cells from human cord blood by Ficoll-Paque density gradient. Curr Protoc Stem Cell Biol Chapter 2: Unit.
19. Aktas M, Radke TF, Strauer BE, Wernet P, Kogler G. (2008) Separation of adult bone marrow mononuclear cells using the automated closed separation system Sepax. Cytotherapy 10: 203–211.
20. Martin-Rendon E, Brunskill SJ, Hyde CJ, Stanworth SJ, Mathur A et al. (2008) Autologous bone marrow stem cells to treat acute myocardial infarction: a systematic review. Eur Heart J 29: 1807–1818.
21. Renzi P, Ginns LC (1987) Analysis of T cell subsets in normal adults. Comparison of whole blood lysis technique to Ficoll-Hypaque separation by flow cytometry. J Immunol Methods 98: 53–56.
22. Romeu MA, Mestre M, Gonzalez L, Valls A, Verdaguer J et al. (1992) Lymphocyte immunophenotyping by flow cytometry in normal adults. Comparison of fresh whole blood lysis technique, Ficoll-Paque separation and cryopreservation. J Immunol Methods 154: 7–10.
23. Ahmadbeigi N, Soleimani M, Babaeijandaghi F, Mortazavi Y, Gheisari Y et al. (2012) The aggregate nature of human mesenchymal stromal cells in native bone marrow. Cytotherapy 14: 917–924.
24. Bhartiya D, Shaikh A, Nagvenkar P, Kasiviswanathan S, Pethe P et al. (2012) Very small embryonic-like stem cells with maximum regenerative potential get discarded during cord blood banking and bone marrow processing for autologous stem cell therapy. Stem Cells Dev 21: 1–6.
25. Nieto JC, Canto E, Zamora C, Ortiz MA, Juarez C et al. (2012) Selective loss of chemokine receptor expression on leukocytes after cell isolation. PLoS One 7: e31297.
26. Naranbhai V, Bartman P, Ndlovu D, Ramkalawon P, Ndung'u T et al. (2011) Impact of blood processing variations on natural killer cell frequency, activation, chemokine receptor expression and function. J Immunol Methods 366: 28–35.
27. Rosca AM, Burlacu A (2010) Isolation of a mouse bone marrow population enriched in stem and progenitor cells by centrifugation on a Percoll gradient. Biotechnol Appl Biochem 55: 199–208.
28. Preobrazhensky SN, Bahler DW (2009) Immunomagnetic bead separation of mononuclear cells from contaminating granulocytes in cryopreserved blood samples. Cryobiology 59: 366–368.
29. Baksh D, Song L, Tuan RS. (2004) Adult mesenchymal stem cells: characterization, differentiation, and application in cell and gene therapy. J Cell Mol Med 8: 301–316.
30. Luttmann W, Bratke K, Kupper M, Myrtek D (2006) Immunology. Academic Press. 264 p.
31. Stelzer GT, Marti G, Hurley A, McCoy P Jr, Lovett EJ et al. (1997) U.S.-Canadian Consensus recommendations on the immunophenotypic analysis of hematologic neoplasia by flow cytometry: standardization and validation of laboratory procedures. Cytometry 30: 214–230.
32. Ghodsizad A, Klein HM, Borowski A, Stoldt V, Feifel N et al. (2004) Intraoperative isolation and processing of BM-derived stem cells. Cytotherapy 6: 523–526.
33. Tendera M, Wojakowski W, Ruzyllo W, Chojnowska L, Kepka C et al. (2009) Intracoronary infusion of bone marrow-derived selected CD34+CXCR4+ cells and non-selected mononuclear cells in patients with acute STEMI and reduced left ventricular ejection fraction: results of randomized, multicentre Myocardial Regeneration by Intracoronary Infusion of Selected Population of Stem Cells in Acute Myocardial Infarction (REGENT) Trial. Eur Heart J 30: 1313–1321.
34. Yerebakan C, Kaminski A, Westphal B, Donndorf P, Glass A et al. (2011) Impact of preoperative left ventricular function and time from infarction on the long-term benefits after intramyocardial CD133(+) bone marrow stem cell transplant. J Thorac Cardiovasc Surg 142: 1530–1539.
35. Federmann B, Bornhauser M, Meisner C, Kordelas L, Beelen DW et al. (2012) Haploidentical allogeneic hematopoietic cell transplantation in adults using CD3/CD19 depletion and reduced intensity conditioning: a phase II study. Haematologica 97: 1523–31.
36. Lannert H, Able T, Becker S, Sommer M, Braun M et al. (2008) Optimizing BM harvesting from normal adult donors. Bone Marrow Transplant 42: 443–447.
37. Goodchild TT, Robinson KA, Pang W, Tondato F, Cui J et al. (2009) Bone marrow-derived B cells preserve ventricular function after acute myocardial infarction. JACC Cardiovasc Interv 2: 1005–1016.
38. Medina RJ, Kataoka K, Miyazaki M, Huh NH (2006) Efficient differentiation into skin cells of bone marrow cells recovered in a pellet after density gradient fractionation. Int J Mol Med 17: 721–727.
39. D'Ippolito G, Diabira S, Howard GA, Menei P, Roos BA et al. (2004) Marrow-isolated adult multilineage inducible (MIAMI) cells, a unique population of postnatal young and old human cells with extensive expansion and differentiation potential. J Cell Sci 117: 2971–2981.
40. Timmermans F, Plum J, Yoder MC, Ingram DA, Vandekerckhove B et al. (2009) Endothelial progenitor cells: identity defined? J Cell Mol Med 13: 87–102.
41. Koskenvuo JW, Sievers RE, Zhang Y, Angeli FS, Lee B et al. (2012) Fractionation of mouse bone-marrow cells limits functional efficacy in non-reperfused mouse model of acute myocardial infarction. Ann Med: epub ahead of print.

2.2 Bone marrow cell transplantation time-dependently abolishes efficacy of G-CSF after stroke in hypertensive rats

Titel: Bone marrow cell transplantation time-dependently abolishes efficacy of G-CSF after stroke in hypertensive rats

Autoren: Claudia Pösel, Johanna Scheibe, Alexander Kranz, Viktoria Bothe, Elfi Quente, Wenke Fröhlich, Franziska Lange, Wolf-Rüdiger Schäbitz, Jens Minnerup, Johannes Boltze*, Daniel-Christoph Wagner*
* geteilte Autorenschaft

eingereicht am: 10.12.2013

akzeptiert am: 21.05.2014

Veröffentlichung: Stroke 2014; 45 (8):2431-2437

Stroke
Journal of the American Heart Association

Bone Marrow Cell Transplantation Time-Dependently Abolishes Efficacy of Granulocyte Colony-Stimulating Factor After Stroke in Hypertensive Rats

Claudia Pösel, Johanna Scheibe, Alexander Kranz, Viktoria Bothe, Elfi Quente, Wenke Fröhlich, Franziska Lange, Wolf-Rüdiger Schäbitz, Jens Minnerup, Johannes Boltze and Daniel-Christoph Wagner

Stroke. 2014;45:2431-2437; originally published online July 1, 2014;
doi: 10.1161/STROKEAHA.113.004460
Stroke is published by the American Heart Association, 7272 Greenville Avenue, Dallas, TX 75231

Print ISSN: 0039-2499. Online ISSN: 1524-4628

Bone Marrow Cell Transplantation Time-Dependently Abolishes Efficacy of Granulocyte Colony-Stimulating Factor After Stroke in Hypertensive Rats

Claudia Pösel, Dipl Ing (FH); Johanna Scheibe, PhD; Alexander Kranz, MD; Viktoria Bothe, MSc; Elfi Quente; Wenke Fröhlich; Franziska Lange, PhD; Wolf-Rüdiger Schäbitz, MD; Jens Minnerup, MD; Johannes Boltze, MD, PhD*; Daniel-Christoph Wagner, MD*

Background and Purpose—We aimed to determine a possible synergistic effect of granulocyte colony-stimulating factor (G-CSF) and bone marrow–derived mononuclear cells (BM MNC) after stroke in spontaneously hypertensive rats.

Methods—Male spontaneously hypertensive rats were subjected to middle cerebral artery occlusion and randomly assigned to daily injection of 50 µg/kg G-CSF for 5 days starting 1 hour after stroke (groups 1, 2, and 3) with additional intravenous transplantation of 1.5×10E7 BM MNC per kilogram at 6 hours (group 2) or 48 hours (group 3) after stroke, or control treatment (group 4). Circulating leukocyte counts and functional deficits, infarct volume, and brain edema were repeatedly assessed in the first week and first month.

Results—G-CSF treatment led to a significant neutrophilia, to a reversal of postischemic depression of circulating leukocytes, and to a significantly improved functional recovery without affecting the infarct volume or brain edema. BM MNC cotransplantation was neutral after 6 hours, but reversed the functional effect of G-CSF after 48 hours. Short-term investigation of combined G-CSF and BM MNC treatment at 48 hours indicated splenic accumulation of granulocytes and transplanted cells, accompanied by a significant rise of granulocytes in the circulation and the ischemic brain.

Conclusions—G-CSF improved functional recovery in spontaneously hypertensive rats, but this effect was abolished by cotransplantation of BM MNC after 48 hours. In the spleen, transplanted cells may hinder the clearance of granulocytes that were massively increased by G-CSF. Increased circulation and infiltration of granulocytes into the ischemic brain may be detrimental for stroke outcome. **(*Stroke*. 2014;45:2431-2437.)**

Key Words: cell- and tissue-based therapy ■ granulocyte colony-stimulating factor ■ immune system ■ stroke

Stroke remains a major challenge of modern medicine, belonging to the most frequent causes of death and permanent disability, whereas causal treatment is not applicable to most patients. Unfortunately, many promising drug candidates got lost in translation, with the hematopoietic hormone granulocyte colony-stimulating factor (G-CSF) being one of the most recent examples.[1] However, this result strikingly contrasts with the convincing preclinical data for G-CSF[2,3] and may be owed to the fact that therapeutic effect sizes decline with increasing study population heterogeneity and complexity. Hence, enhancing the therapeutic effect, for instance, by synergistic combination[4] of G-CSF with another favorable approach may afford its clinical use.

Evidence exists that the mobilization of bone marrow (BM) cells, either as endogenous response,[5] or by G-CSF treatment[6] is protective after stroke and significantly improves neurological outcome. However, the latter process requires a successive degradation of cell-arresting stromal cell-derived factor 1 within the BM[7] and thus begins delayed after stroke. By contrast, intravenously transplanted BM-derived mononuclear cells (BM MNC) rapidly increase cerebral blood flow and reduced tissue damage after acute and chronic brain ischemia.[8,9] We, therefore, hypothesized that the delayed mobilization by G-CSF could be compensated by early cotransplantation of BM MNC, which is also an established preclinical stroke therapy.[10]

To test this hypothesis, we applied a classical G-CSF regime extended by cotransplantation of syngeneic BM MNC at 6 or 48 hours after experimental stroke. The study was planned in line with recommendations for good preclinical stroke research,[11] including the use of comorbid animals and long-term monitoring

Received December 10, 2013; final revision received May 14, 2014; accepted May 21, 2014.

From the Fraunhofer Institute for Cell Therapy and Immunology, Leipzig, Germany (C.P., J.S., A.K., E.Q., W.F., F.L., J.B., D.-C.W.); Translational Centre for Regenerative Medicine, Leipzig, Germany (A.K., V.B., E.Q., W.F., J.B., D.-C.W.); EVK Bielefeld, Bethel, Neurologische Klinik, Bielefeld, Germany (W.-R.S.); Department of Neurology, University of Münster, Germany (J.M.); and Massachusetts General Hospital and Harvard Medical School, Boston (J.B.).

Guest Editor for this article was Costantino Iadecola, MD.

*Drs Boltze and Wagner contributed equally.

The online-only Data Supplement is available with this article at http://stroke.ahajournals.org/lookup/suppl/doi:10.1161/STROKEAHA.113.004460/-/DC1.

Correspondence to Claudia Pösel, Dipl Ing (FH), Fraunhofer Institute for Cell Therapy and Immunology, Perlickstrasse 1, 04103 Leipzig, Germany. E-mail claudia.poesel@izi.fraunhofer.de

***Stroke* is available at http://stroke.ahajournals.org** **DOI: 10.1161/STROKEAHA.113.004460**

of functional and imaging end points. Surprisingly, our study showed that combining G-CSF and BM MNC at 48 hours had significant adverse effects on the neurological outcome. Further mechanistic experiments indicated an interaction of granulocytes, which were massively mobilized by G-CSF, and transplanted BM MNC in the spleen. The consecutive spillover of granulocytes may finally explain the unfavorable outcome. Although our experiments failed to provide a novel preclinical approach for stroke, it emphasizes the importance of the immune system for the development and translation of stroke therapies.

Materials and Methods

A detailed description of materials and methods is provided in the online-only Data Supplement.

Experimental Stroke

Animal experiments were performed according to the *Guide for the Care and Use of Laboratory Animals* published by the US National Institutes of Health (NIH Publication No. 85-23, revised 1996) and approved by legal authorities (TVV 12/11). Spontaneously hypertensive rats (SHR; Charles River, Sulzfeld, Germany; 12 weeks of age) were anesthetized with ketamine/xylazine and subjected to permanent right middle cerebral artery occlusion (pMCAO).

Experimental Set Up and Treatment

Animals were randomly assigned to following experimental groups: (1) G-CSF monotherapy (G-CSF; n=18) with daily intraperitoneal injection of 50 µg/kg body weight G-CSF for 5 days starting 1 hour after pMCAO; (2) G-CSF plus intravenous transplantation of 1.5×10E7 BM MNC per kilogram body weight at 6 hours after pMCAO (G-CSF+BM MNC 6 hours; n=18); (3) G-CSF plus intravenous transplantation of 1.5×10E7 BM MNC per kilogram body weight at 48 hours after pMCAO (G-CSF+BM MNC 48 hours; n=18); (4) control group (control; n=18) receiving phosphate buffered saline instead of G-CSF and BM MNC. Stroke induction, treatments, and analyses were performed by investigators blinded to group allocation.

Study End Points

Infarct volume and space-occupying effect were determined by magnetic resonance imaging at days 1, 3, 7, and 30. Neurological deficits were assessed by the adhesive removal test at days 2, 7, 14, 21, and 28. Circulating leukocytes were identified by specific antigens (Table I in the online-only Data Supplement) within the first week after stroke using flow cytometry. Cytokine levels were repeatedly measured by multiparametric enzyme-linked immunosorbent assay. At day 30 after stroke, expressions of plasticity and inflammation-related genes were assessed by quantitative real-time polymerase chain reaction. T cells were visualized by immunofluorescence staining and counted within the infarct border and the entire ischemic hemisphere.

Biodistribution and Short-Term Effects of Cell Transplantation

In a subgroup analysis, animals were randomly assigned to groups 1, 3, and 4 (n=3 per group). Distribution of PKH26-labeled BM MNC and immune cell frequencies were determined in the blood, BM, and single cell lysates of the spleen and brain at 52 hours after stroke by flow cytometry. Splenic gene expression of pro- and anti-inflammatory cytokines was investigated by real-time polymerase chain reaction.

Results

Study Enrollment

All animals except for 1 control (1.4%) survived pMCAO. One animal of G-CSF+BM MNC 6 hours group was excluded because of partial infarction. Two animals (one in control and one in G-CSF+BM MNC 6 hours) died during day 3 magnetic resonance imaging. Further animals were excluded solely from magnetic resonance imaging because of technical problems (Table II in the online-only Data Supplement). Finally, 1 animal with G-CSF monotherapy was excluded from behavioral tests because of lack of compliance.

Characterization of Cell Graft

Previously isolated and cryopreserved syngeneic BM MNC grafts were thawed and characterized by flow cytometry. We observed only minor variation of the main leukocyte populations among the different cohorts (n=8). Mature B cells compromised the major part of the graft (48.2±6.5%), followed by myeloid $CD11b^+$ cells (22.2±3.0%), T cells (4.9±0.5%), and remaining uncharacterized leukocytes (CD45only: 27.2±3.7%). 7.1±1.3% of BM MNC expressed the CXC chemokine receptor-4 (CXCR4), whereas we did not found detectable CXCR4 expression by $CD34^+$ cells. Hematopoietic progenitor cells analyzed by coexpression of CD45 and CD34 accounted for 5.0±1.5% of all BM MNC with a frequency of 2.0±0.3% for granulocyte/monocyte progenitors determined by colony-forming unit–granulocyte/macrophage. Analysis of programmed cell death among the graft revealed 23.5±3.3% early apoptotic cells, 6.7±2.5% late apoptotic cells, and 1.9±1.0% necrotic cells.

Peripheral Leukocyte Counts

The impact of G-CSF administration and additional BM MNC transplantation on peripheral leukocyte counts was analyzed 6, 48, 52, 96, and 144 hours after pMCAO. Expectably, G-CSF treatment caused a distinct increase of peripheral leukocyte counts, reaching its peak at 48 hours with a successive normalization until 144 hours after stroke. However, additional administration of BM MNC after either 6 or 48 hours did not impact overall leukocyte counts (Figure 1). The increase of leukocytes was predominantly driven by granulocytes and, to a much lesser extent, by monocytes, T cells, B cells, and natural killer cells (Figure 1). Four hours after transplantation of BM MNC at 48 hours, we observed a statistically significant increase of granulocyte counts in the G-CSF+BM MNC 48 hours group compared with the G-CSF monotherapy (Figure 1). When comparing leukocyte counts of stroke and naive animals, we observed a considerable decrease of T and B cells, monocytes and natural killer cells 48 hours after stroke. This observation is consistent with recent studies and corresponds to the phenomenon of poststroke immunodepression.[12] Although the suppression of T cells, monocytes, and natural killer cells was limited to 48 hours, we found a persistent depression of B cells (Figure 1). Interestingly, at 48 hours after stroke, poststroke cellular immunodepression was largely reversed by G-CSF treatment, independent of a concomitant cell therapy. Moreover, G-CSF provoked a significant downregulation of CXCR4 on peripheral blood mononuclear cells at 48 hours (Figure 1). CXCR4 expression completely recovered in groups with G-CSF monotherapy or additional early (6 hours) BM MNC administration, but remained suppressed in the G-CSF+BM MNC 48 hours group. Finally, differentiation of T cells into T helper cells, cytotoxic T cells, CD4/CD8 double-positive, as well as CD4/CD8 double-negative T cells (data not

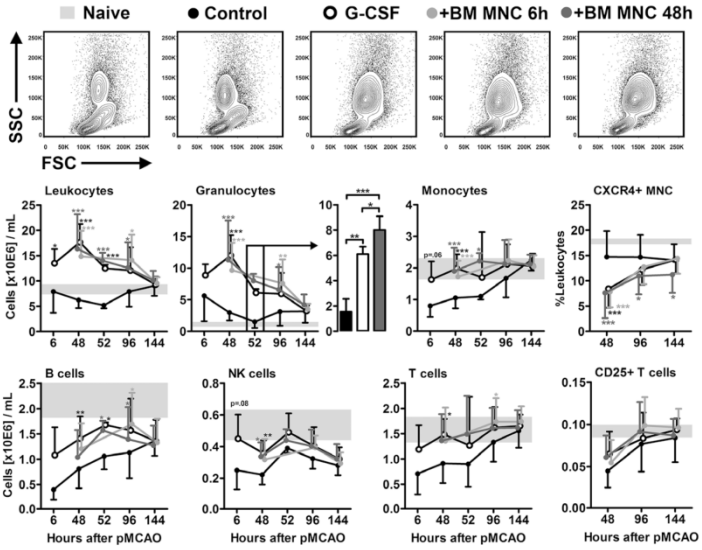

Figure 1. Influence of experimental treatments on peripheral leukocyte counts. Cell counts from naive spontaneously hypertensive rats (SHR) were included as reference (grey area: upper and lower SD; n=3). All animals that received granulocyte colony-stimulating factor (G-CSF) showed a 3-fold increase of leukocytes at 48 hours that successively normalized until 144 hours. As illustrated by exemplary flow cytometric forward/side scatter (FSC/SSC) plots of blood samples at 48 hours, granulocytes were the main contributors of leukocytosis. At 52 hours, transplantation of bone marrow–derived mononuclear cells (BM MNC) after 48 hours caused a significant increase of granulocytes compared with G-CSF monotherapy. The transient decline of monocytes, T, and natural killer (NK) cells in consequence of stroke was reversed by G-CSF at 48 hours and partly at 96 hours. The suppression of B cells was persistent until 144 hours and was only partially attenuated by G-CSF. The initial decline of CXC chemokine receptor-4 (CXCR4) expression was transient after G-CSF or G-CSF+BM MNC 6 hours, but persistent over the first 144 hours after G-CSF+BM MNC 48 hours. pMCAO indicates permanent right middle cerebral artery occlusion. *P<0.05, **P<0.01, ***P<0.001 compared with control group determined by 1-way ANOVA; n=14 to 17 (48, 96, and 144 hours) or n=3 to 6 (6 and 52 hours) animals per group.

shown) and regulatory T cells (Figure 1) revealed no statistically significant differences among the treatment groups.

Serum Cytokines

Serum concentrations of interleukin (IL)-4, IL-10, IL-17A, monocyte chemotactic protein-1, and macrophage inflammatory protein-1α changed significantly as a function of time (P<0.05), whereas interferon-γ levels remained stable ≤144 hours after stroke (Figure I in the online-only Data Supplement). At 96 hours, the serum level of macrophage inflammatory protein-1α was slightly but statistically significant reduced by G-CSF+BM MNC 48 hours. Besides that, none of the treatments had significant influence on cytokine levels (Figure I in the online-only Data Supplement).

Infarct Volume and Brain Edema

At day 1 after stroke, the mean edema-corrected infarct volume (%HLVe) amounted to 15.7±4.5% of the hemisphere without any differences between the experimental groups. Although the infarct volume remained constant during the first week after stroke, we observed a 30% increase of the infarct volume to 19.2±3.7% at day 30 (Figure 2). G-CSF monotherapy or combination therapy had no detectable impact on the infarct volume at any time point. The space-occupying effect of the ischemic lesion (%HSE) was maximally pronounced at day 1 after stroke and successively declined during the first week (Figure 2). At day 30, we measured negative values for %HSE that likely correspond to loss of hemispheric brain tissue and is consistent with the aforementioned increase of infarct volume at the same time point. Neither the early edema–related space-occupying effect nor the delayed brain atrophy was influenced by one of the treatments (Figure 2).

Functional Outcome After Stroke

We next used the adhesive removal test to monitor the clinical course within 30 days after stroke. To clearly define a hypothesis (treatment improves or impairs functional improvement), we a priori decided to perform a summarized analysis of the functional development by means of an area under the curve. At the baseline prior to stroke induction, rats needed ≈5 seconds to notice and remove the sticky tape from their contralateral forelimb. As expected, we observed a substantial increase of the tape removal time after stroke (to 91±37 seconds in the pMCAO-only control), which subsequently declined by ≈50% within 7 days to reach a constant level reflecting the permanent neurological deficit (Figure 3A). The area under the curve analysis revealed a statistically significant decrease of the tape removal time in G-CSF and a strong trend in the G-CSF+BM MNC 6 hours group (P=0.05). By contrast, the latter effect was

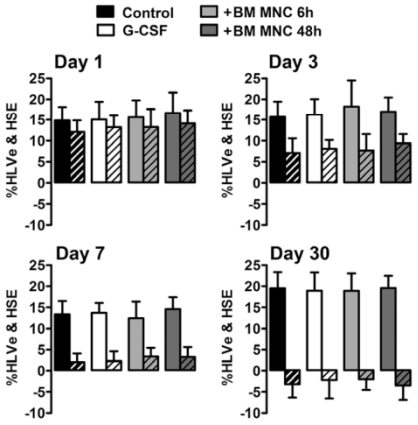

Figure 2. Determination of the corrected hemispheric infarct volume (%HLVe; solid bars) and space-occupying effect (%HSE; striped bars) at day 1, 3, 7, and 30. The %HSE was maximal at day 1 and successively declined until day 7 (ie, brain edema). The increase of %HLVe between days 7 and 30 was accompanied by negative values of %HSE at day 30 (ie, brain atrophy). None of the parameters (corrected lesion volume, brain edema, and brain atrophy) was influenced by any of the treatments; n=11 to 16 animals per group.

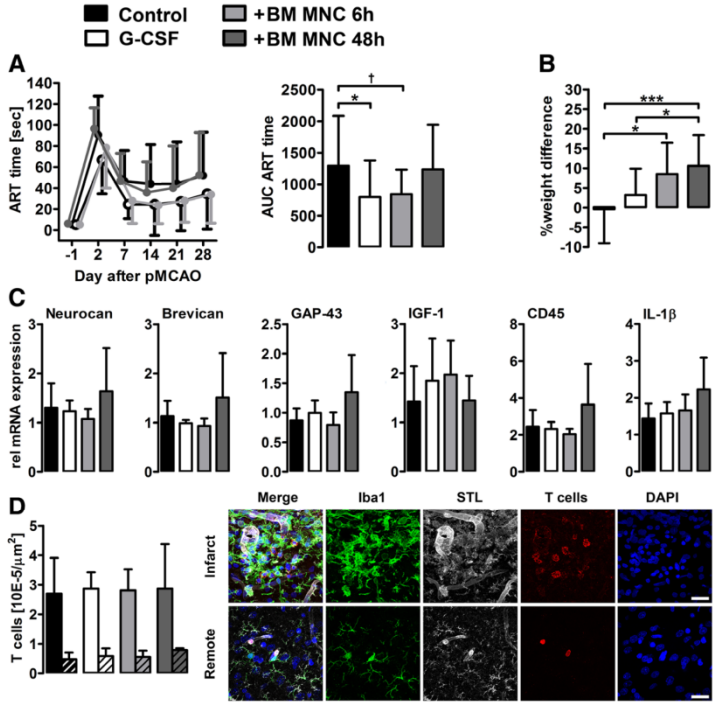

Figure 3. A, Assessment of neurological deficits using the adhesive removal test (ART). Experimental stroke caused a significant increase of ART time in all experimental groups, which was less pronounced after granulocyte colony-stimulating factor (G-CSF) and G-CSF plus bone marrow–derived mononuclear cells (BM MNC) 6 hours treatment. BM MNC transplantation at 48 hours was performed 12 hours before the ART at day 2. The area under the curve (AUC) analysis revealed a significantly improved functional recovery after G-CSF monotherapy and a strong trend by G-CSF+BM MNC 6 hours; †P=0.05. **B**, BM MNC therapy after 6 and 48 hours caused a significant increase of the body weight at day 30. **C**, Gene expression analysis of markers associated with inflammation and neural plasticity at day 30 after stroke. Treatment with G-CSF, G-CSF+BM MNC 6 hours or G-CSF+BM MNC 48 hours had no impact on the expression of analyzed genes (n=6 samples per group). **D**, T-cell counts in the ischemic lesion border (open bars) and the entire ipsilateral hemisphere (striped bars) were not altered by G-CSF or cell transplantation. The representative illustration of the infarct border zone showed a massive activation of ionized calcium-binding adapter molecule-1 (Iba1)–positive microglia/macrophages and abundance of extravascular T cells (vessels were stained with solanum tuberosum lectin [STL]). By contrast, T cells remote from the ischemic lesion were exclusively found within vessels. pMCAO indicates permanent right middle cerebral artery occlusion. *P<0.05, ***P<0.001 determined by 1-way ANOVA; n=16 to 17 animals per group; bars: 20 µm.

abolished in the G-CSF+BM MNC 48 hours group (Figure 3A). Body weights of all animals completely attained presurgery levels within the following days after stroke. Interestingly, after 30 days, we observed a significant increase of body weight in animals receiving BM MNC at 6 or 48 hours (Figure 3B).

Expression of Plasticity-Related Genes and Chronic Inflammation

Next, we investigated the expression of genes that are involved in neural regeneration and delayed inflammation in the ischemic hemisphere. Thirty days after stroke, the expression of Brevican, Neurocan, Gap-43 (Figure 3C), Versican, MARCKS, and Slit1 (Table III in the online-only Data Supplement) was not affected by any treatment. The growth factors insulin-like growth factor-1 (Figure 3C) and brain-derived neurotrophic factor (Table III in the online-only Data Supplement) showed a 1.5- to 2-fold increase in the ischemic hemisphere, but were not altered by G-CSF or G-CSF+BM MNC. Similarly, expression levels of IL-1β and CD45 were increased in the ischemic hemisphere 30 days after stroke, but did not differ among the experimental groups (Figure 3C). Immunohistochemical investigation revealed numerous T cells in the ischemic lesion 30 days after pMCAO, most of them located in the cortical infarct border. Neither G-CSF monotherapy nor cotransplantation of BM MNC altered T-cell counts in the ischemic brain (Figure 3D).

Short-Term Effects of Delayed Combination Treatment

Finally, we tried to elucidate the mechanisms behind the antagonizing effect of late BM MNC transplantation on the protective effect of G-CSF. Therefore, BM MNC were stained by the lipophilic membrane dye PKH26 to track short-term biodistribution. Labeling efficiency was 99.3±0.08% (n=3), and the dye had no impact on composition or vitality of the graft (data not shown). Four hours after intravenous transplantation of labeled BM MNC, we could identify PKH26$^+$ cells in all samples investigated (blood, spleen, BM, and brain tissue; Table). The composition of recovered PKH26$^+$ cells varied from the original graft, indicating differences in biodistribution or survival among the BM MNC subpopulations (Figure 4A). In the spleen, numerous PKH26$^+$ cells were found in the marginal zone between red and white pulp (Figure 4A), partly internalized by ionized calcium-binding adapter molecule-1–positive marginal zone macrophages (Figure II in the online-only Data Supplement). Gene expression analysis of spleen tissue revealed a significant increase of monocyte chemotactic protein-1 and IL-10 solely in the BM MNC 48 hours group (Figure 4B). By contrast, we observed a G-CSF–related increase of IL-1β mRNA (Figure 4B). Gene expression of chemokine (CC motif) ligand 6, chemokine (CXC motif) ligand 2, chemokine (CXC motif) ligand 5, high-mobility group box 1, IL-6, and tumor necrosis factor-α did not differ among the treatment groups (Table IV in the online-only Data Supplement). Spleen weights were significantly increased by G-CSF treatment, but not further influenced by BM MNC transplantation (control 530±23 mg versus G-CSF 640±41 mg versus G-CSF+BM MNC 48 hours, 629±14 mg; P<0.05 by 1-way ANOVA). Flow cytometric analyses exposed that the increased spleen weights were primarily caused by a tremendous increase of splenic granulocytes in both groups receiving G-CSF. The latter effect was most pronounced after BM MNC transplantation at 48 hours (Figure 4C). By using an annexin V/7-aminoactinomycin D flow cytometric assay,

Table. Total Amount of PKH26⁺ Cells 4 Hours After Transplantation

	PKH26⁺ Cells (Mean±SD)
Graft (in 0.8 mL), body weight–adapted	4 065 000±187 350
Blood (in 1 mL)	1219±584
Spleen	67 788±11 119
Bone marrow (1 femur bone)	4281±1071
Brain: stroke hemisphere	284±127
Brain: contralateral hemisphere	112±78

we found most of the splenic granulocytes being vital. A small fraction of necrotic granulocytes was also increased by BM MNC when compared with the G-CSF group (Figure 4C). Finally, we quantified immune cells within the ischemic (Figure 4D) and contralateral hemisphere (Figure III in the online-only Data Supplement) 52 hours after experimental stroke. Transplantation of BM MNC after 48 hours caused a significant increase of vital granulocytes in the ischemic hemisphere when compared with the G-CSF or control group (Figure 4D). Interestingly, almost half of all granulocytes in the ischemic brain were early apoptotic; however, neither G-CSF monotherapy nor BM MNC cotransplantation had an effect on the extent of this fraction (Figure 4D).

Discussion

In this study, we aimed to investigate the potential synergistic effect of 2 successfully tested experimental treatments for stroke: the repeated injection of G-CSF combined with transplantation of BM MNC. Our study yielded 3 major findings: first, we observed that G-CSF, neither alone nor in combination with BM MNC, had any impact on our primary end point, the infarct volume. Second, we found that a monotherapy with G-CSF and the cotransplantation of BM MNC after 6 hours significantly improved functional recovery. Surprisingly, this effect was entirely abolished when BM MNC were given after 48 hours. Finally, we found that G-CSF with and without auxiliary cell therapy significantly altered systemic immune responses to stroke.

The neuroprotective effect of G-CSF has been discovered and mechanistically defined in a landmark study by Schneider et al,[13] who showed that G-CSF provides strong antiapoptotic effects in neurons exposed to ischemia. Many studies

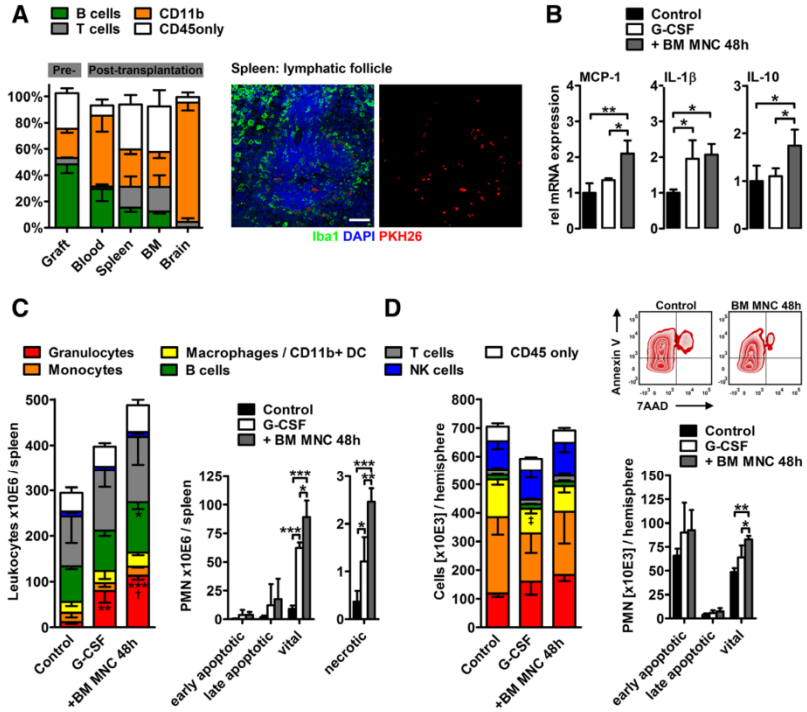

Figure 4. Short-term effects of the combined treatment with granulocyte colony-stimulating factor (G-CSF) and bone marrow–derived mononuclear cells (BM MNC) at 48 hours after stroke. **A**, Biodistribution analysis 4 hours after cell transplantation revealed a reduced proportion of B cells in the blood, spleen, bone marrow (BM), and brain. In the circulation, primarily CD11b⁺ monocytes were positive for the cell marker PKH26, whereas T cells and CD45-only cells were enriched in the spleen and BM. Almost all PKH26⁺ cells in the brain were CD11b⁺. Immunofluorescence staining of spleen sections revealed an accumulation of PKH26⁺ cells in the marginal zone around the lymphatic follicles. **B**, Gene expression analysis of the spleen showed a significant increase of monocyte chemotactic protein-1 (MCP-1) and interleukin (IL)-10 after BM MNC transplantation. By contrast, IL-1β mRNA was increased by G-CSF, but not further affected by cell therapy. **C**, Flow cytometric quantification of major leukocyte populations in the spleen showed a distinct increase of granulocytes after G-CSF treatment, further increased by BM MNC transplantation. The vast majority of splenic granulocytes were vital, reflecting the group differences of total granulocytes. Necrotic granulocyte counts were doubled by G-CSF and quintupled by G-CSF+BM MNC 48 hours. **D**, Major leukocyte subpopulation in the ischemic brain did not differ between the experimental groups; however, vital granulocytes were significantly increased after BM MNC transplantation. Iba1 indicates ionized calcium-binding adapter molecule-1; and PMN, polymorphonuclear cells (granulocytes). †P<0.05 vs G-CSF, *P<0.05, **P<0.01, ***P<0.001, ‡P=0.06 determined by 1-way ANOVA; n=3 animals per group; bar: 20 μm.

reproduced this finding and 2 meta-analyses consistently confirmed a significant impact of G-CSF on the infarct volume, the most frequently used surrogate for neuroprotection.[2,3] Interestingly, the same meta-analysis revealed, in contrast to one recent study,[14] that the infarct volume was not influenced by G-CSF treatment in permanent stroke,[2] likely owing to the fact that the neuroprotective time window is shorter in permanent stroke (3 hours) compared with the classical ischemia/reperfusion models (up to 12 hours).[15] In SHR, neuroprotection is even limited to the first 60 minutes after MCAO.[16] We hence reasoned that the lack of influence of G-CSF treatment and cell transplantation on the ischemic lesion is likely caused by the absence of reperfusion and the comorbidities present in SHR. Conversely, the functional effect of G-CSF observed in our study is likely mediated by mechanism beyond neuroprotection. This is highly relevant for translational stroke research,[11,15] but it should also be noted that inbred SHR may be compromised by genetic aberrations that could bias the value of our experiment.

G-CSF has an impact on various pathophysiological aspects relevant for stroke outcome: it promotes endogenous neurogenesis and angiogenesis, modulates immune responses, reduces brain edema, and enhances structural and functional regeneration capacities of the central nervous system.[17] These mechanisms could explain the significant functional improvement after G-CSF treatment that was prevalent in most of the published preclinical experiments[2,3] being corroborated by ours. Angiogenesis and neurogenesis were not investigated here. However, we examined the expression of various growth-promoting and growth-inhibiting genes during the late stage of poststroke axonal sprouting[18] (day 30) but found no differences between any treatment regime and control. Furthermore, and again in contrast to another study using a reperfusion model of stroke,[19] we found that the brain edema was also not influenced by G-CSF.

With respect to the early functional improvement observed in our study, we suggest acute immunologic interactions as one key mechanism for the efficacy of G-CSF and its antagonization by late BM MNC transplantation. Two days after stroke, we found a significant decline of circulating $CXCR4^+$ mononuclear cells in all treatment groups, likely as a consequence of chemokine receptor downregulation by G-CSF.[20] Recent studies showed that early CXCR4 antagonism significantly improved outcome after stroke by regulating the infiltration of leukocytes into the ischemic brain.[21] In this manner, G-CSF may dampen central nervous system inflammation and damage, and in fact, we found a strong trend toward less macrophages/dendritic cells infiltrating the ischemic lesion in G-CSF–treated animals.

Interestingly, we found a recovery of depressed spleen weights and circulating leukocyte counts in all groups receiving G-CSF. Postischemic immunodepression is a consequence of an overactivated cholinergic anti-inflammatory pathway finally contributing to morbidity after stroke.[12] We found no evidence for infections, such as increased mortality or decreased body weights in our study, but the restoration of immunocompetence by G-CSF may have protected the brain from chronic central nervous system inflammation.[22] In fact, we found ongoing immune responses including an accumulation of T cells at the infarct border at day 30 after stroke, but T-cell counts and brain atrophy were not influenced by G-CSF treatment or accompanying cell therapy.

One surprising finding of our study was that transplantation of BM MNC after 48 hours completely neutralized the beneficial effect of G-CSF. Early transplantation of BM MNC after transient stroke in SHR have had no positive or negative impact on functional outcome[23]; however, it is possible that late BM MNC transplantation is detrimental after stroke and simply deleted the protective effects of the accompanying G-CSF therapy. This notion remains hypothetical because we did not investigate the exclusive effect of late BM MNC transplantation here. Nevertheless, adverse effects of BM-derived cells have been described in animal models of diabetes mellitus and arteriosclerosis,[24,25] suggesting a compromised cell graft under translationally relevant conditions of hyperglycemia and hypertension.[26,27]

We found almost 30% of the BM MNC being apoptotic before transplantation, a finding that may reflect hypertension-related oxidative stress in the BM.[26,27] In steady state, circulating apoptotic cells were trapped by specialized splenic macrophages in the marginal zone between red and white pulp.[28] This endogenous scavenging system carefully downregulates immune-stimulatory functions and helps to maintain self-tolerance.[29] It is thus tempting to speculate that the intravenous transplantation of numerous (pre)apoptotic BM MNC may induce endogenous anti-inflammatory programs,[30,31] and in fact, we found an accumulation of BM MNC in the splenic marginal zones together with increased expression of anti-inflammatory mediators.

Intriguingly, this assumed universal mechanism for intravenously administered cells may also explain the interaction effect between late BM MNC and G-CSF found in our study. Circulating granulocytes have a short half-life and are continuously cleared in the splenic marginal zone. Mice deficient for marginal zone macrophages develop increased granulocyte counts and IL-1β levels.[32] Accordingly, we found that treatment with G-CSF caused a 10-fold increase of splenic granulocytes and 2-fold increase of IL-1β expression, indicating an overload of the granulocyte clearance system. The simultaneous engagement of marginal zone macrophages with transplanted BM MNC and massively increased granulocytes may further overload this scavenging system, as it has been shown after the application of polystyrene particles.[33] This would explain the significant increase of vital granulocytes in the blood, spleen, and brain of animals that received BM MNC at the peak point of G-CSF–induced neutrophilia. Higher neutrophil counts in the brain could finally explain the negative functional effect either by disturbing the microcirculation or by releasing toxic mediators.[34]

Conclusions

In our study, we could confirm the beneficial effect of G-CSF on long-term functional recovery, but not on neuroprotection after stroke in hypertensive rats. The cotreatment with BM MNC was without effect after 6 hours, but reversed the protective effect of G-CSF after 48 hours, probably by overloading the splenic scavenging system by the apoptotic fraction of BM MNC and massively increased granulocytes.

Acknowledgments

We thank Isabelle Glocke, Sebastian Baasch, Christin Kellner, Isabell Schulz, and Natalia Shurawel for excellent technical support, and Karoline Möller and Dr Gesa Weise for helpful discussions.

Sources of Funding

This work was supported by the German Federal Ministry of Education and Research (grant number 01GN0981).

Disclosures

Dr Schäbitz is an inventor on a patent claiming the use of granulocyte colony-stimulating factor for the treatment of stroke. The other authors report no conflicts.

References

1. Ringelstein EB, Thijs V, Norrving B, Chamorro A, Aichner F, Grond M, et al; AXIS 2 Investigators. Granulocyte colony-stimulating factor in patients with acute ischemic stroke: results of the AX200 for Ischemic Stroke trial. *Stroke*. 2013;44:2681–2687.
2. England TJ, Gibson CL, Bath PM. Granulocyte-colony stimulating factor in experimental stroke and its effects on infarct size and functional outcome: a systematic review. *Brain Res Rev*. 2009;62:71–82.
3. Minnerup J, Heidrich J, Wellmann J, Rogalewski A, Schneider A, Schäbitz WR. Meta-analysis of the efficacy of granulocyte-colony stimulating factor in animal models of focal cerebral ischemia. *Stroke*. 2008;39:1855–1861.
4. O'Collins VE, Macleod MR, Donnan GA, Howells DW. Evaluation of combination therapy in animal models of cerebral ischemia. *J Cereb Blood Flow Metab*. 2012;32:585–597.
5. Dunac A, Frelin C, Popolo-Blondeau M, Chatel M, Mahagne MH, Philip PJ. Neurological and functional recovery in human stroke are associated with peripheral blood CD34+ cell mobilization. *J Neurol*. 2007;254:327–332.
6. England TJ, Abaei M, Auer DP, Lowe J, Jones DR, Sare G, et al. Granulocyte-colony stimulating factor for mobilizing bone marrow stem cells in subacute stroke: the stem cell trial of recovery enhancement after stroke 2 randomized controlled trial. *Stroke*. 2012;43:405–411.
7. Petit I, Szyper-Kravitz M, Nagler A, Lahav M, Peled A, Habler L, et al. G-CSF induces stem cell mobilization by decreasing bone marrow SDF-1 and up-regulating CXCR4. *Nat Immunol*. 2002;3:687–694.
8. Fujita Y, Ihara M, Ushiki T, Hirai H, Kizaka-Kondoh S, Hiraoka M, et al. Early protective effect of bone marrow mononuclear cells against ischemic white matter damage through augmentation of cerebral blood flow. *Stroke*. 2010;41:2938–2943.
9. Kasam M, Yang B, Strong R, Schaar K, Misra V, Xi X, et al. Nitric oxide facilitates delivery and mediates improved outcome of autologous bone marrow mononuclear cells in a rodent stroke model. *PLoS One*. 2012;7:e32793.
10. Savitz SI, Misra V, Kasam M, Juneja H, Cox CS Jr, Alderman S, et al. Intravenous autologous bone marrow mononuclear cells for ischemic stroke. *Ann Neurol*. 2011;70:59–69.
11. Sena E, van der Worp HB, Howells D, Macleod M. How can we improve the pre-clinical development of drugs for stroke? *Trends Neurosci*. 2007;30:433–439.
12. Prass K, Meisel C, Höflich C, Braun J, Halle E, Wolf T, et al. Stroke-induced immunodeficiency promotes spontaneous bacterial infections and is mediated by sympathetic activation reversal by poststroke T helper cell type 1-like immunostimulation. *J Exp Med*. 2003;198:725–736.
13. Schneider A, Krüger C, Steigleder T, Weber D, Pitzer C, Laage R, et al. The hematopoietic factor G-CSF is a neuronal ligand that counteracts programmed cell death and drives neurogenesis. *J Clin Invest*. 2005;115:2083–2098.
14. Bråtane BT, Bouley J, Schneider A, Bastan B, Henninger N, Fisher M. Granulocyte-colony stimulating factor delays PWI/DWI mismatch evolution and reduces final infarct volume in permanent-suture and embolic focal cerebral ischemia models in the rat. *Stroke*. 2009;40:3102–3106.
15. Hossmann KA. The two pathophysiologies of focal brain ischemia: implications for translational stroke research. *J Cereb Blood Flow Metab*. 2012;32:1310–1316.
16. Legos JJ, Lenhard SC, Haimbach RE, Schaeffer TR, Bentley RG, McVey MJ, et al. SB 234551 selective ET(A) receptor antagonism: perfusion/diffusion MRI used to define treatable stroke model, time to treatment and mechanism of protection. *Exp Neurol*. 2008;212:53–62.
17. Minnerup J, Sevimli S, Schäbitz WR. Granulocyte-colony stimulating factor for stroke treatment: mechanisms of action and efficacy in preclinical studies. *Exp Transl Stroke Med*. 2009;1:2.
18. Carmichael ST, Archibeque I, Luke L, Nolan T, Momiy J, Li S. Growth-associated gene expression after stroke: evidence for a growth-promoting region in peri-infarct cortex. *Exp Neurol*. 2005;193:291–311.
19. Gibson CL, Jones NC, Prior MJ, Bath PM, Murphy SP. G-CSF suppresses edema formation and reduces interleukin-1beta expression after cerebral ischemia in mice. *J Neuropathol Exp Neurol*. 2005;64:763–769.
20. Kim HK, De La Luz Sierra M, Williams CK, Gulino AV, Tosato G. G-CSF down-regulation of CXCR4 expression identified as a mechanism for mobilization of myeloid cells. *Blood*. 2006;108:812–820.
21. Huang J, Li Y, Tang Y, Tang G, Yang GY, Wang Y. CXCR4 antagonist AMD3100 protects blood-brain barrier integrity and reduces inflammatory response after focal ischemia in mice. *Stroke*. 2013;44:190–197.
22. Becker KJ, Kindrick DL, Lester MP, Shea C, Ye ZC. Sensitization to brain antigens after stroke is augmented by lipopolysaccharide. *J Cereb Blood Flow Metab*. 2005;25:1634–1644.
23. Minnerup J, Wagner DC, Strecker JK, Pösel C, Sevimli-Abdis S, Schmidt A, et al. Bone marrow-derived mononuclear cells do not exert acute neuroprotection after stroke in spontaneously hypertensive rats. *Front Cell Neurosci*. 2014;7:288.
24. Chen J, Ye X, Yan T, Zhang C, Yang XP, Cui X, et al. Adverse effects of bone marrow stromal cell treatment of stroke in diabetic rats. *Stroke*. 2011;42:3551–3558.
25. Silvestre JS, Gojova A, Brun V, Potteaux S, Esposito B, Duriez M, et al. Transplantation of bone marrow-derived mononuclear cells in ischemic apolipoprotein E-knockout mice accelerates atherosclerosis without altering plaque composition. *Circulation*. 2003;108:2839–2842.
26. Campagnaro BP, Tonini CL, Doche LM, Nogueira BV, Vasquez EC, Meyrelles SS. Renovascular hypertension leads to DNA damage and apoptosis in bone marrow cells. *DNA Cell Biol*. 2013;32:458–466.
27. Karcher JR, Greene AS. Bone marrow mononuclear cell angiogenic competency is suppressed by a high-salt diet. *Am J Physiol Cell Physiol*. 2014;306:C123–C131.
28. Miyake Y, Asano K, Kaise H, Uemura M, Nakayama M, Tanaka M. Critical role of macrophages in the marginal zone in the suppression of immune responses to apoptotic cell-associated antigens. *J Clin Invest*. 2007;117:2268–2278.
29. Green DR, Ferguson T, Zitvogel L, Kroemer G. Immunogenic and tolerogenic cell death. *Nat Rev Immunol*. 2009;9:353–363.
30. Voll RE, Herrmann M, Roth EA, Stach C, Kalden JR, Girkontaite I. Immunosuppressive effects of apoptotic cells. *Nature*. 1997;390:350–351.
31. Yang B, Migliati E, Parsha K, Schaar K, Xi X, Aronowski J, et al. Intra-arterial delivery is not superior to intravenous delivery of autologous bone marrow mononuclear cells in acute ischemic stroke. *Stroke*. 2013;44:3463–3472.
32. Gordy C, Pua H, Sempowski GD, He YW. Regulation of steady-state neutrophil homeostasis by macrophages. *Blood*. 2011;117:618–629.
33. Knudsen E, Benestad HB, Seierstad T, Iversen PO. Macrophages in spleen and liver direct the migration pattern of rat neutrophils during inflammation. *Eur J Haematol*. 2004;73:109–122.
34. Segel GB, Halterman MW, Lichtman MA. The paradox of the neutrophil's role in tissue injury. *J Leukoc Biol*. 2011;89:359–372.

SUPPLEMENTAL MATERIAL

Bone marrow cell transplantation time-dependently abolishes efficacy of G-CSF after stroke in hypertensive rats

#Claudia Pösel, Dipl Ing FH; Johanna Scheibe, PhD; Alexander Kranz, MD; Viktoria Bothe, MSc; Elfi Quente; Wenke Fröhlich; Franziska Lange, PhD; Wolf-Rüdiger Schäbitz, MD; Jens Minnerup, MD; *Johannes Boltze, MD, PhD; *Daniel-Christoph Wagner, MD

Supplemental methods

Experimental stroke

Animal experiments were conducted according to the Guide for the Care and Use of Laboratory Animals published by the US National Institutes of Health (NIH Publication No. 85-23, revised 1996), and approved by the appropriate regional authorities (reference number TVV 12/11). A total of 81 spontaneously hypertensive rats (SHR; Charles River, Sulzfeld, Germany) at the age of 12 weeks were anesthetized with ketamine hydrochloride (100mg/kg) and xylazine (10mg/kg) given as an intraperitoneal injection. During the surgical procedure, body core temperature was constantly measured and maintained at 37.5°C. Experimental stroke was induced by permanent occlusion of the right middle cerebral artery (pMCAO) as described previously.[1] Briefly, the right temporal scull bone and dura mater were opened, and the subjacent middle cerebral artery was permanently occluded by thermocoagulation. Health status including the body weight was monitored daily within the first week after stroke and weekly thereafter. The exclusion criteria were defined as follows: i) weight loss of more than 20% body weight during week 1; ii) absence of a cortical brain lesion typical for distal MCAO in the MR sequence; iii) incomplete injection of G-CSF, cell suspension or vehicle solution.

Experimental group allocation

In the first study, we defined the reduction of the infarct volume (%HLVe, see below) by at least 30% as primary endpoint. Accordingly, the sample sizes were a priori calculated for an expected difference of the mean of 30% with α=0.05 and β=0.8 for a one-way ANOVA (Sigma Plot version 11.0). The expected standard deviation (σ=3.2 %HLVe) was obtained from a previous study (day 1 and day 3 after pMCAO from SHRs).[2] SHRs were randomly assigned (balanced randomization by lot) to one of the following experimental groups: (i) G-CSF monotherapy group (henceforth G-CSF, n=18) with a daily intraperitoneal injection of 50 µg/kg Neupogen (rhG-CSF; Amgen GmbH, Thousand Oaks, USA) for 5 days starting 1h after pMCAO; (ii) combination group with early cell transplantation (henceforth G-CSF+BM MNC 6h, n=18) with a G-CSF schedule according to (i) and an additional transplantation of 1.5x10E7 BM MNCs per kg bodyweight at 6h after pMCAO; (iii) combination group with late cell transplantation (henceforth G-CSF+BM MNC 48h, n=18) with a G-CSF schedule according to (i) and an additional transplantation of 1.5x10E7 BM MNCs per kg bodyweight at 48h after pMCAO; (iv) control group (henceforth control, n=18) receiving phosphate buffered saline (PBS) instead of G-CSF and BM MNCs. The administrations in all treatment groups were completely controlled by PBS injections, meaning, for instance, that the G-CSF group received PBS injections at 6h and 48h after stroke.

In the second study, we investigated the distribution of PKH26-labeled BM MNC and the short-term immunological responses to late transplantation of BM MNC (48h). Nine animals were randomly assigned to the following experimental groups (in accordance with the first study): (i) G-CSF, n=3; (iii) G-CSF+BM MNC 48h, n=3; (iv) control group, n=3.

BM MNC isolation and transplantation

Syngeneic rat bone marrow mononuclear cells (BM MNC) were enriched by magnetic depletion of granulocytes as described previously[3] and cryo-preserved until further use. At the day of cell transplantation, BM MNCs were re-thawed in Dulbecco's modified Eagle's medium containing 4.5g/L glucose (PAA Laboratories, Cölbe, Germany) and 10% fetal calf serum (FCS; PAN Biotech, Aidenbach, Germany), washed twice in medium. Vital cell numbers were determined by the trypan blue exclusion method using a hemocytometer. Cellular composition of cell grafts was characterized by flow cytometry for B cells (CD45R+), T cells (CD3+) and myeloid cells (CD11b+ and RP1-; for details please refer to supplemental table I). CXCR4+ BM MNC were identified by polyclonal rabbit anti-rat CXCR4 (Abcam, Cambridge, UK) which was secondly labeled with donkey anti-rabbit PE (ebioscience, San Diego, USA). Hematopoietic progenitors expressing CD34 (polyclonal goat anti-rat; R&D Systems, Minneapolis, USA) were secondly conjugated with donkey anti-goat PE-Cy™5 (Santa Cruz Biotechnology, Dallas, USA) and differentiated in bipotent hematopoietic progenitors using granulocyte-macrophage colony forming unit assay (CFU-GM) as described elsewhere.[3]

For the analysis of the biodistribution, BM MNC were labeled with the red fluorescent dye PKH26 according to the manufacturer's instructions (Sigma Aldrich, St. Louis, USA).

Prior to transplantation, 1.5x10E7 BM MNCs per kg bodyweight were resuspended in 800µl PBS. Cell suspension was slowly administered via the tail vein. The application of G-CSF, BM MNCs or vehicle solution was performed by an investigator blinded to the group allocation 12h prior to functional testing and MR imaging.

Analysis of peripheral blood leukocytes and cytokine levels

Peripheral blood and serum samples were collected at 6h, 48h, 52h, 96h and 144h after pMCAO. Anticoagulated blood samples were harvested in 0,2M EDTA and stored in EDTA-monovettes for hematological analysis. Absolute leukocyte counts were determined by an animal blood cell counter (scil Vet abc, SCIL animal care company GmbH, Viernheim, Germany). Leukocyte subsets were identified and categorized according to their antigen expression (for details please refer to supplemental table I) using multichannel flow cytometry. Natural killer (NK) cells were identified by biotinylated anti-CD161a and secondly conjugated with streptavidin Horizon™V500 (BD Pharmingen, Heidelberg, Germany). Purified CXCR4 was secondly labeled with donkey anti–rabbit PE as mentioned above (ebioscience, San Diego, USA). For this, 50µL of blood were diluted in 50µL PBS and incubated with a mixture of monoclonal antibodies (supplemental table I) for 20min at 4°C. Erythrocytes were lysed by short-term incubation (30 seconds) with distilled water followed by two washing steps with PBS containing 3% fetal calf serum (PBS/3% FCS). Remaining leukocytes were resuspended in 300µL PBS/3% FCS. Flow cytometric acquisition and analysis was performed using a FACS Canto II equipped with FACS Diva software (BD Biosciences, Heidelberg, Germany). For the quantification of circulating cytokine levels, serum (n=6 per group and day, randomly assigned by lot) was separated from 300µl coagulated blood samples by centrifugation at 5000 rpm for 5min and stored in aliquots at -80°C. Cytokine secretion levels of IFNγ, IL-4, IL-10, IL-17A, MCP-1 and MIP-1α were analyzed by multiparametric ELISA (Multimetrix GmbH, Regensburg, Germany).

Biodistribution study and flow cytometric analysis of spleen and brain tissue

Animals from the second study were sacrificed exactly 52h after stroke and transcardially perfused with 200mL of ice-cold PBS. Spleens, femur bones and brains were removed. Spleens were weighed and segmented into three parts for (i) histological analyses, (ii) for gene expression analysis and (iii) for flow cytometric analyses.

For flow cytometry, spleens were mechanically dissected using razor blades and further dissociated through 100µm and 40µm cell strainers using glass pestles. Bone marrow was harvested from one femur bone by repeated flushing with PBS. Total cell counts and viability were determined by trypan blue exclusion in a hemocytometer. Total leukocyte counts were defined by counting in Turk's solution. Single cell suspensions of the ischemic and contralateral brain hemispheres were isolated by mechanical dissection and enzymatic digestion as described previously[4]. Immune cells were separated by density gradient centrifugation on discontinuous Percoll (GE Healthcare, München, Germany) gradients composed of four sequent layers (80%/38%/21% Percoll covered with cell culture medium). Cells accumulating in between 80%/38% Percoll were harvested and washed repeatedly. Total counts of brain leukocytes were determined by additional Trucount Tube measurements (BD Biosciences). Frequencies of PKH26+ cells and of major leukocyte populations were assessed by flow cytometry. In total, 1x10E6 isolated spleen or bone marrow cells and 2x10E5 brain cells were incubated with a specific FC-blocking reagent (purified anti-rat CD32; BD Bioscience) for 10min at 4°C and labeled with a mixture of monoclonal antibodies (supplemental table I). After incubation for 20min at 4°C, cells were washed and incubated with annexin V PE-Cy™7 (ebioscience, San Diego, USA) in 100 µL annexin V binding buffer for 15min at room temperature. After washing, cells were stained with 7-AAD viability staining solution (ebioscience). Flow cytometric acquisition and analysis was performed by an investigator blinded to the group allocation using a 3-laser FACS Canto II equipped with FACS Diva software (BD Biosciences).

Determination of infarct volume

The infarct volume and space occupying effect of the lesion were determined in vivo by means of magnetic resonance imaging (MRI) at day 1, 3, 7 and 30. Image sequences were acquired in clinical MR scanner (1.5 T Gyroscan Intera human whole-body spectrometer equipped with a 47mm loop RF-Coil, Philips). Briefly, animals were anesthetized as described above. T2-weighted sequences (T2-TSE) consisting of 20 transverse slices (matrix: 224×224; field of view: 50mm; slice thickness: 1mm) were acquired. Hemispheric lesion volume corrected for edema (%HLVe) and hemispheric space occupying effect (%HSE) of the lesion were calculated by a blinded investigator as described previously.[5]

Assessment of functional recovery

Neurological deficits were repeatedly assessed by means of the adhesive removal test (ART) as described previously.[6] Animals were allowed to adapt to the ART conditions for 3 days. The baseline data was ascertained one day before pMCAO. Following pMCAO, ART was performed at day 2, 7, 14, 21 and 28 by an investigator blinded to group allocation. The time needed to remove the adhesive tape was measured in technical triplicates that were averaged for one individual at each day. For the statistical analysis, time series data was summarized as individual area under the curve (AUC).

Quantitative RT-PCR

Animals were sacrificed and transcardially perfused with 200mL of ice-cold PBS. Spleen segments, ipsilateral and contralateral brain tissue were manually dissociated by razor blades. Next, total RNA of 100mg tissue was extracted by homogenization in 1mL Trizol using a ULTRA-TURRAX® (Ika, Staufen, Germany) and further purified by RNeasy Mini Kit (Qiagen, Hilden, Germany). Single-strand cDNA copies were generated from 1µg of total purified RNA by using random primers (Promega, Mannheim, Germany) and Superscript III reverse transcriptase (Invitrogen/Life Technologies, Darmstadt, Germany) according to manufacturer's instructions. Quantification of mRNA expression was performed and monitored using an ABI 7900 real-time PCR system (Applied Biosystems, Darmstadt,

Germany) applying the following conditions: initial denaturation at 95°C for 10min, followed by 50 cycles at 95°C for 15s and 55°C for 1min. All qRT-PCR reactions were conducted in a total volume of 15µL with addition of Power SYBR Green I PCR Master Mix (Applied Biosystems, Darmstadt, Germany) and gene specific QuantiTect® Primer Assay (supplemental table III for brain and supplemental table IV for spleen; Qiagen, Hilden, Germany). Data was analyzed using the relative standard curve method, normalized on the average cycle threshold of the housekeeping genes *B2m* (QT00176295, NM_012512), *Rpl13a* (QT00425873, NM_173340), *Rpl22* (QT00385119, NM_031104) and *Yhwaz* (QT02382184, NM_013011) and normalized to the control group (spleen tissue) or to the contralateral hemisphere (brain tissue).

Histological analysis

30 days after stroke, animals were sacrificed and transcardially perfused with 200mL of PBS and 200mL of formalin solution (4%). Removed brains were vitrified in sucrose solution (30%) and cryoconserved at -80°C. Frozen brains were cut into 20µm coronal sections and mounted on coated slides. Brain sections (n=4 animals per group, randomly assigned by lot) were incubated with 5% goat serum and 0.3% Trition-X-100 for 30 minutes, followed by polyclonal rabbit anti-Iba1 (Ionized calcium binding adaptor molecule 1; 1:200; Wako Chemicals, Neuss, Germany), monoclonal mouse anti-15-16A1 (1:500; Hycult Biotech, Beutelsbach, Germany; for T cells) and biotinylated solanum tuberosum lectin (STL; 1:300; Linaris, Dossenheim, Germany) for 24h at 4°C. Sections were then incubated with goat anti-rabbit IgG (1:200, Invitrogen), goat anti-mouse IgG (1:200, Invitrogen) or streptavidin (Dianova) conjugated with either Alexa Fluor® 488, 546 or Cy5 for 1h at room temperature. Sections were counterstained with DAPI (2.5µg/mL, Sigma). Fluorescence images were acquired using a Zeiss LSM710 confocal laser-scanning microscope (Objective: Plan-Apochromat 63x / 1.40 oil). T cells were counted in 4 brain regions (Bregma anteroposterior +1.5mm, 1.0mm, 0.5mm and 0.0mm) in technical duplicates using a Stereo Investigator system (MBF Bioscience). Briefly, two regions of interest (ROI) were defined as “ipsilateral hemisphere” and “infarct border”, the latter define as a 100µm deep band adjacent to the border of the pseudocyst. The area of the ROIs, and the T cell count within the ROIs were determined by an investigator blinded to the group allocation. Finally, T cell counts were summarized for each biological replicate and indicated as cells per area.

Spleen segments were fixed in formalin solution (4%) for 48h, vitrified in sucrose solution (30%) and cryoconserved at -80°C. Frozen spleens were cut into 20µm coronal sections and mounted on coated slides. Sections were incubated with 5% goat serum and 0.3% Trition-X-100 for 30 minutes, followed by primary incubation with polyclonal rabbit anti-Iba1 for 24h at 4°C and secondary labeling with Alexa Fluor® 488 conjugated goat anti-rabbit IgG for 1h at room temperature. Sections were counterstained with DAPI (2.5µg/mL, Sigma).

Statistical analysis

Peripheral leukocyte counts, summarized ART data, brain histology were analyzed by one-way ANOVA followed by Bonferroni’s post-hoc test. Time series of serum cytokine levels and MR investigations were analyzed by repeated measures two-way ANOVA followed by Bonferroni’s post-hoc test. Immune cell distribution in spleen and brain tissue was analyzed by one-way ANOVA followed by Newman-Keuls test. A p-value of less than 0.05 was considered statistically significant. All data were displayed as mean ± standard deviation (SD). Data analysis was performed by Graph Pad Prism (version 5.03).

Supplemental Tables

Supplemental Table I
Anti-rat monoclonal antibodies used for flow cytometry

		Panel		Identification						
Antigen	**Conjugate**	**Clone**	**Manufacturer**	**B cells**	**T cells**	**NK cells**	**Mo***	**Ma#**	**PMN†**	**CD45 only**
CD11b	Pacific Blue™	MRC OX-42	Abd Serotec	-	-	+	+	+	+	-
CD161a	Biotin	Okt 78	BD Bioscience	-	-	+	n.a.$	n.a.$	-	-
CD3	APC	1F4	BD Bioscience	-	+	-	-	-	-	-
CD4	PE-Cy™7	W3/25	Biolegend	-	(+)	-	n.a.$	n.a.$	-	-
CD45	APC-Cy™7	OX-1	BD Bioscience	+	+	+	+	+	+	+
CD45R	FITC	HIS24	BD Bioscience	+	-	-	-	-	-	-
CD8a	PerCP	OX-8	BD Bioscience	-	(+)	(+)	n.a.$	n.a.$	-	-
MHCII	Alexa Fluor® 488	OX-6	Abd Serotec	+	n.a.$	n.a.$	-	+	-	-
PMN†	PE	RP-1	BD Bioscience	-	-	-	-	-	+	-

*Monocytes; #Macrophages; †Polymorphonuclear cells (Granulocytes) $not analyzed

Supplemental Table II
Animals excluded from MR investigation

	Day			
	1	**3**	**7**	**30**
Control	1	4	2	2
G-CSF	0	2	1	1
GCSF+BM MNC 6h	1	2	2	1
GCSF+BM MNC 48h	2	2	1	1

Supplemental Table III
Relative mRNA expression within the ischemic hemisphere 30 days after stroke

	QuantiTect primer assay	**Transcript**	**Control**		**G-CSF**		**+BM MNC 6h**		**+BM MNC 48h**	
			M$	SD#	M	SD	M	SD	M	SD
BDNF	QT00375998	NM_012513	1.61	1.15	1.29	0.73	1.34	0.56	1.55	0.91
Brevican	QT00176638	NM_012916	0.97	0.06	0.96	0.10	0.88	0.12	1.05	0.32
CD45	QT01797957	NM_001109887	2.11	0.49	2.21	0.39	1.80	0.27	2.43	0.47
Gap-43	QT00184520	NM_017195	0.83	0.11	1.01	0.14	0.77	0.16	1.03	0.42
IGF-1	QT01745373	NM_001082479	1.28	0.64	1.67	0.73	1.61	0.58	1.72	1.13
IL-1ß	QT00181657	NM_031512	1.27	0.40	1.42	0.23	1.42	0.32	1.60	0.32
MARCKS	QT01573418	XM_001060954	0.99	0.24	1.20	0.29	1.00	0.13	1.15	0.37
Neurocan	QT00177240	NM_031653	1.14	0.26	1.17	0.21	0.97	0.12	1.19	0.29
Slit1	QT00189007	NM_022953	0.86	0.09	1.02	0.15	0.96	0.21	1.06	0.34
Versican	QT01598814	XM_001058160	1.07	0.22	1.10	0.13	0.94	0.19	1.14	0.33

$mean; #standard deviation; n=6 per group

Supplemental Table IV
Relative mRNA expression within the spleen 52h after stroke

	QuantiTect primer assay	Transcript	Control		G-CSF		+BM MNC 48h	
			M[$]	SD[#]	M	SD	M	SD
CCL6	QT01573523	NM_001004202	1.00	0.13	1.70	0.17	1.60	0.20
CXCL2	QT00184891	NM_053647	1.00	0.56	1.70	0.31	2.50	0.49
CXCL5	QT00392777	NM_022214	1.00	0.07	0.84	0.10	1.10	0.18
HMGB1	QT00368410	NM_012963	1.00	0.04	0.92	0.05	0.94	0.05
IL-1ß	QT00181657	NM_031512	1.00	0.05	2.00	0.30	2.10	0.17
IL-6	QT00182896	NM_012589	1.00	0.08	0.80	0.10	0.85	0.05
IL-10	QT00177618	NM_012854	1.00	0.19	1.10	0.09	1.70	0.19
MCP-1	QT00183253	NM_031530	1.00	0.15	1.35	0.03	2.10	0.21
TNFα	QT00178717	NM_012675	1.00	0.11	0.79	0.22	0.95	0.20

[$]mean; [#]standard deviation; n=3 per group

Supplemental Figures

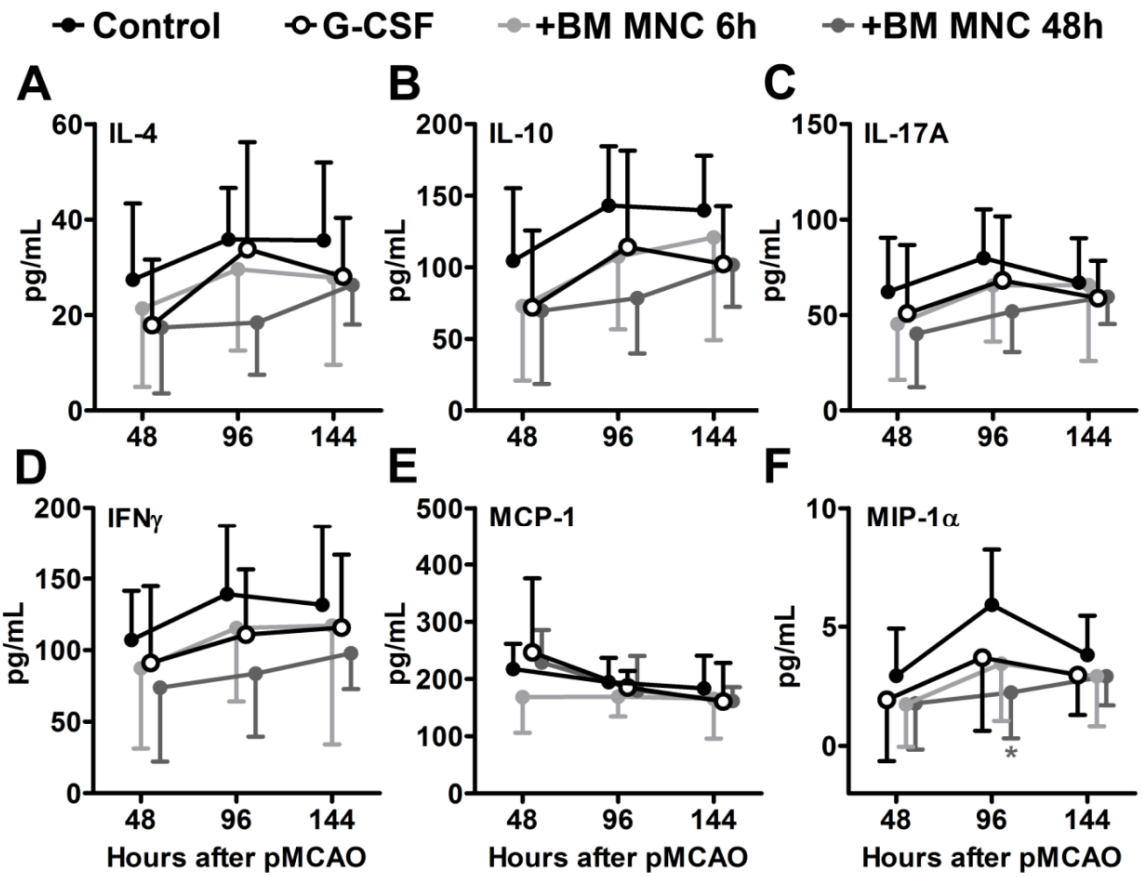

Supplemental Figure I
Serum protein levels of inflammatory cytokines 48, 96 and 144 hours after stroke onset. Serum levels of anti-inflammatory (Interleukin (IL)-4, IL-10) and pro-inflammatory (IL-17A, interferon (IFN) γ and macrophage inflammatory protein (MIP)-1α) cytokines showed a moderate increase from 48h to 96h. The chemotactic molecule monocyte chemotactic protein (MCP)-1 was detectable at relatively high serum levels (around 200 pg/mL serum) but without any relevant kinetics during the observation period. At 96h, the serum level of MIP-1α was slightly, but statistically significant reduced by G-CSF+BM MNC 48h. Apart from that, none of the treatment regimes had a significant influence on the cytokine levels. *$p<0.05$ compared to control group determined by repeated measurement two-way ANOVA; n=14-17 animals per group.

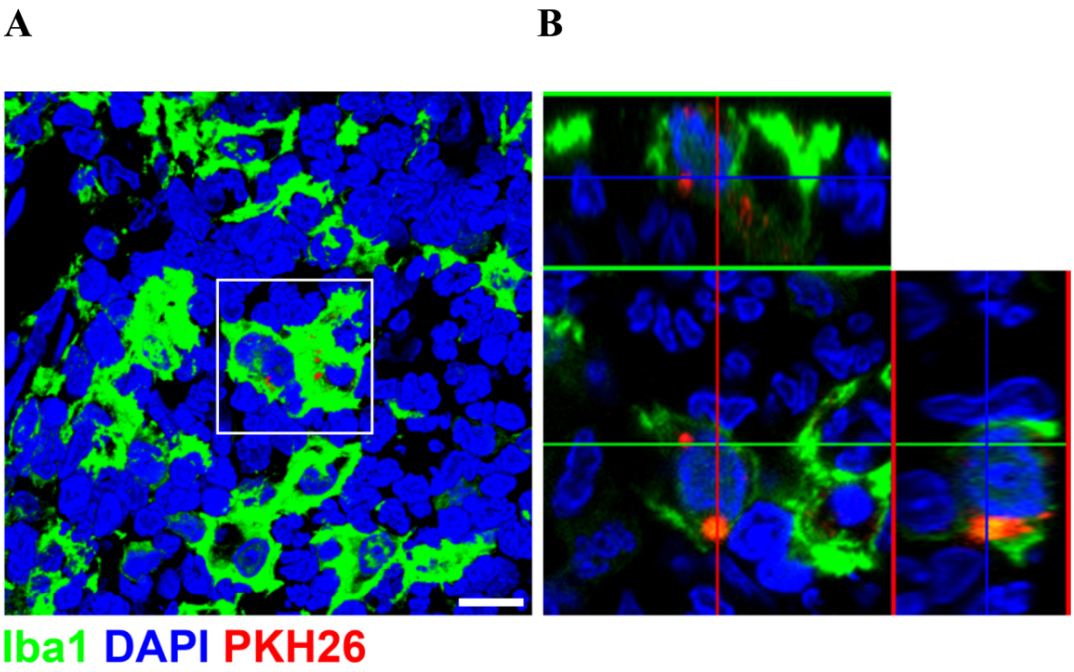

Supplemental Figure II
Laser scanning microscopy of the splenic marginal zone. **A**, a maximum intensity projection of a 15µm thick confocal stack showed various ionized calcium binding adapter molecule 1 (Iba1)+ macrophages. **B**, the detail is displayed as orthographic projection. PKH26+ signals could be clearly localized within the cytoplasm of the macrophage. Bar: 10µm

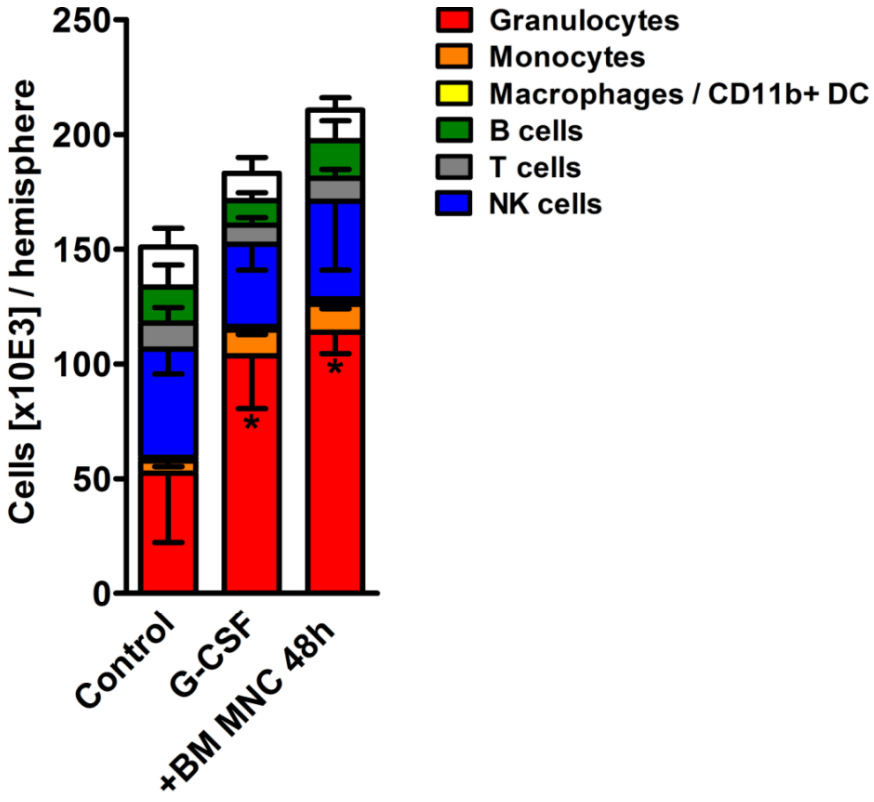

Supplemental Figure III
Flow cytometric analysis of major leukocyte populations in the contralateral hemisphere 52h after stroke. G-CSF treatment caused a significant increase of granulocytes that was not further influenced by BM MNC transplantation at 48h. *$p<0.05$ determined by one-way ANOVA; n=3 animals per group.

Reference List

(1) Tamura A, Graham DI, McCulloch J, Teasdale GM. Focal cerebral ischaemia in the rat: 1. Description of technique and early neuropathological consequences following middle cerebral artery occlusion. *J Cereb Blood Flow Metab*. 1981;1:53-60.

(2) Wagner DC, Deten A, Hartig W, Boltze J, Kranz A. Changes in T2 relaxation time after stroke reflect clearing processes. *Neuroimage*. 2012;61:780-785.

(3) Posel C, Moller K, Frohlich W, Schulz I, Boltze J, Wagner DC. Density gradient centrifugation compromises bone marrow mononuclear cell yield. *PLoS One*. 2012;7:e50293.

(4) Moller K, Stahl T, Boltze J, Wagner DC. Isolation of inflammatory cells from rat brain tissue after stroke. *Exp Transl Stroke Med*. 2012;4:20.

(5) Gerriets T, Stolz E, Walberer M, Muller C, Kluge A, Bachmann A et al. Noninvasive quantification of brain edema and the space-occupying effect in rat stroke models using magnetic resonance imaging. *Stroke*. 2004;35:566-571.

(6) Freret T, Chazalviel L, Roussel S, Bernaudin M, Schumann-Bard P, Boulouard M. Long-term functional outcome following transient middle cerebral artery occlusion in the rat: correlation between brain damage and behavioral impairment. *Behav Neurosci*. 2006;120:1285-1298.

2.3 Beantwortung initialer Fragestellungen

Mit den Ergebnissen dieser Arbeit und dem Auseinandersetzen mit der aktuellen Literatur kann eine klare Beantwortung der initial gestellten Fragen erfolgen:

1. *Welchen Einfluss hat die Aufreinigungsmethode auf das Zelltransplantat? In welcher Zusammensetzung und Vitalität steht das mononukleäre Zelltransplantat für die multimodale Therapie zur Verfügung?*
   In der publizierten Arbeit „Density gradient centrifugation compromises bone marrow mononuclear cell yield“ konnte gezeigt werden, dass bei der Aufreinigung des BM MNC-Transplantates mit der standardisierten Dichtegradientenzentrifugation ein Verlust an Zielzellen um bis zu 75% einhergeht. Mit der Etablierung einer neuen Depletionsmethode basierend auf der magnetischen Abbindung von PMN konnte der Verlust auf 30% minimiert werden. Unabhängig der Methode erstreckte sich der Zellverlust homogen auf alle Zellpopulationen und es wurden BM MNC mit einer Reinheit von über 90% angereichert. Mit der höheren BM MNC-Ausbeute nach immunomagnetischer Separation wurden zugleich zahlenmäßig mehr bipotente hämatopoetische als auch nicht-hämatopoetische Vorläuferzellen isoliert.
   Für die präklinische Wirksamkeitsstudie des kombinierten Therapieansatzes wurden BM MNC durch immunmagnetische Depletion der PMN isoliert. Die BM MNC setzten sich überwiegend aus B-Zellen, mononukleären myeloiden Zellen, T-Zellen sowie wenigen hämatopoetischen Vorläuferzellen zusammen und wiesen nach Kryokonservierung eine durchschnittliche Apoptoserate von 30% auf.

2. *Können die vielversprechenden neuroprotektiven und neuroregenerativen Effekte von G-CSF auch in einer prämorbiden Ratte nach experimentellem Schlaganfall nachgewiesen werden? Welche zusätzliche Wirkung ist durch die wiederholte G-CSF Behandlung zu beobachten?*
   In der publizierten Studie „Bone marrow cell transplantation time-dependently abolishes efficacy of G-CSF after stroke in hypertensive rats“ konnte erstmals durch eine G-CSF-Therapie neurologische Funktionen nach einem permanenten Schlaganfall in einer prämorbiden Ratte verbessert werden. Die G-CSF-Behandlung hatte keinen Einfluss auf das Infarktvolumen oder Hirnödem, was auf ein kürzeres Zeitfenster der Neuroprotektion in einem permanenten Schlaganfallmodell zurückzuführen ist. Des Weiteren gab es keine Anhaltspunkte für verbesserte neuroregenerative Effekte durch G-CSF. In den ersten Tagen nach Schlaganfall fiel in der Kontrollgruppe eine auffällige Reduktion der zirkulierenden Immunzellen im Blut

auf. Die wiederholte G-CSF-Gabe führte dagegen zu einem deutlichen Anstieg von PMN, Lymphozyten und Monozyten im Blut und hob die in der Kontrollgruppe beobachtete Immundepression auf. Die Einzeltherapie mit G-CSF führte ebenso zu einer vermehrten Ansammlung von vitalen als auch nekrotischen PMN in der Milz sowie zu einem Anstieg der Sekretion des pro-inflammatorischen Zytokins IL-1ß. In der ischämischen Hemisphäre konnte indessen keine erhöhte Infiltration von PMN beobachtet werden, dennoch kam es zu einer zahlenmäßigen Abnahme von infiltrierten Makrophagen durch die G-CSF-Behandlung.

3. *Wie wirkt sich die zusätzliche Zelltherapie zu einem frühen oder späteren Transplantationszeitpunkt auf die Studienendpunkte aus? Welche Wechselwirkungen können innerhalb der Kombinationstherapie beobachtet werden?*
   Die mononukleäre Zelltherapie 6h nach Schlaganfall zeigte weder einen fördernden noch schädlichen Einfluss auf die G-CSF-Effekte. Demgegenüber führte die zusätzliche Zelltherapie nach 48h zur vollständigen Aufhebung des protektiven Therapieeffektes von G-CSF und wies demnach ein neurologisches Defizit vergleichbar zur unbehandelten Kontrollgruppe auf. Die Entwicklung des Infarktvolumens oder des Hirnödems sowie die neuroregenerativen Prozesse wurden weder durch die frühe noch durch die späte Zelltherapie verändert. Die Aufhebung des G-CSF-Therapieeffektes durch eine zusätzliche Zelltransplantation nach 48h ist vermutlich auf nachteilige immunologische Interaktionen in der Milz zurückzuführen. So konnten 4h nach Injektion des Zelltransplantates fluoreszenzmarkierte BM MNC durchflusszytometrisch in Blut, Milz, Knochenmark und Hirn lokalisiert und differenziert werden, wobei ein Großteil der transplantierten Zellen in der Milz akkumulierte. Die histologische Analyse ergab, dass zahlreiche BM MNC zwischen roter und weißer Pulpa in direkter Nachbarschaft zu Makrophagen der Marginalzone lokalisiert waren. In Anbetracht der Tatsache, dass diese Makrophagen vor allem für den Abbau von zirkulierenden seneszenten und apoptotischen Zellen verantwortlich sind, könnte die G-CSF-bedingte Neutrophilie und die zusätzliche Injektion von apoptotischen BM MNC eine doppelte Belastung des Systems bewirkt haben. Die kompetitive Hemmung des Granulozytenabbaus in der Milz führte zu einer Akkumulation der PMN im Blut und bewirkte eine vermehrte Infiltration von vitalen PMN in die ischämische Hemisphäre. Dies könnte schließlich den negativen Einfluss auf die funktionelle Erholung erklären. Die untersuchte Kombinationstherapie war also je nach Therapiebeginn ohne Vorteil oder sogar schädlich und es konnten sowohl für die G-CSF- als auch die zusätzliche Zelltherapie interessante immunologische Wechselwirkungen beobachtet werden.

3 Zusammenfassung

Kumulative Dissertation zur Erlangung des akademischen Grades Dr. rer. med.

Effizienz einer Kombinationstherapie aus G-CSF und mononukleären Knochenmarkzellen in einem präklinischen Schlaganfallmodell

eingereicht von: Claudia Pösel, geb. Schnepp

angefertigt am: Fraunhofer-Institut für Zelltherapie und Immunologie, Abteilung Zelltherapie, Arbeitsgruppe Ischämieforschung

betreut von: Prof. Dr. Frank Emmrich (Universität Leipzig)
Prof. Dr. Hans-Jürgen Mägert (Hochschule Anhalt, Köthen)

Oktober 2014

In Deutschland ist der Schlaganfall die zweithäufigste Todesursache sowie oftmals der Grund für erworbene Behinderungen im Erwachsenenalter. Trotz intensiver Forschung in den letzten Jahrzehnten existiert bis heute nur eine kausale Therapiemöglichkeit: die Auflösung des gefäßverschließenden Blutgerinnsels mit gewebsspezifischem Plasminogenaktivator (Thrombolyse). Das Zeitfenster für diese Notfallbehandlung ist auf maximal viereinhalb Stunden nach Auftreten des Schlaganfalls limitiert, und weitere Begleitumstände führen dazu, dass nur ca. 15% aller Schlaganfallpatienten eine Thrombolyse erhalten. Ein wichtiges Ziel der Schlaganfallforschung ist die Entwicklung neuer Therapien, die in einem ausgedehnten Zeitfenster einsetzbar sind und somit mehr Patienten eine kausale Therapie ermöglichen. In Hinblick auf die komplexen pathophysiologischen Vorgänge nach einem Schlaganfall stellt die Kombination aus mehreren therapeutisch-wirksamen Kandidaten einen interessanten Ansatzpunkt dar. Die vorliegende Dissertation beschreibt die präklinische Prüfung eines multimodalen Therapiekonzeptes, dass die wiederholte Applikation des Wachstumshormones G-CSF (engl. *granulocyte-colony stimulating factor*, Granulozyten-Kolonie stimulierender Faktor) mit der Transplantation syngener, mononukleärer Knochenmarkzellen kombiniert. Die Effektivität der Therapie wurde für die Endpunkte Neuroprotektion und Neuroregeneration beurteilt. Aufgrund der immunmodulatorischen Eigenschaften von G-CSF wurde zudem die Wirkung der Kombinationstherapie auf die periphere und zerebrale Immunantwort nach Schlaganfall betrachtet.

G-CSF zeigte in verschiedenen präklinischen Schlaganfallstudien eine neuroprotektive und neuroregenerative Wirkung: beispielweise aktiviert G-CSF multiple Zellüberlebenskaskaden und führt so zu einer Verringerung des finalen Infarktvolumens. Weiterhin fördert G-CSF die adulte Neurogenese und unterstützt die Gefäßneubildung nach einem Schlaganfall. Als hämatopoetisches Wachstumshormon regt G-CSF die Reifung und Proliferation von therapeutisch relevanten Vorläuferzellen an und bewirkt deren Mobilisation aus dem Knochenmark in die Blutbahn. Da diese mobilisierende Eigenschaft des G-CSF zeitverzögert stattfindet, könnte eine zusätzliche, frühzeitige Zelltransplantation mit mononukleären Knochenmarkzellen eine synergistische Therapieoption zur Behandlung des Schlaganfalls darstellen. Zelltherapeutische Ansätze weisen ebenfalls ein vielfältiges Wirkungsspektrum auf, zu der die Hemmung des apoptotischen oder nekrotischen Zellsterbens, die Förderung der Neurogenese und der neuronalen Plastizität, der Wiederaufbau eines nährstoffversorgenden Gefäßsystems und die Immunmodulation durch die Sekretion trophischer Faktoren gehören. Die in dieser Arbeit verwendeten mononukleären Zellen des Knochenmarks (engl. *bone marrow mononuclear cells*, BM MNC) stellen als heterogenes Zellgemisch aus reifenden B-Lymphozyten, T-Lymphozyten, Monozyten sowie hämatopoetischen, endothelialen und mesenchymalen Stammzellen ein vielversprechendes Zelltransplantat dar. Die unkomplizierte Entnahme und Aufbereitung macht eine autologe Anwendung innerhalb weniger Stunden möglich.

Das in der Kombinationstherapie mit G-CSF verwendete mononukleäre Zelltransplantat (BM MNC) wurde aus dem Knochenmark von syngenen, spontan hypertensiven Ratten (SHR) gewonnen. Die Separation der BM MNC von der polymorphonukleären Zellfraktion (PMN, Granulozyten) erfolgte über immunmagnetische Depletion (engl. *magnetic activated cell sorting*, MACS) der PMN. Die im Rahmen dieser Arbeit etablierte Depletionsmethode zur Isolation der murinen BM MNC wurde mit den standardisierten Sedimentationsmethoden über Dichtegradientenzentrifugation mit Ficoll- oder Percoll-Medien verglichen. Mittels MACS konnten 72,3 ± 6,7% der BM MNC aus dem murinen Knochenmark isoliert werden. Demgegenüber reicherte die Dichtesedimentation nur ein Viertel (Ficoll: 25,6 ± 5,8%) bzw. die Hälfte (Percoll: 51,5 ± 2,3%) der BM MNC Fraktion an. Unabhängig von der Isolationsmethode erstreckte sich der ermittelte Zellverlust homogen auf alle Zellpopulationen, so dass sich die angereicherten BM MNC-Faktionen in ihrer zellulären Verteilung nicht von der des Knochenmarks unterschieden. Die Separation mit Ficoll führte zu einer prozentualen Anreicherung von hämatopoetischen Vorläuferzellen (engl. *hematopoietic stem cell*, HSC) im BM MNC-Transplantat, jedoch konnten aufgrund der geringeren BM MNC-Ausbeute im Ficoll-Ansatz zahlenmäßig nur

halb so viele HSC isoliert werden als nach Percoll-Dichtegradientenzentrifugation oder immunmagnetischer Separation (HSC-Gehalt nach Ficoll: 10700 ± 4066; Percoll: 20099 ± 5317 oder MACS: 20092 ± 3229, $p<0,05$). Für die präklinische Wirksamkeitsstudie des kombinierten Therapieansatzes wurden BM MNC durch immunmagnetische Depletion der PMN aus dem Knochenmark von SHR gewonnen und bis zur Transplantation kryokonserviert.

Die Wirksamkeit der Kombinationstherapie wurde in einem experimentellen Schlaganfallmodell in der komorbiden SHR geprüft. Unter Einhaltung tierschutzrechtlicher Vorgaben wurde in 81 männlichen SHRs die rechte mittlere Hirnarterie permanent verschlossen (engl. *permanent middle cerebral artery occlusion*, pMCAO). Die Tiere wurden randomisiert einer der vier Experimentalgruppen zugeteilt: drei Gruppen erhielten täglich eine intraperitoneale Injektion von 50µg G-CSF je kg Körpergewicht für insgesamt 5 Tage, beginnend eine Stunde nach pMCAO. Zusätzlich erhielten zwei der mit G-CSF behandelten Gruppen eine einmalige intravenöse Zelltherapie mit $1,5 \times 10^7$ syngenen BM MNC je kg Körpergewicht nach entweder 6h oder 48h nach Schlaganfall. Die Kontrollgruppe wurde zu allen Zeitpunkten der G-CSF- oder Zellapplikation mit einer Pufferlösung behandelt.
Zur Bewertung der Therapieeffizienz wurde über einen Zeitraum von 30 Tagen wiederholt das Infarktvolumen und das Hirnödem mittels Magnetresonanztomographie bestimmt. Die neurologische Entwicklung wurde mit dem *Adhesive Removal Test* (ART) über 28 Tage bestimmt und anhand der Fläche unter der Kurve (engl. *area under the curve*, AUC) quantifiziert. Weder in der Gruppe mit alleiniger G-CSF-Behandlung noch in den Gruppen mit zusätzlicher Zelltherapie nach 6h oder 48h wurde eine Beeinflussung des Infarktvolumens oder des Hirnödems festgestellt. Dennoch konnte bei Tieren mit einer G-CSF-Monotherapie eine Reduktion des funktionellen Defizites nachgewiesen werden (pMCAO AUC: 1291 ± 768; pMCAO+G-CSF AUC: 797 ± 581, $p<0,05$). Die zusätzliche Zelltherapie 6h nach Schlaganfall bewirkte keine weitere Veränderung dieses Befundes (pMCAO+G-CSF+BM MNC 6h AUC: 843 ± 391, $p>0,05$), interessanterweise führte jedoch die zusätzliche Zelltherapie nach 48h zur vollständigen Aufhebung des G-CSF Therapieeffektes (pMCAO+G-CSF+BM MNC 48h AUC: 1238 ± 707, $p>0,05$). Dies ließ eine nachteilige Interaktion zwischen der G-CSF- und Zelltherapie nach 48h vermuten. Die erhöhte Expression der Leukozyten-spezifischen Tyrosinphosphatase (CD45) und des entzündungsfördernden Interleukins-1β in der ischämischen Hirnhemisphäre, sowie zahlreiche T-Lymphozyten im Randbereich der ischämischen Läsion wiesen auf einen andauernden Entzündungsprozess im Spätstadium des Schlaganfalls hin. Jedoch wurden die Prozesse weder durch G-CSF noch durch die zusätzliche Zelltherapie moduliert.

Innerhalb der ersten 5 Tage nach Schlaganfall wurde im Blut der Kontrollgruppe erwartungsgemäß eine auffällige Reduktion an zirkulierenden Immunzellen nach Schlaganfall festgestellt. Im Gegensatz dazu bewirkte die G-CSF-Therapie einen deutlichen Anstieg von PMN, Lymphozyten und Monozyten. Die Transplantation von BM MNC nach 6h hatte zu keinem der untersuchten Zeitpunkte einen signifikanten Einfluss auf die Leukozytenverteilung. Interessanterweise konnte jedoch in der späten Zelltherapiegruppe (48h) bereits vier Stunden nach Zelltransplantation ein signifikanter Anstieg der zirkulierenden PMN beobachtet werden (pMCAO: 1,54 ± 1,01 $x10^6$ PMN/ml; pMCAO+G-CSF: 6,11 ± 0,58 $x10^6$ PMN/ml; pMCAO+G-CSF+BM MNC 48h: 8,01 ± 1,09 $x10^6$ PMN/ml, $p<0,05$).
Um eine potenziell immunologische Interaktion zwischen der G-CSF-Therapie und der späten Zelltherapie ermitteln zu können, wurde zunächst die Verteilung der spät-transplantierten (48h) BM MNC 4h nach Injektion in Blut, Milz, Knochenmark und Gehirn untersucht. Die fluoreszenzmarkierten BM MNC konnten durchflusszytometrisch in allen untersuchten Organen lokalisiert und differenziert werden, wobei der Großteil der transplantierten Zellen in der Milz akkumulierte. Die histologische Analyse der Milz ergab, dass zahlreiche BM MNC zwischen roter und weißer Pulpa in direkter Nachbarschaft zu Makrophagen der Marginalzone lokalisiert waren. Diese sogenannten *Marginal Zone Macrophages* (MZM) sind für den Abbau von zirkulierenden seneszenten und apoptotischen Zellen verantwortlich. Möglicherweise hat die doppelte Belastung dieses Systems durch die massive G-CSF-bedingte Neutrophilie und die Injektion von teilweise apoptotischen BM MNC zu einer kompetitiven Hemmung des Granulozytenabbaus geführt. Tatsächlich konnte nach einer späten Zelltherapie sowohl einen Anstieg der zirkulierenden PMN als auch deren vermehrte Infiltration in die ischämische Hirnhemisphäre nachgewiesen werden. Dies könnte schließlich den negativen Einfluss auf die funktionelle Verbesserung erklären.

Zusammenfassend konnte in dieser Arbeit erstmals die Wirksamkeit von G-CSF auf die funktionelle Erholung nach einem permanenten Schlaganfallmodell in einer komorbiden Ratte bestätigt werden. Während die zusätzliche Transplantation von BM MNC nach 6h keinen weiteren Therapieeffekt zeigte, führte die Zelltransplantation nach 48h, wahrscheinlich aufgrund einer immunologischen Interaktion, zu einer Aufhebung des protektiven G-CSF-Effektes. Die untersuchte Kombinationstherapie war also je nach Therapiebeginn ohne Vorteil oder sogar schädlich. Die zugrundeliegenden Interaktionsmechanismen werfen ein interessantes Licht auf die mögliche Wirkungsweise von Zelltherapien und unterstreichen die entscheidende Rolle des Immunsystems in der Pathophysiologie des Schlaganfalls.

Literaturverzeichnis

(1) Kolominsky-Rabas PL, Heuschmann PU, Marschall D, Emmert M, Baltzer N, Neundorfer B, et al. Lifetime cost of ischemic stroke in Germany: results and national projections from a population-based stroke registry: the Erlangen Stroke Project. Stroke 2006 May;37(5):1179-83.

(2) Roger VL, Go AS, Lloyd-Jones DM, Adams RJ, Berry JD, Brown TM, et al. Heart disease and stroke statistics--2011 update: a report from the American Heart Association. Circulation 2011 Feb 1;123(4):e18-e209.

(3) Adams HP, Jr., Bendixen BH, Kappelle LJ, Biller J, Love BB, Gordon DL, et al. Classification of subtype of acute ischemic stroke. Definitions for use in a multicenter clinical trial. TOAST. Trial of Org 10172 in Acute Stroke Treatment. Stroke 1993 Jan;24(1):35-41.

(4) Dirnagl U, Iadecola C, Moskowitz MA. Pathobiology of ischaemic stroke: an integrated view. Trends Neurosci 1999 Sep;22(9):391-7.

(5) Broughton BR, Reutens DC, Sobey CG. Apoptotic mechanisms after cerebral ischemia. Stroke 2009 May;40(5):e331-e339.

(6) Hossmann KA. Periinfarct depolarizations. Cerebrovasc Brain Metab Rev 1996;8(3):195-208.

(7) Chamorro A, Meisel A, Planas AM, Urra X, van de BD, Veltkamp R. The immunology of acute stroke. Nat Rev Neurol 2012 Jul;8(7):401-10.

(8) Dirnagl U, Klehmet J, Braun JS, Harms H, Meisel C, Ziemssen T, et al. Stroke-induced immunodepression: experimental evidence and clinical relevance. Stroke 2007 Feb;38(2 Suppl):770-3.

(9) Prass K, Meisel C, Hoflich C, Braun J, Halle E, Wolf T, et al. Stroke-induced immunodeficiency promotes spontaneous bacterial infections and is mediated by sympathetic activation reversal by poststroke T helper cell type 1-like immunostimulation. J Exp Med 2003 Sep 1;198(5):725-36.

(10) Offner H, Vandenbark AA, Hurn PD. Effect of experimental stroke on peripheral immunity: CNS ischemia induces profound immunosuppression. Neuroscience 2009 Feb 6;158(3):1098-111.

(11) Haeusler KG, Schmidt WU, Fohring F, Meisel C, Helms T, Jungehulsing GJ, et al. Cellular immunodepression preceding infectious complications after acute ischemic stroke in humans. Cerebrovasc Dis 2008;25(1-2):50-8.

(12) Meisel C, Schwab JM, Prass K, Meisel A, Dirnagl U. Central nervous system injury-induced immune deficiency syndrome. Nat Rev Neurosci 2005 Oct;6(10):775-86.

(13) Howells DW, Porritt MJ, Rewell SS, O'Collins V, Sena ES, van der Worp HB, et al. Different strokes for different folks: the rich diversity of animal models of focal cerebral ischemia. J Cereb Blood Flow Metab 2010 Aug;30(8):1412-31.

(14) Stroke Therapy Academic Industry Roundtable (STAIR). Recommendations for standards regarding preclinical neuroprotective and restorative drug development. Stroke 1999 Dec;30(12):2752-8.

(15) Stem Cell Therapies as an Emerging Paradigm in Stroke Participants. Stem Cell Therapies as an Emerging Paradigm in Stroke (STEPS): bridging basic and clinical science for cellular and neurogenic factor therapy in treating stroke. Stroke 2009 Feb;40(2):510-5.

(16) Kilkenny C, Browne WJ, Cuthill IC, Emerson M, Altman DG. Improving bioscience research reporting: the ARRIVE guidelines for reporting animal research. PLoS Biol 2010;8(6):e1000412.

(17) Crossley NA, Sena E, Goehler J, Horn J, van der WB, Bath PM, et al. Empirical evidence of bias in the design of experimental stroke studies: a metaepidemiologic approach. Stroke 2008 Mar;39(3):929-34.

(18) Swislocki A, Tsuzuki A. Insulin resistance and hypertension: glucose intolerance, hyperinsulinemia, and elevated free fatty acids in the lean spontaneously hypertensive rat. Am J Med Sci 1993 Nov;306(5):282-6.

(19) Bauhofer A, Tischer B, Middeke M, Plaul U, Lorenz W, Torossian A. The genetic background of hypertensive, septic rats determines outcome improvement with antibiotic and G-CSF prophylaxis. Shock 2003 Oct;20(4):326-31.

(20) Tamura A, Graham DI, McCulloch J, Teasdale GM. Focal cerebral ischaemia in the rat: 1. Description of technique and early neuropathological consequences following middle cerebral artery occlusion. J Cereb Blood Flow Metab 1981;1(1):53-60.

(21) Wagner DC, Deten A, Hartig W, Boltze J, Kranz A. Changes in T2 relaxation time after stroke reflect clearing processes. Neuroimage 2012 Jul 16;61(4):780-5.

(22) Blinzler C, Breuer L, Huttner HB, Schellinger PD, Schwab S, Kohrmann M. Characteristics and outcome of patients with early complete neurological recovery after thrombolysis for acute ischemic stroke. Cerebrovasc Dis 2011;31(2):185-90.

(23) Sutherland BA, Minnerup J, Balami JS, Arba F, Buchan AM, Kleinschnitz C. Neuroprotection for ischaemic stroke: translation from the bench to the bedside. Int J Stroke 2012 Jul;7(5):407-18.

(24) O'Collins VE, Macleod MR, Donnan GA, Howells DW. Evaluation of combination therapy in animal models of cerebral ischemia. J Cereb Blood Flow Metab 2012 Apr;32(4):585-97.

(25) O'Collins VE, Macleod MR, Donnan GA, Horky LL, van der Worp BH, Howells DW. 1,026 experimental treatments in acute stroke. Ann Neurol 2006 Mar;59(3):467-77.

(26) Hossmann KA. The two pathophysiologies of focal brain ischemia: implications for translational stroke research. J Cereb Blood Flow Metab 2012 Jul;32(7):1310-6.

(27) Shuaib A, Lees KR, Lyden P, Grotta J, Davalos A, Davis SM, et al. NXY-059 for the treatment of acute ischemic stroke. N Engl J Med 2007 Aug 9;357(6):562-71.

(28) Endres M, Engelhardt B, Koistinaho J, Lindvall O, Meairs S, Mohr JP, et al. Improving outcome after stroke: overcoming the translational roadblock. Cerebrovasc Dis 2008;25(3):268-78.

(29) Sena ES, van der Worp HB, Bath PM, Howells DW, Macleod MR. Publication bias in reports of animal stroke studies leads to major overstatement of efficacy. PLoS Biol 2010 Mar;8(3):e1000344.

(30) Bliss TM, Andres RH, Steinberg GK. Optimizing the success of cell transplantation therapy for stroke. Neurobiol Dis 2010 Feb;37(2):275-83.

(31) Minnerup J, Heidrich J, Wellmann J, Rogalewski A, Schneider A, Schabitz WR. Meta-analysis of the efficacy of granulocyte-colony stimulating factor in animal models of focal cerebral ischemia. Stroke 2008 Jun;39(6):1855-61.

(32) England TJ, Gibson CL, Bath PM. Granulocyte-colony stimulating factor in experimental stroke and its effects on infarct size and functional outcome: A systematic review. Brain Res Rev 2009 Dec 11;62(1):71-82.

(33) Hill CP, Osslund TD, Eisenberg D. The structure of granulocyte-colony-stimulating factor and its relationship to other growth factors. Proc Natl Acad Sci U S A 1993 Jun 1;90(11):5167-71.

(34) Nicola NA, Begley CG, Metcalf D. Identification of the human analogue of a regulator that induces differentiation in murine leukaemic cells. Nature 1985 Apr 18;314(6012):625-8.

(35) Kawakami M, Tsutsumi H, Kumakawa T, Abe H, Hirai M, Kurosawa S, et al. Levels of serum granulocyte colony-stimulating factor in patients with infections. Blood 1990 Nov 15;76(10):1962-4.

(36) Vellenga E, Rambaldi A, Ernst TJ, Ostapovicz D, Griffin JD. Independent regulation of M-CSF and G-CSF gene expression in human monocytes. Blood 1988 Jun;71(6):1529-32.

(37) Koeffler HP, Gasson J, Ranyard J, Souza L, Shepard M, Munker R. Recombinant human TNF alpha stimulates production of granulocyte colony-stimulating factor. Blood 1987 Jul;70(1):55-9.

(38) Zsebo KM, Yuschenkoff VN, Schiffer S, Chang D, McCall E, Dinarello CA, et al. Vascular endothelial cells and granulopoiesis: interleukin-1 stimulates release of G-CSF and GM-CSF. Blood 1988 Jan;71(1):99-103.

(39) Begley CG, Lopez AF, Nicola NA, Warren DJ, Vadas MA, Sanderson CJ, et al. Purified colony-stimulating factors enhance the survival of human neutrophils and eosinophils in vitro: a rapid and sensitive microassay for colony-stimulating factors. Blood 1986 Jul;68(1):162-6.

(40) Bober LA, Grace MJ, Pugliese-Sivo C, Rojas-Triana A, Waters T, Sullivan LM, et al. The effect of GM-CSF and G-CSF on human neutrophil function. Immunopharmacology 1995 Mar;29(2):111-9.

(41) Yoshino T, Tamura M, Hattori K, Kawamura A, Imai N, Ono M. Effects of recombinant human granulocyte colony-stimulating factor on neutrophil function in normal rats. Int J Hematol 1991 Dec;54(6):455-62.

(42) Arcese W, De AG, Cerretti R. Granulocyte-mobilized bone marrow. Curr Opin Hematol 2012 Nov;19(6):448-53.

(43) Frampton JE, Lee CR, Faulds D. Filgrastim. A review of its pharmacological properties and therapeutic efficacy in neutropenia. Drugs 1994 Nov;48(5):731-60.

(44) Rutella S, Zavala F, Danese S, Kared H, Leone G. Granulocyte colony-stimulating factor: a novel mediator of T cell tolerance. J Immunol 2005 Dec 1;175(11):7085-91.

(45) Hartung T, Doecke WD, Bundschuh D, Foote MA, Gantner F, Hermann C, et al. Effect of filgrastim treatment on inflammatory cytokines and lymphocyte functions. Clin Pharmacol Ther 1999 Oct;66(4):415-24.

(46) Boneberg EM, Hareng L, Gantner F, Wendel A, Hartung T. Human monocytes express functional receptors for granulocyte colony-stimulating factor that mediate suppression of monokines and interferon-gamma. Blood 2000 Jan 1;95(1):270-6.

(47) Sloand EM, Kim S, Maciejewski JP, Van RF, Chaudhuri A, Barrett J, et al. Pharmacologic doses of granulocyte colony-stimulating factor affect cytokine production by lymphocytes in vitro and in vivo. Blood 2000 Apr 1;95(7):2269-74.

(48) Nicola NA, Metcalf D. Binding of 125I-labeled granulocyte colony-stimulating factor to normal murine hemopoietic cells. J Cell Physiol 1985 Aug;124(2):313-21.

(49) Avalos BR. Molecular analysis of the granulocyte colony-stimulating factor receptor. Blood 1996 Aug 1;88(3):761-77.

(50) Shimoda K, Okamura S, Harada N, Kondo S, Okamura T, Niho Y. Identification of a functional receptor for granulocyte colony-stimulating factor on platelets. J Clin Invest 1993 Apr;91(4):1310-3.

(51) Franzke A, Piao W, Lauber J, Gatzlaff P, Konecke C, Hansen W, et al. G-CSF as immune regulator in T cells expressing the G-CSF receptor: implications for transplantation and autoimmune diseases. Blood 2003 Jul 15;102(2):734-9.

(52) Bussolino F, Ziche M, Wang JM, Alessi D, Morbidelli L, Cremona O, et al. In vitro and in vivo activation of endothelial cells by colony-stimulating factors. J Clin Invest 1991 Mar;87(3):986-95.

(53) Schneider A, Kruger C, Steigleder T, Weber D, Pitzer C, Laage R, et al. The hematopoietic factor G-CSF is a neuronal ligand that counteracts programmed cell death and drives neurogenesis. J Clin Invest 2005 Aug;115(8):2083-98.

(54) Demetri GD, Griffin JD. Granulocyte colony-stimulating factor and its receptor. Blood 1991 Dec 1;78(11):2791-808.

(55) Hernandez JM, Castilla C, Gutierrez NC, Isidro IM, Delgado M, de las RJ, et al. Mobilisation with G-CSF in healthy donors promotes a high but temporal deregulation of genes. Leukemia 2005 Jun;19(6):1088-91.

(56) Six I, Gasan G, Mura E, Bordet R. Beneficial effect of pharmacological mobilization of bone marrow in experimental cerebral ischemia. Eur J Pharmacol 2003 Jan 5;458(3):327-8.

(57) Sevimli S, Diederich K, Strecker JK, Schilling M, Klocke R, Nikol S, et al. Endogenous brain protection by granulocyte-colony stimulating factor after ischemic stroke. Exp Neurol 2009 Jun;217(2):328-35.

(58) Kleinschnitz C, Schroeter M, Jander S, Stoll G. Induction of granulocyte colony-stimulating factor mRNA by focal cerebral ischemia and cortical spreading depression. Brain Res Mol Brain Res 2004 Nov 24;131(1-2):73-8.

(59) Schabitz WR, Kollmar R, Schwaninger M, Juettler E, Bardutzky J, Scholzke MN, et al. Neuroprotective effect of granulocyte colony-stimulating factor after focal cerebral ischemia. Stroke 2003 Mar;34(3):745-51.

(60) Komine-Kobayashi M, Zhang N, Liu M, Tanaka R, Hara H, Osaka A, et al. Neuroprotective effect of recombinant human granulocyte colony-stimulating factor in transient focal ischemia of mice. J Cereb Blood Flow Metab 2006 Mar;26(3):402-13.

(61) Solaroglu I, Cahill J, Tsubokawa T, Beskonakli E, Zhang JH. Granulocyte colony-stimulating factor protects the brain against experimental stroke via inhibition of apoptosis and inflammation. Neurol Res 2009 Mar;31(2):167-72.

(62) Lee ST, Chu K, Jung KH, Ko SY, Kim EH, Sinn DI, et al. Granulocyte colony-stimulating factor enhances angiogenesis after focal cerebral ischemia. Brain Res 2005 Oct 5;1058(1-2):120-8.

(63) Taguchi A, Wen Z, Myojin K, Yoshihara T, Nakagomi T, Nakayama D, et al. Granulocyte colony-stimulating factor has a negative effect on stroke outcome in a murine model. Eur J Neurosci 2007 Jul;26(1):126-33.

(64) Ringelstein EB, Thijs V, Norrving B, Chamorro A, Aichner F, Grond M, et al. Granulocyte colony-stimulating factor in patients with acute ischemic stroke: results of the AX200 for Ischemic Stroke trial. Stroke 2013 Oct;44(10):2681-7.

(65) Rosenberg GA. Matrix metalloproteinases in neuroinflammation. Glia 2002 Sep;39(3):279-91.

(66) Gidday JM, Gasche YG, Copin JC, Shah AR, Perez RS, Shapiro SD, et al. Leukocyte-derived matrix metalloproteinase-9 mediates blood-brain barrier breakdown and is proinflammatory after transient focal cerebral ischemia. Am J Physiol Heart Circ Physiol 2005 Aug;289(2):H558-H568.

(67) Gibson CL, Jones NC, Prior MJ, Bath PM, Murphy SP. G-CSF suppresses edema formation and reduces interleukin-1beta expression after cerebral ischemia in mice. J Neuropathol Exp Neurol 2005 Sep;64(9):763-9.

(68) Wagner DC, Posel C, Schulz I, Schicht G, Boltze J, Lange F, et al. Allometric dose retranslation unveiled substantial immunological side effects of granulocyte colony-stimulating factor after stroke. Stroke 2014 Feb;45(2):623-6.

(69) Kurozumi K, Nakamura K, Tamiya T, Kawano Y, Ishii K, Kobune M, et al. Mesenchymal stem cells that produce neurotrophic factors reduce ischemic damage in the rat middle cerebral artery occlusion model. Mol Ther 2005 Jan;11(1):96-104.

(70) Llado J, Haenggeli C, Maragakis NJ, Snyder EY, Rothstein JD. Neural stem cells protect against glutamate-induced excitotoxicity and promote survival of injured motor neurons through the secretion of neurotrophic factors. Mol Cell Neurosci 2004 Nov;27(3):322-31.

(71) Taguchi A, Soma T, Tanaka H, Kanda T, Nishimura H, Yoshikawa H, et al. Administration of CD34+ cells after stroke enhances neurogenesis via angiogenesis in a mouse model. J Clin Invest 2004 Aug;114(3):330-8.

(72) Jiang Q, Zhang ZG, Ding GL, Zhang L, Ewing JR, Wang L, et al. Investigation of neural progenitor cell induced angiogenesis after embolic stroke in rat using MRI. Neuroimage 2005 Nov 15;28(3):698-707.

(73) Chen J, Zhang ZG, Li Y, Wang L, Xu YX, Gautam SC, et al. Intravenous administration of human bone marrow stromal cells induces angiogenesis in the ischemic boundary zone after stroke in rats. Circ Res 2003 Apr 4;92(6):692-9.

(74) Shen LH, Li Y, Chen J, Zhang J, Vanguri P, Borneman J, et al. Intracarotid transplantation of bone marrow stromal cells increases axon-myelin remodeling after stroke. Neuroscience 2006;137(2):393-9.

(75) Xiao J, Nan Z, Motooka Y, Low WC. Transplantation of a novel cell line population of umbilical cord blood stem cells ameliorates neurological deficits associated with ischemic brain injury. Stem Cells Dev 2005 Dec;14(6):722-33.

(76) Nakatomi H, Kuriu T, Okabe S, Yamamoto S, Hatano O, Kawahara N, et al. Regeneration of hippocampal pyramidal neurons after ischemic brain injury by recruitment of endogenous neural progenitors. Cell 2002 Aug 23;110(4):429-41.

(77) Iihoshi S, Honmou O, Houkin K, Hashi K, Kocsis JD. A therapeutic window for intravenous administration of autologous bone marrow after cerebral ischemia in adult rats. Brain Res 2004 May 8;1007(1-2):1-9.

(78) Kamiya N, Ueda M, Igarashi H, Nishiyama Y, Suda S, Inaba T, et al. Intra-arterial transplantation of bone marrow mononuclear cells immediately after reperfusion decreases brain injury after focal ischemia in rats. Life Sci 2008 Sep 12;83(11-12):433-7.

(79) Giraldi-Guimaraes A, Rezende-Lima M, Bruno FP, Mendez-Otero R. Treatment with bone marrow mononuclear cells induces functional recovery and decreases neurodegeneration after sensorimotor cortical ischemia in rats. Brain Res 2009 Feb 9.

(80) Brenneman M, Sharma S, Harting M, Strong R, Cox CS, Jr., Aronowski J, et al. Autologous bone marrow mononuclear cells enhance recovery after acute ischemic stroke in young and middle-aged rats. J Cereb Blood Flow Metab 2010 Jan;30(1):140-9.

(81) Nakano-Doi A, Nakagomi T, Fujikawa M, Nakagomi N, Kubo S, Lu S, et al. Bone marrow mononuclear cells promote proliferation of endogenous neural stem cells through vascular niches after cerebral infarction. Stem Cells 2010 Jul;28(7):1292-302.

(82) Sharma S, Yang B, Strong R, Xi X, Brenneman M, Grotta JC, et al. Bone marrow mononuclear cells protect neurons and modulate microglia in cell culture models of ischemic stroke. J Neurosci Res 2010 Oct;88(13):2869-76.

(83) Wagner DC, Bojko M, Peters M, Lorenz M, Voigt C, Kaminski A, et al. Impact of age on the efficacy of bone marrow mononuclear cell transplantation in experimental stroke. Exp Transl Stroke Med 2012;4(1):17.

(84) Minnerup J, Wagner DC, Strecker JK, Posel C, Sevimli-Abdis S, Schmidt A, et al. Bone marrow-derived mononuclear cells do not exert acute neuroprotection after stroke in spontaneously hypertensive rats. Front Cell Neurosci 2014;7:288.

(85) Fujita Y, Ihara M, Ushiki T, Hirai H, Kizaka-Kondoh S, Hiraoka M, et al. Early protective effect of bone marrow mononuclear cells against ischemic white matter damage through augmentation of cerebral blood flow. Stroke 2010 Dec;41(12):2938-43.

(86) Terada N, Hamazaki T, Oka M, Hoki M, Mastalerz DM, Nakano Y, et al. Bone marrow cells adopt the phenotype of other cells by spontaneous cell fusion. Nature 2002 Apr 4;416(6880):542-5.

(87) Lu P, Blesch A, Tuszynski MH. Induction of bone marrow stromal cells to neurons: differentiation, transdifferentiation, or artifact? J Neurosci Res 2004 Jul 15;77(2):174-91.

(88) Fischer UM, Harting MT, Jimenez F, Monzon-Posadas WO, Xue H, Savitz SI, et al. Pulmonary passage is a major obstacle for intravenous stem cell delivery: the pulmonary first-pass effect. Stem Cells Dev 2009 Jun;18(5):683-92.

(89) Barbosa da Fonseca LM, Gutfilen B, Rosado de Castro PH, Battistella V, Goldenberg RC, Kasai-Brunswick T, et al. Migration and homing of bone-marrow mononuclear cells in chronic ischemic stroke after intra-arterial injection. Exp Neurol 2010 Jan;221(1):122-8.

(90) Yang B, Migliati E, Parsha K, Schaar K, Xi X, Aronowski J, et al. Intra-arterial delivery is not superior to intravenous delivery of autologous bone marrow mononuclear cells in acute ischemic stroke. Stroke 2013 Dec;44(12):3463-72.

(91) Savitz SI, Misra V, Kasam M, Juneja H, Cox CS, Jr., Alderman S, et al. Intravenous autologous bone marrow mononuclear cells for ischemic stroke. Ann Neurol 2011 Jul;70(1):59-69.

(92) Aktas M, Radke TF, Strauer BE, Wernet P, Kogler G. Separation of adult bone marrow mononuclear cells using the automated closed separation system Sepax. Cytotherapy 2008;10(2):203-11.

(93) van Beem RT, Hirsch A, Lommerse IM, Zwaginga JJ, Noort WA, Biemond BJ, et al. Recovery and functional activity of mononuclear bone marrow and peripheral blood cells after different cell isolation protocols used in clinical trials for cell therapy after acute myocardial infarction. EuroIntervention 2008 May;4(1):133-8.

(94) Minnerup J, Seeger FH, Kuhnert K, Diederich K, Schilling M, Dimmeler S, et al. Intracarotid administration of human bone marrow mononuclear cells in rat photothrombotic ischemia. Exp Transl Stroke Med 2010;2(1):3.

(95) Yang B, Strong R, Sharma S, Brenneman M, Mallikarjunarao K, Xi X, et al. Therapeutic time window and dose response of autologous bone marrow mononuclear cells for ischemic stroke. J Neurosci Res 2011 Jun;89(6):833-9.

(96) Yang B, Xi X, Aronowski J, Savitz SI. Ischemic stroke may activate bone marrow mononuclear cells to enhance recovery after stroke. Stem Cells Dev 2012 Dec 10;21(18):3332-40.

(97) Rogalewski A, Schneider A, Ringelstein EB, Schabitz WR. Toward a multimodal neuroprotective treatment of stroke. Stroke 2006 Apr;37(4):1129-36.

(98) Petit I, Szyper-Kravitz M, Nagler A, Lahav M, Peled A, Habler L, et al. G-CSF induces stem cell mobilization by decreasing bone marrow SDF-1 and up-regulating CXCR4. Nat Immunol 2002 Jul;3(7):687-94.

Erklärung über die eigenständige Abfassung der Arbeit

Hiermit erkläre ich, dass ich die vorliegende Arbeit, mit dem Titel „*Effizienz einer Kombinationstherapie aus G-CSF und mononukleären Knochenmarkzellen in einem präklinischen Schlaganfallmodell*“ selbständig und ohne unzulässige Hilfe oder Benutzung anderer als der angegebenen Hilfsmittel angefertigt habe. Ich versichere, dass Dritte von mir weder unmittelbar noch mittelbar geldwerte Leistungen für Arbeiten erhalten haben, die im Zusammenhang mit dem Inhalt der vorgelegten Dissertation stehen, und dass die vorgelegte Arbeit weder im Inland noch im Ausland in gleicher oder ähnlicher Form einer anderen Prüfungsbehörde zum Zweck einer Promotion oder eines anderen Prüfungsverfahrens vorgelegt wurde. Alles aus anderen Quellen und von anderen Personen übernommene Material, das in der Arbeit verwendet wurde oder auf das direkt Bezug genommen wird, wurde als solches kenntlich gemacht. Insbesondere wurden alle Personen genannt, die direkt an der Entstehung der vorliegenden Arbeit beteiligt waren.

.....	.....
Datum	Unterschrift

Danksagung

An dieser Stelle möchte ich allen danken, die zum Gelingen dieser Arbeit beigetragen haben.

Herrn Prof. Dr. Emmrich danke für die Möglichkeit, diese Dissertation am Fraunhofer-Institut für Zelltherapie und Immunologie durchführen zu können. Bei Herrn Prof. Dr. Hans-Jürgen Mägert bedanke ich mich für die Betreuung des kooperativen Promotionsverfahrens vonseiten der Hochschule Anhalt in Köthen.

Herrn Dr. med. Dr. rer. nat. Johannes Boltze möchte ich für das interessante Dissertationsthema, das entgegengebrachte Vertrauen und die langjährige Unterstützung danken.

Mein besonderer Dank geht an Dr. med. Daniel-Christoph Wagner für die hervorragende wissenschaftliche Betreuung und seine ständige Diskussions- und Hilfsbereitschaft. Seine fachliche Kompetenz und kritischen Ratschläge haben mich sehr inspiriert und täglich angespornt. Dr. Gesa Weise, Karoline Möller und Dr. Alexander Deten danke ich für die vielen wissenschaftlichen und konstruktiven Gespräche.

Johanna, Wenke, Elfi und Isabell danke ich für deren Unterstützung bei der Bearbeitung der Projekte. Weiterer Dank gilt der gesamten Arbeitsgruppe für die freundschaftliche Arbeitsatmosphäre und stete Hilfsbereitschaft, die wesentlich zum Gelingen dieser Arbeit beigetragen haben.

Des Weiteren bedanke ich mich bei der Klinik für Diagnostische und Interventionelle Radiologie der Universität Leipzig für die freundliche Zusammenarbeit sowie bei Herrn Dr. med. Alexander Kranz für die Durchführung der Magnetresonanztomographie.

Bei meiner Familie möchte ich mich besonders herzlich bedanken für die uneingeschränkte und liebevolle Unterstützung während der letzten 4 Jahre. Den größten Dank schulde ich meinem Mann Udo. Er hat mir stets zur Seite gestanden, immer Verständnis gehabt, mich liebevoll unterstützt und immerzu motiviert meine Dissertation zu vollenden.

Lebenslauf

Claudia Pösel, geb. Schnepp

Geburtsdatum:	09.04.1982
Geburtsort:	Gera
Nationalität:	deutsch
Familienstand:	verheiratet
Adresse:	Weißenfelser Straße 51, 04229 Leipzig

Schulbildung

1988 – 1994	Grund- und Realschule, Pölzig
1994 – 2000	Otto-Baensch-Gymnasium, Zeitz

Berufsausbildung

2000 – 2005	Studium der Biotechnologie, Hochschule Anhalt Köthen; Abschluss 03/05 als Dipl.Ing. (FH) für Biotechnologie, Spez. Verfahrenstechnik
2010 – 2014	Promotionsarbeit am Fraunhofer Institut für Zelltherapie und Immunologie / Medizinische Fakultät der Universität Leipzig

Beruflicher Werdegang

06/2005 – 06/2008	technische Mitarbeiterin am Institut für Zelltechniken und angewandte Stammzellbiologie, Medizinische Fakultät der Universität Leipzig
07/2008 – 06/2012	technische Mitarbeiterin am Fraunhofer Institut für Zelltherapie und Immunologie, Abteilung Zelltherapie, AG Ischämieforschung, Leipzig
09/2012 –	wissenschaftliche Mitarbeiterin am Fraunhofer Institut für Zelltherapie und Immunologie, Abteilung Zelltherapie, AG Ischämieforschung, Leipzig

Verzeichnis wissenschaftlicher Veröffentlichungen

Publikationen in Zeitschriften mit Gutachtensystem

Bone marrow mononuclear cell transplantation time-dependently abolishes efficacy of G-CSF after stroke in hypertensive rats; **Pösel C.**, Scheibe J., Kranz A., Bothe V., Quente E., Fröhlich W., Schäbitz W.-R., Minnerup J., Boltze J., Wagner D.-C. (2014): Stroke

Bone marrow-derived mononuclear cells do not exert acute neuroprotection after stroke in spontaneously hypertensive rats, Minnerup J., Wagner D.-C., Strecker J.-K., **Pösel C.**, Sevimli-Abdis S., Schmidt A., Schilling M., Boltze J., Diederich K., Schäbitz W.-R. (2014): Frontiers in Cellular Neuroscience

Allometric dose retranslation unveiled substantial immunological side effects of G-CSF after stroke; Wagner D.-C., **Pösel C.**, Schulz I., Schicht G., Boltze J., Lange F., Scheibe J., Möller K., Weise G.(2014): Stroke

Transplantation of cryopreserved human umbilical cord blood mononuclear cells does not induce sustained recovery after experimental stroke in spontaneously hypertensive rats; Weise G., Lorenz M., **Pösel C.**, Riegelsberger U.M., Storbeck V., Kamprad M., Kranz A., Wagner D.-C., Boltze J. (2013): J Cereb Blood Flow Metab.

Sterile inflammation after stroke in hypertensive rats; Möller K., **Pösel C.**, Seeger J., Boltze J., Stahl T., Wagner D.-C. (2013): J Cereb Blood Flow Metab.

Density gradient centrifugation compromises bone marrow mononuclear cell yield; **Pösel C.**, Möller K., Fröhlich W., Schulz I., Boltze J., Wagner D.-C. (2012): PLoS ONE

Comprehensive characterization of chondrocyte cultures in plasma and whole blood biomatrices for cartilage tissue engineering; Schulz R.M., Haberhauer M., Zernia G., **Pösel C.**, Thümmler C., Somerson J.S., Huster D. (2012): J Tissue Eng Regen Med.

Intravenous human umbilical cord blood transplantation for stroke : Impact on infarct volume and caspase3-dependent cell death in spontaneously hypertensive rats; Riegelsberger U.M., Deten A., **Pösel C.**, Zille M., Kranz A., Boltze J., Wagner D.-C. (2011): Exp. Neurology

Allogeneic non-adherent bone marrow cells facilitate hematopoietic recovery but do not lead to allogeneic engraftment; Fricke S., Ackermann M., Stolzing A., Schimmelpfennig C., Hilger N., Jahns J., Hildebrandt G., Emmrich F., Ruschpler P., **Pösel C.**, Kamprad M., Sack U. (2009): PLoS One

Low oxygen expansion of MSC enhance chondrogenic differentiation in pellet culture and collagen scaffold; Zscharnack M., **Pösel C.**, Galle J., Bader A. (2009): Cells Tissues Organs

Cartilage tissue engineering in allogenous plasma and whole blood nanoscaffolds; Haberhauer M., Zernia G., Schulz R., Deiwick A., **Schnepp C.**, Huster D., Bader A.: Adv. Materials

Publikationen in Zeitschriften ohne Gutachtensystem

Entzündung ohne Erreger – Rolle des Immunsystems nach Schlaganfall; Wagner D.-C., Möller K., **Pösel C.** (2014): BIOspektrum 01/2014, Springer

Tracking of Autologous VSOP-Labeled Mesenchymal Stem Cells in the Sheep Brain Using 3.0T MRI; Dreyer A. Y., Lobsien D., **Pösel C.**, Hoffmann K.-T., Nitzsche B., Findeisen M., Stroh A., Boltze J. (2012): Cell-Based Therapies in Stroke, Springer (Buchkapitel)

Frameless stereotaxy in sheep – neurosurgical and imaging techniques for translational stroke research; Dreyer A.Y., Stroh A., **Pösel C.**, Findeisen M., Geymüller T., Lobsien D., Nitsche B., Boltze J. (2011): InTech. (Buchkapitel)

Konferenzbeiträge

Tracking of autologous VSOP-labeled mesenchymal stem cells in the sheep brain using 3T MRI; Dreyer A., Nitzsche B., **Pösel C.**, Zeisig V., Lobsien D., Hoffmann K.T., Boltze J. (2014): Australia Neuroscience Society

Tracking of QuantumDot-labeled human neural stem cells after intracerebral transplantation in ‘humanized mice; Garcia Puig A., **Pösel C.**, Scheibe J., Boltze J., Wagner D.-C., Weise G. (2013): World Conference on Regenerative Medicine, Leipzig

Migratory Behavior of lymphocytes from humanized mouse chimera, Didwischus N., **Pösel C.**, Möller K., Wagner D.-C., Weise G. (2013): World Conference on Regenerative Medicine, Leipzig

Cellular characterization of brain and peripheral immune organs in a humanized mouse model with particular focus on cerebral ischemia and stem cell transplantation; Möller K., **Pösel C.**, Schulz I., Lange F., Bliss T., Boltze, J., Wagner D.-C. (2012): Fraunhofer Life Science Symposium, Leipzig

Molecular Characterization of stably, virally infected GFP-hNSCs compared to non-infected hNSCs; Scheibe J., Hetz S., Fronz U., Deten A., **Pösel C.**, Fröhlich W., Boltze J., Wagner D.-C. (2012): Fraunhofer Life Science Symposium, Leipzig

Molecular Characterization of stably, virally infected GFP-hNSCs compared to non-infected hNSCs; Scheibe J., Hetz S., Fronz U., Deten A., **Pösel C.**, Fröhlich W., Boltze J., Wagner D.-C. (2012): Neuroscience, New Orleans

Identification and characterization of brain infiltrating leukocytes and intracerebrally engrafted human neural stem cells in a humanized mouse model; Möller K., **Pösel C.**, Schulz I., Lange F., Bliss T., Boltze, J., Wagner D.-C. (2012): Cyto, Leipzig

A combined experimental stroke therapy using G-CSF and syngeneic bone marrow mononuclear cells; **Pösel C.**, Scheibe J., Möller K., Quente E., Kranz A., Glocke I., Bothe V., Fröhlich W., Boltze J., Wagner D.-C. (2012): The 7th International Symposium on Neuroprotection and Neurorepair, Potsdam

Cell yield and composition of rat bone marrow mononuclear cells significantly depend on the isolation procedure; **Pösel C.**, Möller K., Fröhlich W., Boltze J., Wagner D.-C. (2012): The 7th International Symposium on Neuroprotection and Neurorepair, Potsdam

Methods for cell trafficking after transplantation in animal stroke models; **Pösel C.**, Riegelsberger U.-M., Emmrich F., Boltze J., Holland H., Wagner D.-C. (2009): World Conference on Regenerative Medicine, Leipzig

Syngeneic transplantation of adipose tissue-derived cells for experimental stroke; Taubert, J., Safdari, S., **Pösel, C.**, Kranz, A., Scheibe, J., Boltze, J., Wagner, D.-C. (2009): World Conference on Regenerative Medicine, Leipzig

Impact of cell therapies on post-ischemic astrogliosis; Wagner, D.-C.; Kranz, A.; Riegelsberger, U.M., **Pösel, C.**, Emmrich, F., Boltze, J. (2009): World Conference on Regenerative Medicine, Leipzig

Intravenous administration of human umbilical cord blood cells did not reduce infarct volume and caspase-3-dependent apoptosis; Kranz, A., Riegelsberger, U.M., **Pösel, C.**, Boltze, J., Emmrich, F., Wagner, D.-C. (2009): World Conference on Regenerative Medicine, Leipzig

Low oxygen during expansion of mesenchymal stem cells increases the following chondrogenic differentiation in pellet culture and collagen gel; Zscharnack M., **Pösel C.**, Marquass B., Bader A. (2007): 2nd Congress of the German Society for Stem Cell Research, Würzburg

Comparison of solid-state NMR and established methods for the characterisation of tissue engineered cartilage; Haberhauer M., Zernia G., Deiwick A., **Schnepp C.**, Huster D., Bader A., (2006): 5th Biotechnology symposium, Leipzig

Tissue Engineering of cartilage: biocompatible scaffolds; Haberhauer M., Deiwick A., **Schnepp C.**, Bader A. (2006): 5th Biotechnology symposium, Leipzig

Solid-state NMR as a non-invasive method for the characterization of tissue engineered cartilage; Haberhauer M., Zernia G., Deiwick A., **Schnepp C.**, Huster D., Bader A. (2006): 2nd international Conference “Stategies in tissue Engineering“, Würzburg

New matrices for tissue engineering of cartilage; Haberhauer M., Deiwick A., **Schnepp C.**, Bader A. (2006): 2nd international Conference “Stategies in tissue Engineering“, Würzburg

Tissue engineered matrices for cartilage Repair; Haberhauer M., Deiwick A., **Schnepp C.**, Bader A. In: Thiery J., Beck- Sickinger A., Emmrich F. (2005): 4th Research festival Life Science, Leipzig